Durham E-Theses

Late Glacial to Holocene relative sea-level change in Assynt, north west Scotland

HAMILTON, CHRISTINE,ANNE

Late Glacial to Holocene relative sea-level change in Assynt, north west Scotland

Christine Anne Hamilton

Thesis submitted for the degree of
Master of Science (by Research)

Department of Geography
Durham University

2014

Christine Anne Hamilton

Late Glacial to Holocene relative sea-level change in Assynt, north west Scotland

This thesis aims to improve the relative sea-level (RSL) reconstruction for the Assynt region, a previously under-studied region of the British Isles, to provide important further constraints on glacial isostatic adjustment (GIA) models for the British Isles. The lack of geological data from this region means that the GIA models are currently poorly constrained for this region of north west Scotland. Evidence from four isolation basins on the north coast of the Assynt region reconstructs post-Last Glacial Maximum (LGM) RSL for previously unstudied time periods, including the Late Glacial and early Holocene. This thesis produces the first Late Glacial sea-level index points for Assynt, providing a critical additional constraint on the GIA model predictions for this early deglacial period, which in general is poorly constrained throughout the British Isles.

Sediment cores were taken at a range of altitudes above present sea level from four isolation basins. Reconstruction of the palaeoenvironment focused on diatom analysis, supported by organic content, particle size and qualitative pollen analysis. A number of clear transitions, from marine to brackish to freshwater conditions, document the isolation or ingression of the basins investigated at Duart. AMS radiocarbon dating of these contacts produced new sea-level index points for the Late Glacial, early and late Holocene for Assynt.

These new sea-level index points show there is poor fit between the model predictions for the Late Glacial RSL fall following the Late Glacial highstand and the RSL rise to the mid-Holocene highstand. There is reasonable data-model fit however from the mid- to late-Holocene as RSL falls to present. This misfit, evident elsewhere in north west Scotland, is potentially due to uncertainties associated with both the global and local ice model employed in the GIA models, providing a context for future study.

Contents

List of tables

List of Figures

Chapter 3:Geographical location & study sites

Chapter 4: Methodology

Chapter 5: Results and Interpretation

Chapter 6: Discussion

Declaration of copyright

I confirm that no part of the material presented in this thesis has previously been submitted by me or any other person for a degree in this or any other university. In all cases, where it is relevant, material from the work of others has been acknowledged.

The copyright of this thesis rests with the author. No quotation from it should be published without prior written consent and information derived from it should be acknowledged.

Acknowledgements

Chapter 1: Introduction

1.1 Introduction

Predictions of future sea-level change are of increasing importance due to the potential impact sea-level rise would have upon the coastal zone. It is estimated that by 2500 median sea level will rise by 1.84 m and 5.49 m based upon the lowest and highest radiative forcing scenarios respectively (Jevrejeva et al. 2012). In 2010, c. 44% of the world's population lived within 150 km of the sea, whilst in England one in six properties are deemed as at risk from flooding in the future (United Nations Environment Programme 2010; Environment Agency 2009). One way to better understand coastal changes, in response to future sea-level change, is to improve our understanding of past changes in relative sea level (RSL) during different climate states. One aspect of this research has been the production of well-constrained records of past sea-level changes which provide information regarding the link between climate and sea level, and can also be used to test and improve models of glacial isostastic adjustment (GIA).

During the Last Glacial Maximum (LGM) the British and Irish Ice Sheet (BIIS) was relatively small in comparison to other ice sheets around the Earth. During deglaciation of the BIIS the interaction between regional GIA, deformation of the ocean geoid and changes in the global ocean volume (eustatic sea level) resulted in a spatially complicated RSL history in the British Isles (Flemming 1982; Shennan 1989). This geographical region is regarded by Peltier (1998) as extremely useful for improving understanding of aspects of GIA modelling because it was glaciated in the north and subject to the collapse of the Fennoscandian forebulge. The RSL record is well documented by a range of geological evidence for much of the UK and these records have been used to refine models (e.g. Shennan 1989; Shennan et al. 2006a). Mismatches, however, between model predictions and the RSL record remain in some parts of the UK and therefore there is a need for further empirical data from these regions.

Scotland has been the focus of sea-level research for over a century, however Assynt remains an understudied region of the British Isles. By comparison, research from the Arisaig area, further south on the west coast of Scotland, has produced the longest and most complete archive of RSL change from the British Isles (Shennan et al. 1996; Shennan et al. 2005). This data has proved critical in testing and improving geophysical models of GIA (e.g. Bradley et al. 2011). Improved RSL reconstructions from the Assynt region will provide an important further test of the model predictions, which have limited constraint in this area.

1.2 Research Design

Project Rationale

Existing RSL data for the Assynt region is confined to Coigach and restricted to the mid- and late Holocene (Shennan et al. 2000). As a result, the current GIA model for the British Isles (Bradley et al. 2011) has limited constraint and no data from the Late Glacial and early Holocene period in this area. Similarly there is very limited data north of Assynt (Barlow et al. 2014). Refinement of geophysical models such as Bradley et al. (2011) and Kuchar et al. (2012), based on additional RSL data, will lead to improved understanding of ice sheet configuration, earth rheology, lithospheric thickness and mantle viscosity. The history of the BIIS remains debated, particularly aspects such as extent and thickness at the LGM and timing of retreat of the ice stream of north west Scotland (McCarroll et al. 1995; Evans et al. 2005; Bradwell et al. 2008). Additional RSL data for the Assynt region can contribute to this debate by constraining the Earth's response to changes in mass balance following deglaciation.

Research aim and objectives

The aim of this research is to develop new sea-level index points for the Assynt region. The sea-level reconstructions produced will be compared to the Bradley et al (2011) model predictions of post-LGM sea-level change in this region. This thesis sets to test the hypothesis that RSL in Assynt during the Late Glacial and early Holocene was higher than predicted by the Bradley et al (2011) model. This is based upon the recent reassessment of trimline data as englacial thermal boundaries (Ballantyne & Hall 2008; Ballantyne 2010; Fabel et al. 2012) therefore constraining the minimum rather than the maximum surface elevation of the BIIS. Thicker ice would result in greater GIA and RSL higher than currently predicted by the Bradley et al (2011) model.

In order to achieve the aim, and test the hypothesis, the objectives are to:

1. Identify the stratigraphic sequence and elevation of the rock sill from isolation basins in the Assynt region.
2. Reconstruct the palaeoenvironment for sediment sequences recovered from isolation basins to identify any changes in marine, brackish and/or freshwater influence.
3. Produce Late Glacial and Holocene sea-level index points by combining the proxy-based analysis with chronological control.
4. Using the new and existing sea-level index points, assess the implications on post-LGM RSL predictions for Assynt and north west Scotland.

1.3 Thesis outline

The following chapters present the context, location, methodology, results, discussion and conclusions of this research. Chapter 2 reviews the literature concerning the reconstruction of the BIIS and post-LGM RSL in north west Scotland as well as the use of GIA models to predict post-LGM RSL. Chapter 3 outlines the geology and geomorphology of the Assynt region and presents the field locations investigated and sampled for this research. Chapter 4 introduces the field and laboratory methodology employed to reconstruct the palaeoenvironment at each site. Chapter 5 outlines the results of these reconstructions whilst Chapter 6 presents the new sea-level index points generated for the region and discusses their potential implication on predictions of RSL change for Assynt and north west Scotland.

Chapter 2: Context of Research

This chapter outlines the glacial, deglacial and RSL history of north west Scotland and discusses the uncertainties associated with the reconstruction of the BIIS. Reconstructions of post-LGM RSL in north west Scotland are presented and predictions of RSL change by the current GIA model for the British Isles are discussed.

2.1 British and Irish Ice Sheet

The extent, geometry and chronology of the BIIS remains debated, despite over 150 years of research (e.g. Geikie 1878; Gregory 1926; Charlesworth 1956; Ballantyne 1990; Evans et al. 2005). Onshore geomorphology, sedimentology and stratigraphy have traditionally been utilised to reconstruct the BIIS, whilst the development of offshore bathymetry, seismostratigraphy and borehole evidence are delivering new measuring techniques (Bradwell et al. 2007; Bradwell et al. 2008). Refinement of the geophysical models, based on additional RSL data, will lead to improved understanding of the history of the BIIS (McCarroll et al. 1995; Evans et al. 2005; Bradwell et al. 2008). Improving the RSL data for the Assynt region can contribute to this debate by constraining the Earth's response to mass balance.

Earlier research, based on bio- and litho-stratigraphic analysis of onshore and offshore sediment cores, suggested that the BIIS had terminated a short distance of the north east coast of the UK (Davies et al. 1984; Sutherland 1984; Bowen et al. 1986). Bowen et al. (1986) proposed an ice sheet of limited extent which did not extend great distances offshore onto the Atlantic shelf or North Sea basin whilst north east Scotland and north west Ireland were believed to be ice-free. These former reconstructions failed to identify the BIIS as marine-based, therefore underestimating the potential influence of sea-level induced collapse, whilst palaeo-ice streams, such as The Minch, were not identified.

Recent reconstructions (Peck et al. 2007; Bradwell et al. 2008; Clark et al. 2012; Everest et al. 2013) reveal an extensive ice sheet, twice the size of that originally proposed by Bowen et al. (1986) (Figure 2.2). Offshore evidence indicating glacial activity, for example moraines preserved north east and north west of Britain and borehole evidence of subglacial till in the Witch Ground Basin, has challenged previous reconstructions (Bradwell et al. 2008; Clark et al. 2012; Everest et al. 2013). Seismic techniques, along with echosound data, enabled the sequential retreat of the ice sheet from the continental shelf edge to be reconstructed (Everest et al. 2013). Cosmogenic exposure dates of glacially transported boulders on North Rona, 70 km north west of Cape Wrath, along with this geological evidence, illustrated that the BIIS extended near to the edge of the continental shelf between 27 and 25 ka BP (Everest et al. 2013). These reconstructions

show that the BIIS was largely marine-based with an aerial extent of c. 840,000 km^2 (Clark et al. 2012) providing empirical evidence of a confluence with the Fennoscandian Ice Sheet during the LGM (Figure 2.2) (Sejrup et al. 2005; Bradwell et al. 2008).
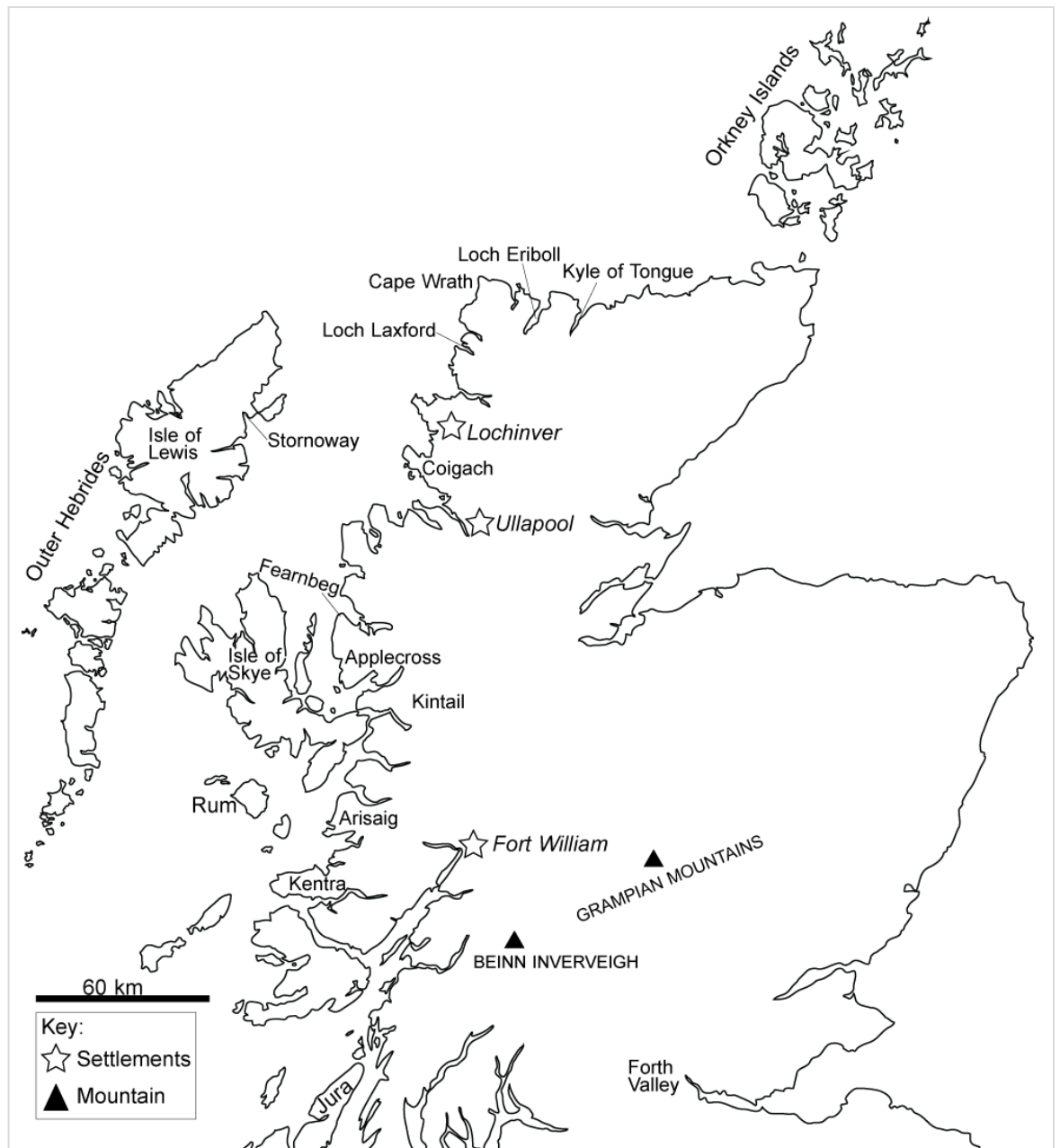
Figure 2.1: Locations and features in Scotland mentioned in the text, with the exception of locations within the Assynt region which are found in Figure 3.1.

Figure 2.2: Contrasting reconstructions of the BIIS during the LGM. The dashed line represents the conservative estimates of Bowen et al. (1986; 2002) whilst the solid line illustrates the recent reconstructions (Sejrup et al. 2005; Bradwell et al. 2008) which reconstruct a confluence with the Fennoscandian Ice Sheet. Source: Ballantyne (2010).

The vertical dimensions of the BIIS have been reconstructed using periglacial trimlines throughout north west Scotland (Figure 2.3). Ballantyne et al. (1998) argued that trimline evidence on Scottish mountains, between Arisaig and Cape Wrath including Skye, Rum and Lewis, is representative of the upper limit of the last ice sheet, below which the glacier eroded frost-weathered material. This argument has been supported by measurements of significantly greater rock breakdown above the trimline (Ballantyne et al. 1998). Reconstructions of the thickness of the last ice sheet using periglacial trimlines has resulted in estimates between 650 m and 750 m for the north west Highlands; the vertical extent at Ullapool was estimated at 750 m whilst, further north, in Lochinver it was

reconstructed at 650 m (Lawson 1995; Ballantyne et al. 1998). These estimates were determined by extrapolating the altitude of the weathering limit from nearby summits such as Ben More Assynt which had a weathering limit of 810-850 m. This interpretation of the evidence has been incorporated into the most recent GIA models (e.g. Shennan et al. 2006a; Bradley et al. 2011).
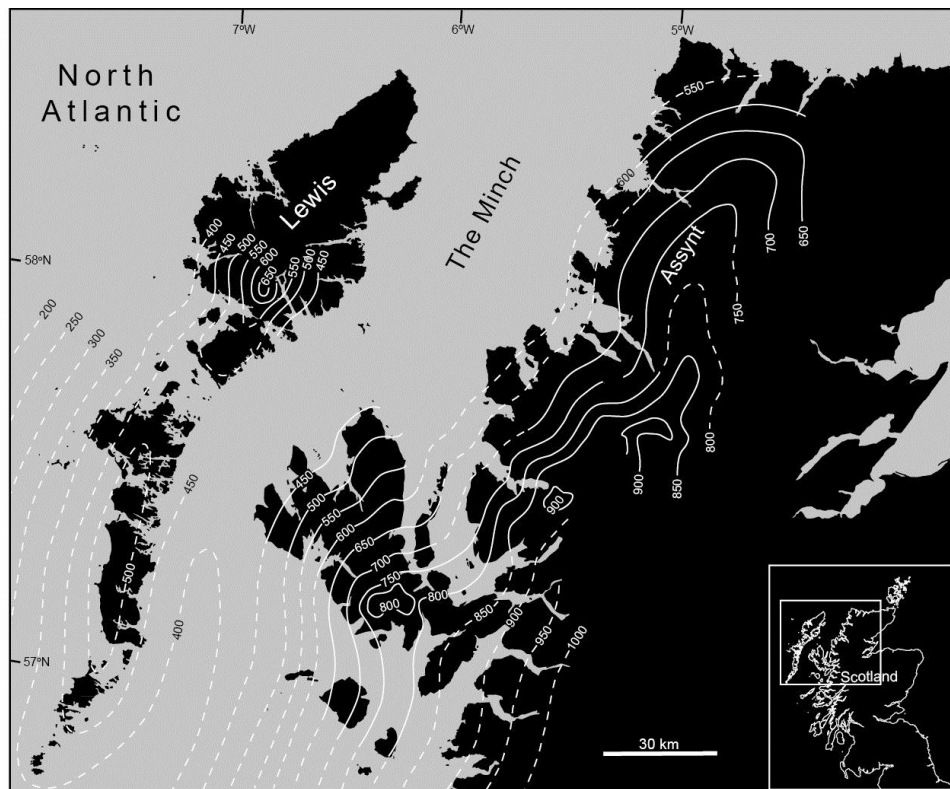
Figure 2.3: Contoured reconstruction of the 'maximum' surface elevation of the BIIS in north west Scotland, based on the altitude of weathering limits (trimlines) and over-ridden mountains (Lawson 1995; McCarroll et al. 1995; Ballantyne et al. 1998). These trimlines are now thought to represent englacial thermal boundaries rather than ice sheet limits (e.g. Ballantyne & Hall 2008; Fabel et al. 2012).

A major re-assessment of trimlines as vertical ice limits, using cosmogenic nuclide analysis, has illustrated that trimlines in the British Isles probably represent englacial thermal boundaries therefore indicating the minimum ice thickness or the maximum elevation of erosive ice (Ballantyne & Hall 2008; Ballantyne 2010; Fabel et al. 2012). A numerical ice sheet model (Boulton & Hagdorn 2006), driven by proxy climate data from Greenland, has been used to alter the ice sheet boundary and climate forcing conditions in order to match the characteristics of the BIIS known from geological evidence. Boulton & Hagdorn (2006) model demonstrated the difficulties of restricting the thickness of the BIIS in north west Scotland to the trimline altitudes mapped by Ballantyne et al. (1998). Kuchar et al. (2012) uses a numerical glaciological model, based upon Hubbard et al. (2009), to create a GIA model for the British Isles and investigate this further. Even the minimal modelled ice reconstruction in the Kuchar et al. (2012) model produces a thicker ice sheet than that from models constrained by trimline observations (e.g. Brooks et al.

2008). The ice in western Scotland is reconstructed up to a kilometre thicker, fitting well with the RSL data for north west Highlands, suggesting that the trimlines are indeed a lower boundary for the ice surface altitude. The lateral, as well as the vertical, extent of the BIIS reconstructed by the Kuchar et al. (2012) model however is not constrained by geomorphological evidence. The next step for modelling the BIIS is to develop models which integrate geological and climate data (e.g. Whitehouse et al. 2012).

Ice streams are regarded as a critical control on the configuration and stability of an ice sheet (Stokes & Clark 2001). Reconstructing these zones of fast flowing ice, responsible for discharging large quantities of ice, improves understanding of the behaviour of previous ice sheets (Boulton & Clark 1990; O'Cofaigh et al. 2003). Ice-streams can rapidly discharge large quantities of freshwater and therefore may be an important mechanism causing a sharp shift in climate (e.g. Heinrich 1988). Ice streaming in north west Scotland has been constrained to 30-15 ka BP by AMS radiocarbon dates of organic deposits from north east Lewis, reconstructing the Tolsta Interstadial (c. 30 k ^{14}C yr BP) using detailed pollen analysis (Whittington & Hall 2002). This is combined with molluscs from borehole 78/4 in the North Minch, 9 km of Stornoway, which reconstruct arctic open-water conditions by 15 k yr BP (Graham et al. 1990). The Minch palaeo-ice stream, c. 200 km long and 50 km wide, drained a substantial volume of the north west section of the last ice sheet (Figure 2.4) (Bradwell et al. 2007). Reconstructions have produced clear evidence of ice streaming on the coast of north west Scotland, particularly around Loch Broom, whilst two of the nine tributaries of the Minch ice stream were identified in the Assynt area in Enard Bay and Eddrachillis Bay (Stoker & Bradwell 2005; Bradwell et al. 2007). New RSL data will refine GIA predictions for the Assynt region and potentially help constrain the timing of the Minch ice-stream.

The climate and glaciation of Scotland during the Late Glacial period (15-11 ka BP) is a topic which remains debated, particularly with respect to the extent, or lack, of ice during the Late Glacial Interstadial (Greenland Interstadial 1; 14.7-12.9 ka BP). A range of scenarios have been presented for the extent of ice during the Late Glacial Interstadial at the margins of the Assynt region; persistence of ice on high-ground (Finlayson et al. 2011), low ground (Bradwell 2006) or complete deglaciation (Sissons 1967; Boulton & Hagdorn 2006). Advances in geomorphological and cosmogenic-isotope evidence as well as onshore-offshore glacial stratigraphy during the last decade has led to the conclusion that glaciation occurred throughout some part of the Late Glacial Interstadial (e.g. Bradwell et al. 2008; Stoker et al. 2009; Ballantyne 2010). The Younger Dryas, referred to as the Loch Lomond Stadial in Britain, is regarded as an analogue for enhancing understanding of rapid change however considerable uncertainty regarding glacier extent is also associated with this Stadial in Assynt and elsewhere in the British Isles (Golledge 2010; Ballantyne 2012). There are two theories of deglaciation for the Loch Lomond

Stadial in north west Scotland. Firstly, that glaciers expanded until the end of the Stadial and then retreated rapidly due to the transition into the Holocene (11.7-11.6 ka) (Sissons 1977; Benn et al. 1992; MacLeod et al. 2011). An alternative theory is that maximum glacier extent was reached during the middle of the Loch Lomond Stadial (12.6-12.4 ka) and gradual retreat, due to warming summer temperatures along with increased aridity occurred, increasing to rapid retreat at the transition into the Holocene (Benn & Ballantyne 2005; Golledge 2010; Lukas & Bradwell 2010; Ballantyne 2012). Reconstructions of the extent of the Loch Lomond Stadial on the margins of the Assynt region, such as the Summer Isles and Ullapool, have indicated that ice masses existed during the Late Glacial Interstadial warming (14.7-12.9 Ka BP) and were therefore present at the beginning of the Loch Lomond Stadial (Bradwell et al. 2008; McIntyre et al. 2011). Lukas & Bradwell (2010) found that large areas of cold-based ice were present on Ben More, Assynt, during the Loch Lomond Stadial however were not able to document the extent or onset of deglaciation. Research undertaken by Bradwell (2006) has indicated that the extent and thickness of ice the Loch Lomond Stadial, in locations adjacent to the Assynt region, was more extensive than previously believed.
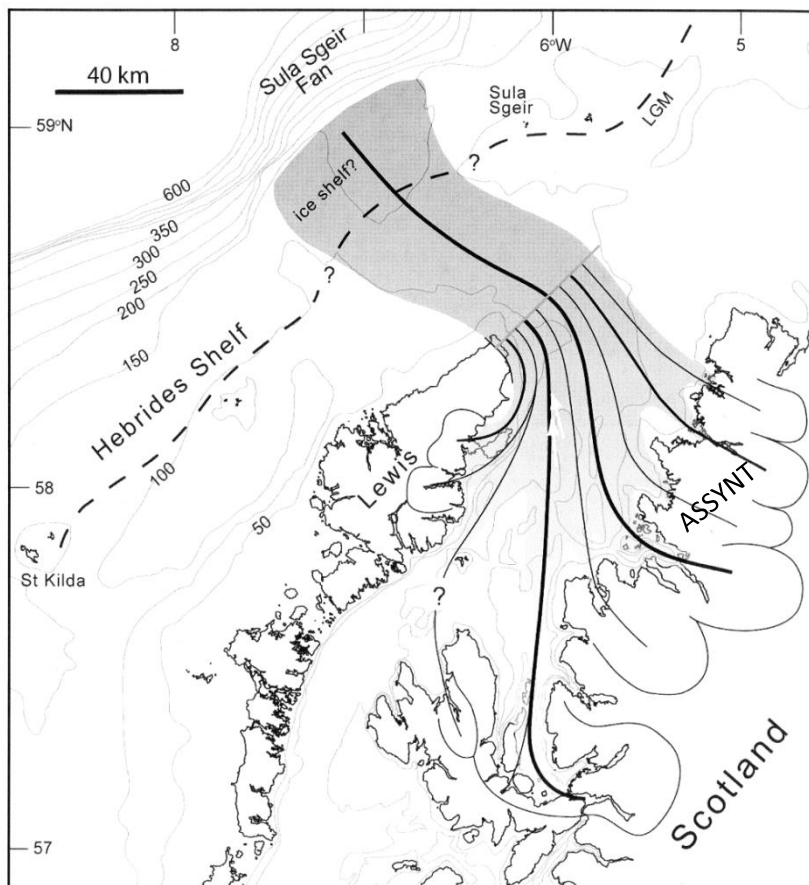
Figure 2.4: Reconstruction of the Minch palaeo-ice stream at maximum extent. The grey shaded area illustrates the flow of the main ice-stream and associated tributaries. Black lines are hypothesised palaeoflow lines, two of which flow from the Assynt region, whilst the dashed line (LGM) shows the probable limit of ground BIIS. Source: Bradwell et al. (2007).

2.2 RSL change in north west Scotland

RSL is defined as the vertical position of the ocean surface (geoid) relative to the present position of the solid land surface. RSL ($\Delta\zeta_{rsl}$) is schematically defined as the complex interplay between the following, at any location in space (σ) and time (τ) (Flemming 1982; Shennan & Horton 2002; Shennan 2007):

$$\Delta\zeta_{rsl}(\tau,\sigma) = \Delta\zeta_{esl}(\tau,\sigma) + \Delta\zeta_{iso}(\tau,\sigma) + \Delta\zeta_{tect}(\tau,\sigma) + \Delta\zeta_{local}(\tau,\sigma)$$

where $\Delta\zeta_{esl}$ is the time-dependent eustatic function, $\Delta\zeta_{iso}$ is the total isostatic effect of the glacial rebound process including both the ice (glacio-isostatic) and water (hydro-isostatic) load contributions and $\Delta\zeta_{tect}$ is the tectonic effect. $\Delta\zeta_{local}$ is the total effect of local processes including the effect of changes in the tidal regime and elevation of the sediment with respect to tide levels when deposited as well as sediment consolidation since deposition. Post-LGM RSL histories from near-field sites are dominated by the process of GIA, due to the removal of the associated ice load, resulting in a sea-level fall for most of the period following the LGM (Milne et al. 2002). The GIA of previously glaciated sites has been considered by a number of studies through the measurement and interpretation of RSL reconstructions (e.g. Lambeck 1993a; Lambeck 1993b; Mitrovica 1996)

RSL change is well constrained for much of the UK (Shennan et al. 2006a) providing a means of testing GIA model predictions, the ability of which to predict the spatial and temporal patterns of RSL change continues to improve (Shennan et al. 2012). The interaction between GIA and global meltwater influx ('eustatic' sea level) since the culmination of the LGM, has resulted in highly spatially and temporally variable RSL change in Scotland due to magnitude similarities (e.g Shennan et al. 2006b). The elevation of the mid-Holocene highstand, for example, is spatially variable, due to GIA and the deformation of the ocean geoid.

Changes in RSL are preserved by geomorphological features such as raised beaches and wave cut platforms as well as depositional features such as isolation basins and salt marsh sediments. Reconstruction of sea level has followed two main approaches in Scotland. Firstly the geomorphological, based upon the identification of raised shorelines or beaches (e.g. Gray 1974; Dawson 1984; Firth & Haggart 1989). For example, Sissons (1963, 1966, 1967, 1983) applied this methodology to the raised features of Forth Valley and identified two major shorelines; the Main Lateglacial Shoreline and the Main Postglacial Shoreline. The Main Lateglacial Shoreline formed during a period of stability and sea-level lowstand following the rapid Late Glacial RSL fall (11200-10800 yr BP). The Main Postglacial Shoreline, by contrast, formed during the mid-Holocene highstand following the early Holocene transgression (6900-5700 yrs BP). Isobase maps, based on altitude measurements of these features in Scotland, illustrate that the greatest land uplift

occurred in the Grampian Highlands (Smith et al. 2000; 2005; 2006; 2012). The inability to obtain an accurate date from these features is a shortcoming of this approach. The second approach uses microfossils in depositional settings, for example identifying the transition from marine to freshwater conditions in environments such as isolation basins and salt marshes (e.g. Lloyd 2000; Barlow et al. 2014). Combining this proxy-based approach with chronological control, such as radiocarbon dating, enables sea-level index points to be established. Depositional features such as isolation basins have been extensively investigated in north west Scotland due to their preservation above current sea level in a region of isostatic uplift (e.g. Shennan et al. 1994; Shennan et al. 1996; Shennan et al. 2005).

Sea-Level Index Points

Sea-level index points were first developed by Godwin (1940) and refined through IGCP Projects 61 and 200. The concept has been widely employed to show vertical movements in sea level (e.g. Shennan 1982; Tooley 1982; van de Plassche 1986). Validated index points require the following to be defined: location, age, indicative meaning and tendency (Devoy 1982; Shennan 1982; van de Plassche 1986). The indicative meaning is a combination of the reference water level (the elevation of a known and measurable water level with respect to a common datum e.g. mean high water of spring tides (MHWST)) and the indicative range (the vertical range over which the indicator under investigation is found in the modern environment) (Devoy 1982; Heyworth & Kidson 1982; Shennan 1982). Tendency describes the trend in marine influence i.e. a positive tendency corresponds to increasing marine influence (Shennan 1982; van de Plassche 1986). The utility of index points in GIA modelling is reduced if these attributes are poorly defined (Bradley et al. 2011).

Isolation basins and RSL reconstruction

An isolation basin is described as a natural rock depression which has, at some point, been isolated or inundated by the sea due to changes in RSL (Lloyd 2000; Lloyd & Evans 2002). Isolation basins preserve relatively undisturbed fine grained sediment which provides a record of environmental change. They ideally require an impervious rock sill which preserves the deposited sediments and restricts post-isolation alteration (Devoy 1982; Shennan 1982; van de Plassche 1986). Near-shore basins accumulate marine sediments when sea level exceeds the elevation of the sill (t_1 in Figure 2.5.A). As RSL falls, the basin will only be connected to the sea periodically at high tide, resulting in a mixture of freshwater, brackish and marine proxies accumulating in the sediment. Further RSL fall results in isolation of the basin due to the sill being raised above the highest tide therefore freshwater sediment accumulation (t_2 in Figure 2.5.A). Microfossil analysis through these sediment sequences can be used to refine palaeoenvironmental

reconstructions, particularly identifying transitions from freshwater to brackish and marine conditions associated with changes in sea level. Kjemperud (1981; 1986) was the first to illustrate, using diatom analysis, the record of changing environmental conditions, from fully marine to fully freshwater, preserved in an isolation basin in Norway. He demonstrated that three isolation contacts (diatomological, hydrological and sedimentological), documenting the relationship between sediment horizons and the timing of the isolation process, were recorded in the sediment sequence. Isolation basins have been extensively utilised in north west Scotland since the early 1990s to reconstruct post-LGM RSL (e.g. Shennan et al. 1994; Shennan et al. 2000; Shennan et al. 2005) and their successful application in the Morar region has resulted in a 16,000 year RSL record being established for Arisaig (Figure 2.7).
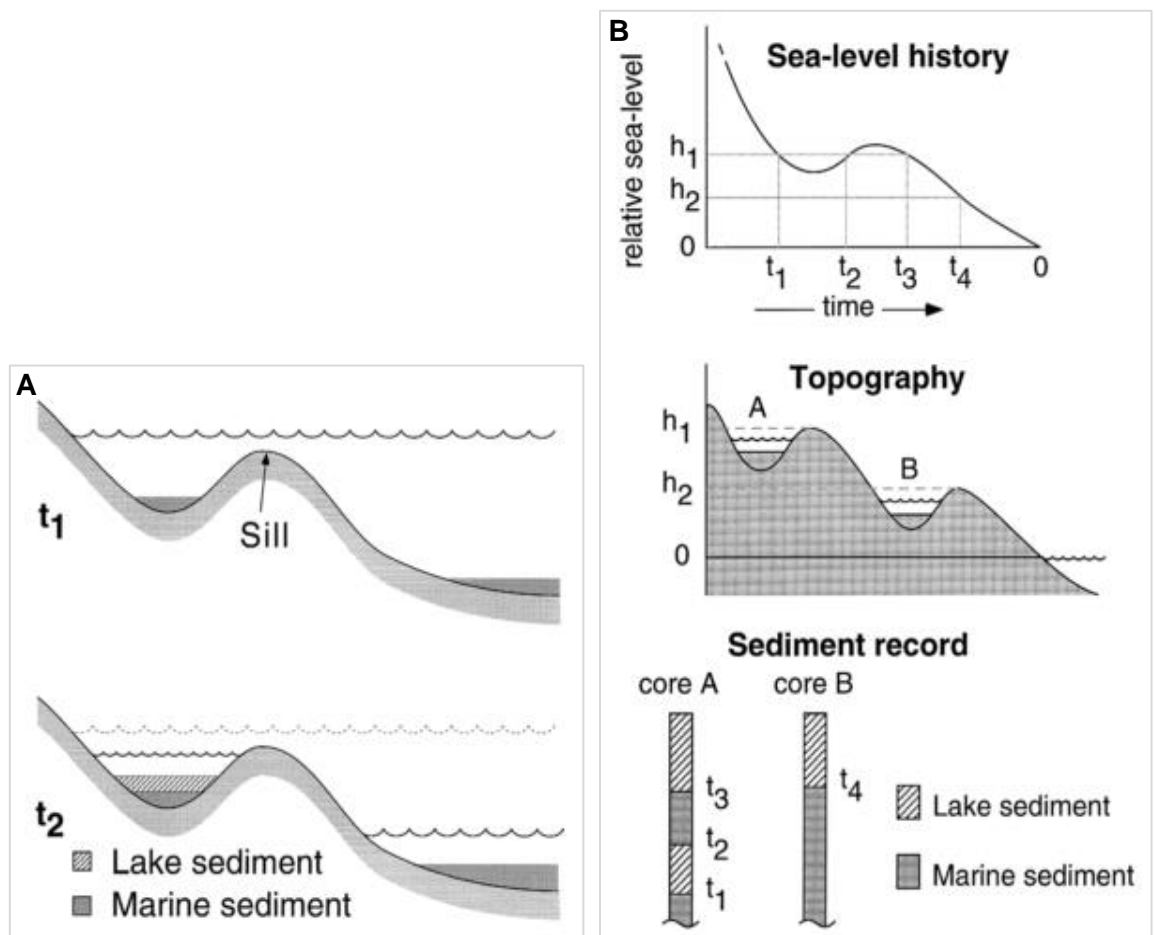
Figure 2.5: (A) Schematic representation of basin isolation during RSL fall and associated sedimentation. At time t_1, marine sediment is deposited when RSL is higher than the sill. At time t_2, RSL has fallen below the elevation of the sill and the basin is isolated, freshwater sediments are deposited in the basin over the older marine sediments. (B) Example of the complex RSL history determined from isolation basins with different sill heights. Dating of each transition in core A and B, corresponding to a point on the RSL curve, constrains the elevations and ages of the RSL highstand and lowstand. Source: Zwartz et al. (1998).

RSL history

Despite the BIIS being small in global terms, the interaction between regional GIA, deformation of the ocean geoid and changes in the global ocean volume, since the LGM, has resulted in a spatially complicated RSL history in Scotland (Figure 2.6) (Flemming 1982; Shennan 1989). Postglacial RSL change in Scotland has been the focus of research for over a century. The RSL record produced for Arisaig, shown in Figure 2.7, is the longest and most complete archive from the British Isles (Shennan et al. 2005; Shennan et al. 1994; Shennan et al. 1996). This data has proved critical in testing and improving geophysical models of GIA (e.g. Bradley et al. 2011).
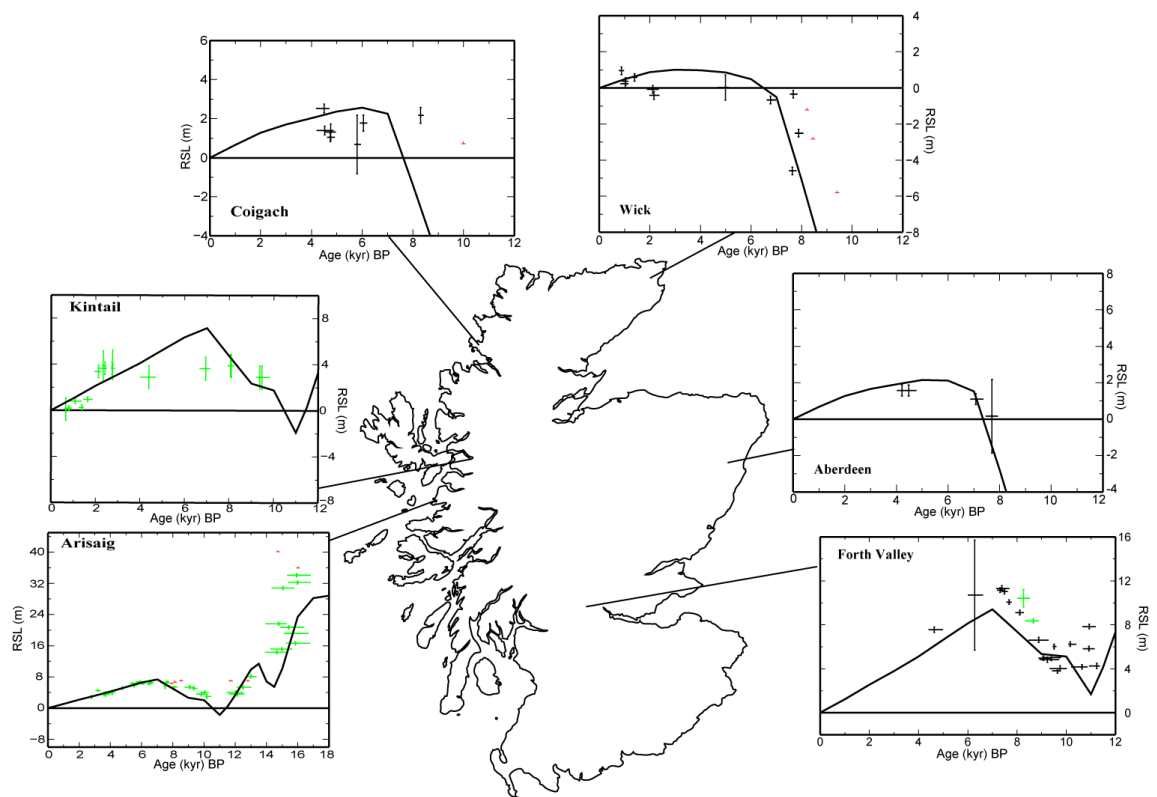
Figure 2.6: Variations in RSL history in Scotland. The proximity of these sites to the centre of uplift, close to Forth Valley, influences the height of the mid-Holocene highstand. For example, a highstand at 6.74 m is recorded at Mointeach Mhor, Arisaig with altitude decreasing northwards. Adapted from Bradley et al. (2011)*.*

RSL reconstructions exist for areas such as Arisaig, Applecross and Kentra however Assynt remains an understudied area of Scotland. Existing sea-level index points in Assynt are confined to Coigach, located 20 km north west of Ullapool. The sea-level index points come from an isolation basin and raised tidal marsh, between Achnahaird and Badentarbet, and utilised a number of microfossil techniques including diatoms, foraminifera and pollen (Shennan et al. 2000). These 8 sea-level index points, shown in

Figure 2.8, are clustered around the mid-Holocene recording a highstand at c. 2.6m above present (Shennan et al. 2000).
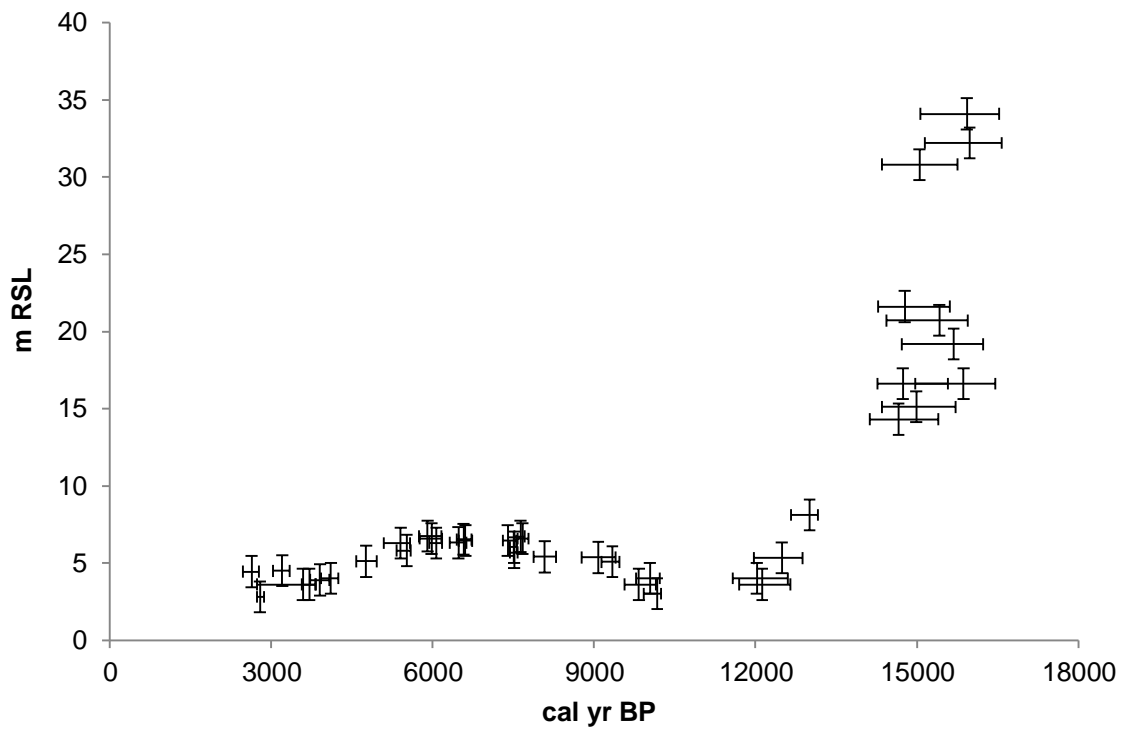
Figure 2.7: The RSL history reconstructed for Arisaig provides one of the most complete records of RSL in the UK from the Late Devensian through to the Holocene. Adapted from Shennan et al. (2005).
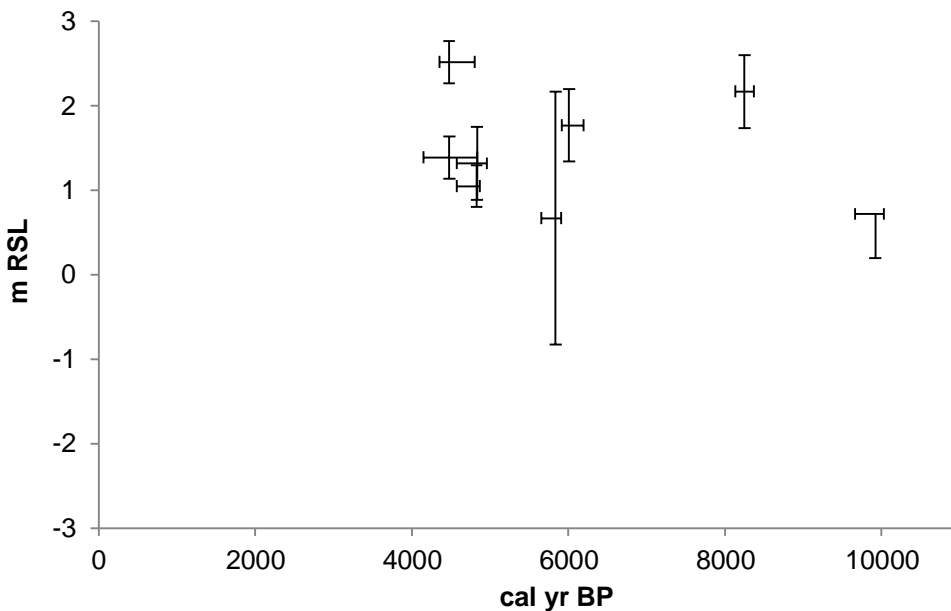
Figure 2.8: Sea-level index points for Coigach. Adapted from Shennan et al. (2000).

2.3 Modelling

Records of past sea-level change enable models of GIA, past ice sheets and RSL to be tested and constrained therefore aiding understanding and improving predictions of future changes (Peltier et al. 1978; Clark et al. 1978). Geophysical models contain 3

components; a model of ice history during the Late Pleistocene; an earth model to replicate the rheology of the solid earth; and a model of sea-level change to determine the redistribution of ocean mass (Farrell & Clark 1976; Lambeck 1993a; Lambeck 1993b; Peltier 1988). Records such as Arisaig (Figure 2.9) (Shennan et al. 2005) provide a strong constraint on GIA models (e.g. Shennan et al. 2006a; Bradley et al. 2011).
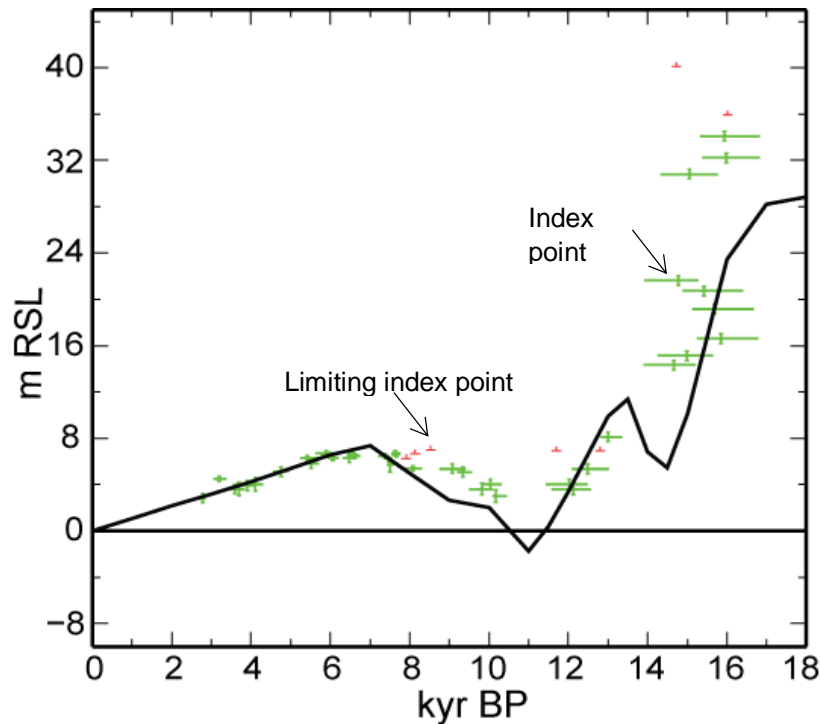
Figure 2.9: Model predictions for Arisaig from Bradley et al. (2011), along with RSL index points from Shennan et al. (2005) demonstrating their ability to test model predictions in this region.

The parameters of GIA models have evolved through time. For example, a range of parameter values for the earth model component have been used to generate predictions of RSL as they are sensitive to variations in shallow earth model parameters, such as lithosphere thickness (Shennan et al. 2000; Shennan et al. 2002). Glacial isostatic rebound in Scotland, in particular, is thought to be extremely sensitive to lithospheric thickness (Peltier et al. 2002). Lambeck (1993a) illustrated this for Edinburgh where RSL predictions for the early Holocene were shown to differ by c. 50 m when lithospheric thickness, ranging between 50 km and 150 km, was investigated. The value associated with this parameter remains uncertain; the conventional thickness was previously identified as 120 km (Peltier 1986) however Lambeck (1995) identified the optimum value to be 65 km in the UK whilst later studies have chosen a higher value of 90 km (Peltier 2002; Shennan et al. 2002; Peltier et al. 2002). This highlights the uncertainty associated with determining parameters which cannot be quantified e.g. mantle viscosity and lithospheric thickness. The Bradley et al. (2011) GIA model determined that the optimal earth model adopted for the British Isles has a 71 km lithosphere thickness, an upper mantle viscosity in the range of 4-6 x 10^{20} Pa s and a lower mantle viscosities ≥ 3 x 10^{22}

Pa s. This is similar to the Shennan et al. (2006a) optimal earth model: lithosphere thickness of 71 km, upper mantle viscosity of 5×10^{20} Pa s and lower mantle viscosity of 3×10^{22} Pa s.

The Bradley et al. (2011) GIA model predictions of RSL for the Assynt region are shown in Figure 2.10. The Bradley et al. (2011) model predicts a mid-Holocene highstand for Coigach similar to that suggested by the RSL data however there is disagreement over the timing of this highstand and its duration (Shennan et al. 2000). RSL data is limited to 4-8 ka yr BP highlighting a need for more RSL data from the deglacial period and early Holocene.
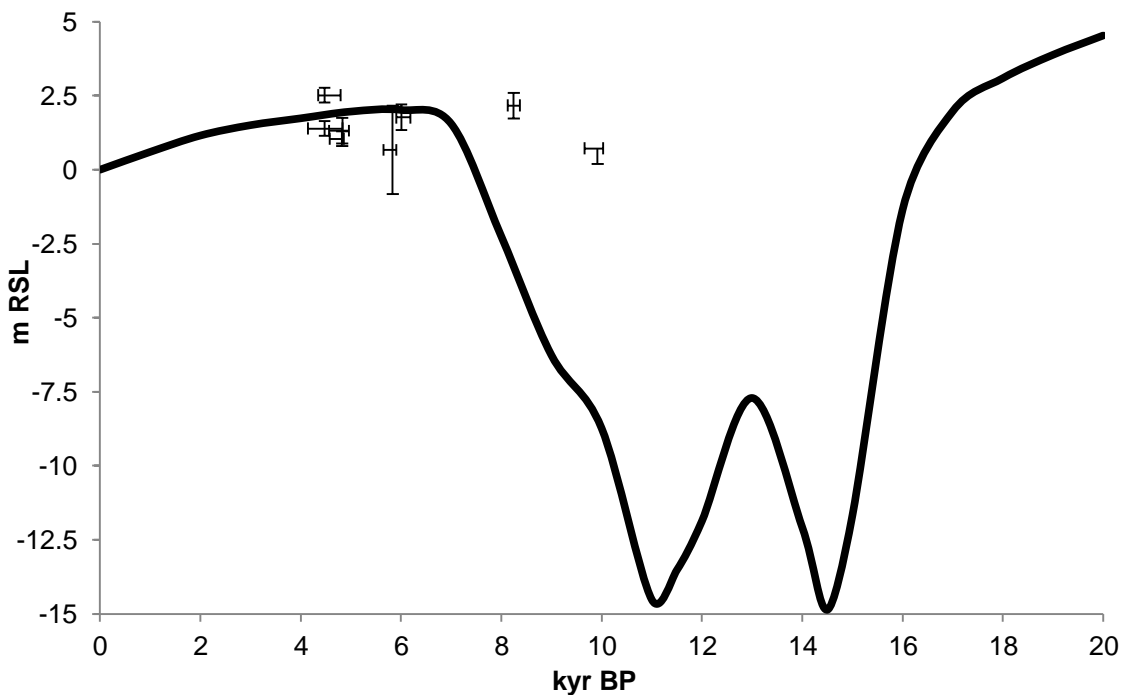
Figure 2.10: Bradley et al. (2011) model predictions for Assynt, including sea-level index points for Coigach (Shennan et al. 2000).

Poor fit between model predictions and sea-level index points, in areas with limited RSL data, in north west Scotland has been attributed to uncertainties associated with the ice model inputs (Shennan et al. 2006a; Bradley et al. 2011; Shennan et al. 2012). For example, depending on the model assumptions, estimates of the maximum ice thickness during the LGM can differ by 25-50% (Lambeck 1995) whilst Shennan et al. (2000) highlighted that previous sea-level inputs had failed to account for the underlying topography when determining the ice thickness. This resulted in an overestimation of ice thickness in areas such as north west Scotland due to similarities in the height of the terrain and the modelled ice (Peltier et al. 2002). Shennan et al. (2006a) demonstrated that applying a terrain correction, to overcome this problem, gave RSL predictions well below RSL data for Arisaig and Forth Valley for both a 71 km and 96 km lithosphere

thickness. Despite these uncertainties, the BIIS is regarded as an accurate test for any ice sheet model due to its dynamism (Peltier 1998; Clark et al. 2012).

Improving the RSL reconstructions in the Assynt region will provide better constraint on model predictions in a region where the RSL record is limited. Further RSL data will enable more vigorous testing of the model components and enhance understanding of the last ice sheet by constraining the Earth's response to mass balance.

Chapter 3: Geographical Location & Study Sites

This chapter provides an overview of the Assynt region, with respect to its geology and landscape, along with an outline of the sites investigated. The field strategies employed, to identify a suitable site for sampling as well as the location and altitude of the rock sill, are introduced. Further details about the methodology used in the field are outlined in Chapter 4 whilst the results of the site surveying, which determined the topography and altitude of the rock sill, are presented in Chapter 5.

3.1 Assynt region

North west Scotland extends from Fort William, in the south, to Cape Wrath, in the north and includes the Isle of Skye and the Outer Hebrides. The Assynt region of north west Scotland stretches from Loch Broom to Eddrachillis Bay and is located north of Ullapool, whilst the population centre is the village of Lochinver (Figure 3.1). Assynt is regarded as a region of classic British geology and contains a number of the oldest rocks in the British Isles. The region has been studied by structural geologists for over a century due to the Moine Thrust Belt (e.g. Peach & Horne 1892; Peach et al. 1913; Lawson 1983), which extends from the Isle of Skye to Loch Eriboll, 27 km north east of Eddrachillis Bay. The glacial history of Assynt, in contrast, has received less attention (e.g. Bradwell 2006; Bradwell et al. 2008; Stoker et al. 2009). Assynts' post-LGM RSL history has been largely under-studied; only the mid-Holocene highstand, for Coigach, has been reconstructed in the region (Shennan et al. 2000). The Assynt region is dominated by the Lewisian Gneiss Complex, which formed during the late Archean, whilst the north west tip of the region is overlain by Torridonian sedimentary rocks (Johnstone & Mykura 1989). The fjord landscape, evident from the coastline of western Scotland, has been sculpted by past glacial cycles resulting in knock-and-lochan topography; the region is dominated by ice-scoured rock outcrop covered by peat (Lawson 1995; Gillen 2003).
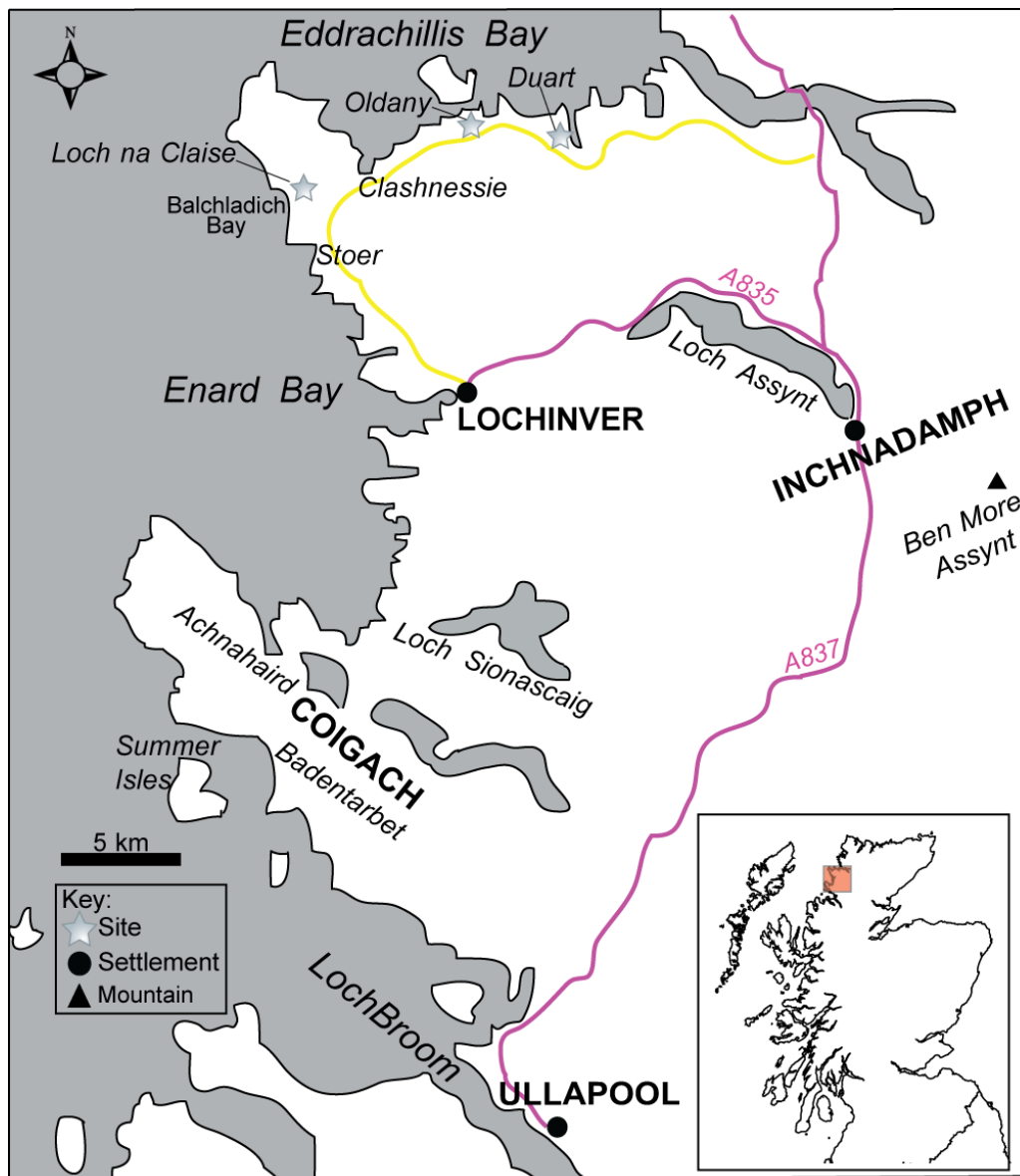
Figure 3.1: Map of the Assynt region showing the locations and features mentioned in the text.

3.2 Study Sites

Potential sites were identified using OS maps and satellite imagery prior to undertaking the fieldwork, from which four were investigated and sampled. The criterion used to determine the ideal sample site is outlined in Chapter 4. The isolation basin sites chosen lie on the north coast of the Assynt region with three of the sites bordering Eddrachillis Bay (Figure 3.1).

Loch na Claise

Loch na Claise is a large freshwater basin, c. 500 x 150 m, on the western coastline of the Assynt region, encircled by steep topography of Torridon Sandstone. The loch, to the east, drains via a channel into Balchladich Bay, through an infilled portion of the basin, to the west. A crannog is located within the loch, several metres from its north east bank. The site can be easily accessed from the road which crosses the drainage channel close

to the present coastline (Figure 3.2). This channel has been straightened and dredged; rock fragments and material line the banks of the channel adjacent to the bridge. Extensive freshwater channels drain into this drainage channel from the surrounding high relief. Initial analysis of the basin morphology led to the identification of two potential sills, one within the drainage channel and the second running parallel to the mouth of the Loch (Figure 3.2). The stratigraphy on the western side of Loch na Claise, on the southern side of the drainage channel, was investigated using a gouge corer. The stratigraphy however consisted of a surface peat underlain by green, brown limus down to bedrock. Further exploration continued on the north side of the drainage channel, in a raised bog. A change in grain-size and colour was noted at the base of the cores investigated in this area. A core for analysis was selected, following the determination of stratigraphy and core depth, using a Russian corer. This sample was in a central location with respect to the bog and the drainage channel. A transect, running south west towards the present coastline, was surveyed within the drainage channel and identified the location and altitude of the rock sill.
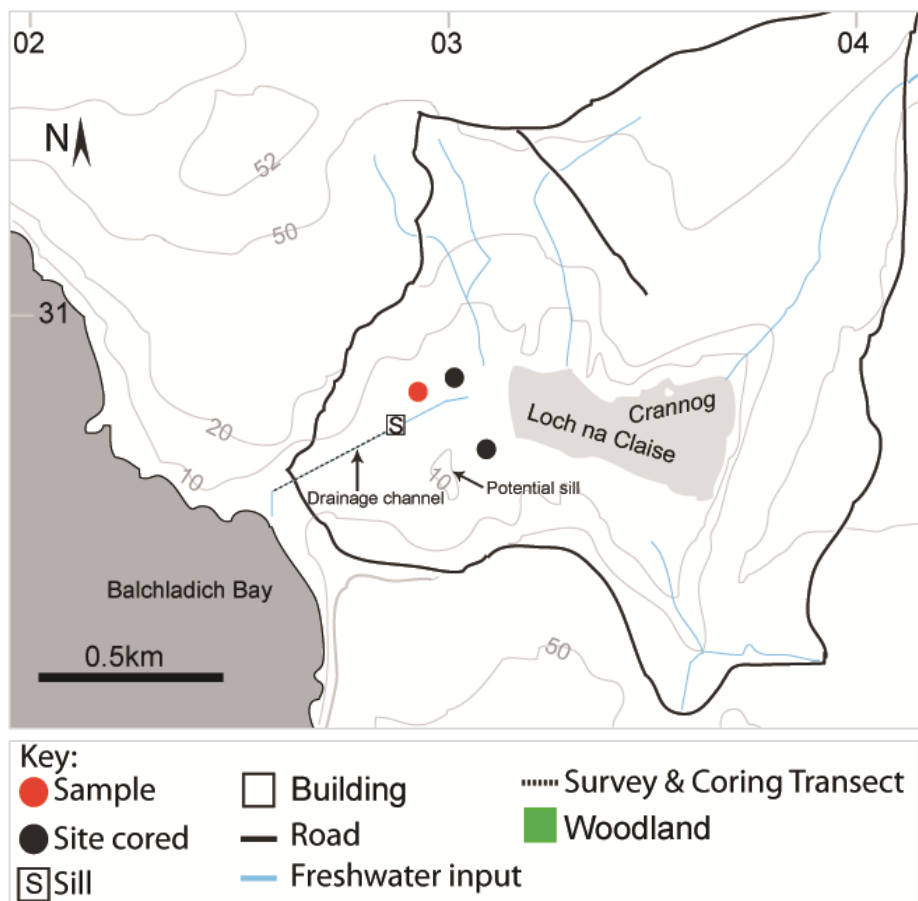
Figure 3.2: Map of the coring locations and surveyed transect at Loch na Claise. The channel draining the loch into Balchladich Bay is marked.

Oldany

Oldany is a very large infilled basin lying just below 10 m OD and sheltered by the surrounding steep topography of Lewisian Gneiss bedrock outcrop. The basin is easily accessed by the road which borders the south eastern margin of the basin, extending north east towards the coastline (Figure 3.3). Initial exploration, using the gouge corer, began on the eastern side of the road, close to the outflow of Oldany River to Lochan na Leobaig, and extended south west towards the basin however the bedrock along this transect was shallow (< 1 m). A transect, extending south west towards the centre of the basin, began close to the intersect between the road and Oldany River. The core depth increased towards the centre of the basin and a sample for analysis was collected near the centre using a Russian corer. A further transect using the gouge corer, within Oldany River, identified the rock sill close to where the road and River intersect.
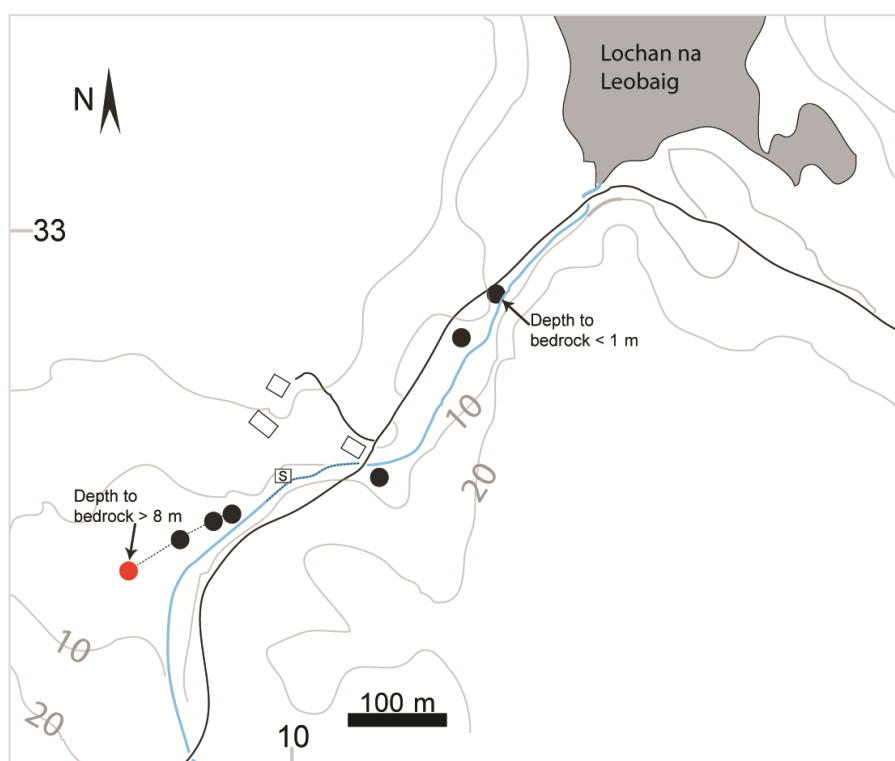
Figure 3.3: Location of the large, infilled basin at Oldany, south west of Lochan na Leobaig (see Figure 3.2 for the key). The map illustrates the number of sites cored to determine the stratigraphy and core depth, extending south west towards this basin. The depth at which the bedrock was reached increased with distance from Lochan na Leobaig.

Duart Bog

Duart Bog is located along the western shoreline of Loch Nedd and is accessible on foot via an off-road path. This low-lying, infilled sediment basin is sheltered by surrounding deciduous woodland with steep topography of Lewisian Gneiss ascending south west of the basin. This site is proximal to Loch Duart Marsh which can be accessed through the woodland encircling Duart Bog (Figure 3.4). A transect, extending from the edge of the

basin, north east, to the present coastline, was cored, using a gouge corer, to identify a representative site near the centre of the basin. The transect identified that the length of the sediment record decreased with proximity to the present coastline, discussed further in Chapter 5. A sample for analysis was collected using a Russian corer, near the south west edge of the basin. The location and altitude of the rock sill was also identified from this coring transect.

Loch Duart Marsh

Loch Duart Marsh is a small, largely infilled basin, c.53 x 23 m with fringing salt marsh, connected to Loch Nedd at high tide by the adjacent tidal basin. A bedrock sill above present, with overlying boulders, separates Loch Duart Marsh, at low tide, from the tidal basin which is also not connected to Loch Nedd during this part of the tidal cycle. The north east and south west edge of the raised marsh, surrounding the infilled basin, was investigated at low tide using a gouge corer. A sample for analysis was collected using a Russian corer from the south west edge of the salt marsh following the determination of stratigraphy and core depth**.** Transects (Figure 3.4), extending north west across the exposed rock sill and north east from the tidal basin to Loch Nedd for example, were surveyed to document the topography of the connection between Loch Nedd, the tidal basin and Loch Duart Marsh.
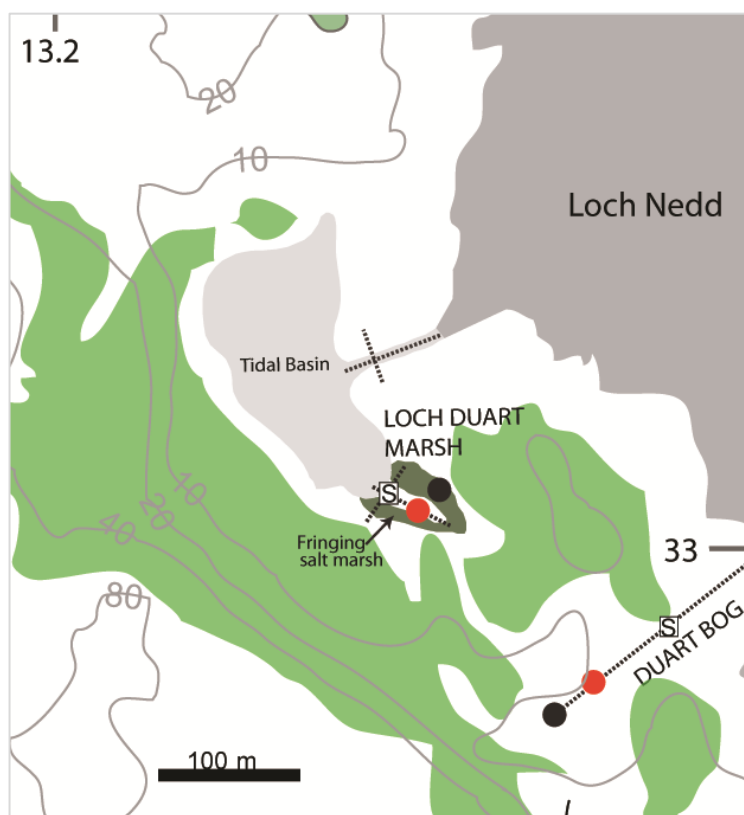
Figure 3.4: Map illustrates the coring locations and survey transects for Duart Bog and Loch Duart Marsh (see Figure 3.2 for the key). Loch Duart Marsh is accessible via the woodland surrounding Duart Bog.

Chapter 4: Methodology

4.1 Field

Fieldwork was carried out between 4th and 8th November 2013. Potential field sites were identified using satellite imagery via google earth prior to undertaking field work. The following criteria were used prior to and during field work to identify the field sites believed to yield suitable locations for coring and determine which cores to collect for further analysis:

1. *Site Elevation*

   The potential field sites identified were at altitudes which would enable critical points in the RSL history to be tested, including the mid-Holocene and Late Glacial highstand. The model predictions for these key points are currently poorly constrained by existing sea-level index points in Assynt (Figure 2.10), particularly for the early Holocene and Late Glacial; this is discussed further in Chapter 2.

2. *Sill determination*

   Isolation basins provide an ideal setting for shifts in environmental conditions to be documented due to the rock sill acting as a 'threshold' which preserves sediment and biota (Lloyd 2000). Determining the elevation of the sill is crucial as it regulates the frequency and proportion of tidal inundation (Zong 1997; Lloyd 2000; Lloyd et al. 2009; Long et al. 2011). The rock sill must be classified as impervious; gravel or sand based barriers allow seawater seepage to percolate, therefore altering the sediments deposited (Lloyd & Evans 2002).

3. *Lake Depth & Size*

   Small, shallow isolation basins produce a better record of RSL change however can suffer from the issue of ice during winter. Deeper lakes may contain older sea water which becomes trapped following isolation (Barland 1991) therefore shallower lakes, subjected to rapid turnover and mixing of water due to wind stress and freshwater input, should be targeted (Snyder et al. 1997). Isolation basins used for the purpose of RSL research tend to be less than 10 m deep and 1 km^2 in size (Long et al. 2011).

4. *Alteration*

   Post-isolation alteration, due to human intervention or natural processes, would lead to the sediment preserved in the basin depression to be disturbed therefore altering the RSL history deciphered. I targeted sites which showed minimal obvious disturbance however Loch na Claise shows this isn't always possible.

5. *Distance between sites*

   Minimising the distance between field sites reduces the effect of differential glacial isostatic uplift between them. Existing sea-level index points in Assynt are located in

Coigach (Shennan et al. 2000); choosing field sites proximal to this area will enable the sea-level index points produced by this research to be combined with existing RSL data.

Determining stratigraphy and identifying sample core

The gouge corer was used to determine changes in the stratigraphic sequence in the basin and identify the location of the deepest core. The stratigraphy was recorded using Troels-Smith classification (Troels-Smith 1955). Locating the deepest core should enable the longest record of environmental change to be identified. Transects were cored between the identified sill and the infilled isolation basin to identify the thickest sequence. Coring strategies focussed on the sediment filled section of the basin due to the difficulty associated with coring using a boat. The position of the core within the basin was considered when identifying a suitable sample core; the centre of the basin is argued to yield a representative record of change (Lloyd 2000).

Once a suitable sample location was determined, a Russian corer was used to retrieve a core for microfossil analysis. Unlike the gouge, the Russian corer contains the sediment within a barrel therefore reducing disturbance. It is best suited to peats and well consolidated limnic sediments and aims to reduce the likelihood of incomplete recovery (Moore & Webb 1978; Glew et al. 2001). A minimum overlap of 5 cm was achieved between cores which were transferred into plastic tubing, wrapped and labelled. Samples were stored in the fridge on return to Durham University.

Identifying the sill

Potential bedrock sill locations were identified upon arrival at the field site based on the morphology of the basin. The sill was buried beneath peat at the well-vegetated field sites (Loch na Claise, Oldany and Duart Bog) therefore requiring stratigraphic investigation using the gouge corer. Coring transects, extending from the sample site to the present coastline, were implemented to identify the rise and fall of the bedrock, representing the impervious sill. The depth at which the bedrock was reached was recorded. The sill at Loch na Claise, as illustrated in Figure 3.2, was located within the main drainage channel which had been dredged and straightened in the upper sections, nearest the present coastline. In this instance, the post-isolation alteration had to be assessed in order to determine if the elevation of the sill had been altered. Due to the dredged material not extending the length of the drainage channel, to the sill location, it was determined that this was not the case.

Surveying

A Sokkia Set 6 Total Station was used to record changes in relief in each basin and the depth of the basins bedrock. Key points at each field site where surveyed including the coring transect, the sample site, the position of the sill and the points investigated to determine the depth of the basin bedrock.

Figure 4.1: Flush bracket 12125 at Clashnessie Bridge, located at 10.343 m OD, used to relate the survey data from each site to the national levelling datum for the UK, Ordnance Datum (Newlyn).

Flush bracket 12125 (NC 0557 3080), located on Clashnessie Bridge on the south side of the road, and the HTM at Clashnessie Beach were surveyed daily to enable the survey data recorded to be related to Ordnance Datum (m OD). The flush bracket benchmark at Clashnessie Bridge was last surveyed in 1976 and is located at 10.343 m OD (Ordnance Survey 2014). This information was used to relate the survey data recorded daily to Ordnance Datum using the relationship between the HTM at Clashnessie and the elevation of the benchmark. Once the HTM at Clashnessie Bridge (Z_1) was corrected to m OD (Y_1), this relationship (X) was used to correct the HTM at the field site to m OD as follows:

$$Z_2 - Z_1 = X$$
$$Y_2 - X = Y_1$$

(Equation 4.1)

where Z_1 is the elevation of the HTM at Clashnessie Bridge (metres), Z_2 the elevation of Clashnessie Flush Bracket (metres) and X is the relationship between the HTM and Flush

Bracket at Clashnessie. Y_2 is the elevation of Clashnessie Flush Bracket (m OD) and Y_1 is the elevation of HTM at Clashnessie Bridge (m OD).

4.2 Laboratory

Combining lithostratigraphy with biological indicators is regarded as an advantageous approach to reconstructing RSL. Lithostratigraphy alone fails to reliably differentiate between freshwater and marine environments (Devoy 1979; Zong & Horton 1999; Murray-Wallace & Woodroffe 2014). A combined litho- and bio-stratigraphic approach, such as that adopted in this study, is more favourable than the morphological approach, adopted by Sissons (1963; 1966; 1967; 1983) and Smith (2000; 2005; 2006; 2012) for example. The shift from marine to terrestrial environments can be determined using the combined approach, enabling the indicative meaning, a requisite for sea-level index points, to be precisely defined. Another advantage is that it allows a larger number of index points, at different altitudes, in close geographical proximity, to be produced therefore generating a well constrained RSL curve from a small geographical area, for example Arisaig (Figure 2.7).

Diatoms

A range of biological indicators, including pollen, diatoms, foraminifera and thecamoebians, have been utilised to reconstruct palaeoenvironments and infer changes in RSL. Diatoms, however, are regarded as an excellent means for accurately identifying the ingression or isolation contacts (Vos & De Wolf 1988; 1993). Diatoms can be used to characterise marine, brackish-water and freshwater phases of the isolation process and are relatively resistant to post-burial alteration (Palmer & Abbott 1986; Denys & De Wolf 1999). These advantageous characteristics along with important methodological advances during the 1980s establishing sea-level index points (Shennan 1982; Tooley 1982; van de Plassche 1986) resulted in diatoms being extensively used for isolation basin-based reconstructions to determine the indicative meaning (Kjemperud 1981; Kaland et al. 1984; Shennan et al. 1994)

Research since the beginning of the 20th century has improved understanding of the relationship between diatom taxa and variables controlling assemblage distribution; salinity was identified as the strongest environmental factor influencing distribution (e.g. Kolbe 1927; Hustedt 1937). This led to diatoms being widely used at the boundary between freshwater and marine environments to determine lake isolation in regions influenced by land uplift (Halden 1929; Fromm 1938; Kjemperud 1981). Earliest application of diatoms to investigate land uplift, shoreline displacement and lake isolation occurred in Scandinavia (Cleve-Euler 1923; Cleve-Euler 1944); Florin (1946) produced a clear and detailed record of the transition from marine to freshwater diatoms in sediments from Myskasjon.

Diatoms have been successfully utilised to reconstruct post-LGM RSL change in north west Scotland, particularly in isolation basins, for locations such as Arisaig, Kentra, Kintail and Applecross (Shennan et al. 1995a; Shennan et al. 1995b; Shennan et al. 1996a; Shennan et al. 1996b; Dawson et al. 1998; Shennan 1999; Selby et al. 2000; Shennan et al. 2000; Shennan et al. 2005; Shennan et al. 2006b). Diatoms were first used in the Assynt region to reconstruct the palaeoenvironment in which lakes and the surrounding catchments were formed (Pennington et al. 1972; Pennington & Sackin 1975; Haworth 1976). Work by Pennington et al. (1972) in Loch Sionascaig, Coigach, provided the first complete, continuous profile of changes in diatom assemblages in northern Scotland.

Despite extensive evidence to support the strong control of salinity on diatom distribution a range of variables, including nutrient content, water temperature, pH and substrate type, also influence distribution (Vos & De Wolf 1993; Sullivan & Currin 2000). Research undertaken in Kentra Moss, for example, highlighted that acidic runoff from a raised bog led to *Eunotia valida*, an acidophilous taxa, being dominant (Zong & Horton 1999). This highlights the importance of ensuring that the relationship between diatom distribution and ecological variables extends beyond salinity. Substrate preference and the primary life form of diatom taxa have also been identified as particularly important when determining diatom assemblage distribution (Vos & De Wolf 1988; Nelson & Kashima 1993). Investigating the relationship between substrate type and diatom taxa has led to an abundance of epipelic diatoms being associated with fine grained sediments whilst episammic taxa have been correlated with sandy substrate (Nelson & Kashima 1993; Zong 1997; Zong & Horton 1998; Zong & Horton 1999). The shift in diatom taxa, from *Paralia sulcata* to *Fragilaria spp.*, has been identified throughout Scottish late Quaternary sediments and associated with a gradual decrease in marine influence (Zong 1997; Selby et al. 2000). Selby et al. (2000) state that this transition cannot be solely explained by salinity and that the importance of organic matter, substrate type and water depth needs to be accounted for. Particle size and organic content were therefore analysed to characterise the substrate. Boomer et al. (2012) illustrated that combining these methods can also yield information regarding deglaciation; coarse material present in sediments from Loch Assynt indicated glacial outwash and supported Bradwell et al. (2008) hypothesis that glaciers were present throughout the Late Glacial period.

Diatom preparation followed the standard method summarised by Palmer & Abbott (1986) and Battarbee (1986). An alternative methodology, designed by Scherer (1994) to determine the absolute abundances of diatoms, was used at the base of the Loch Duart Marsh core due to poor diatom preservation and a high clay content. This settling method produces slides with an even distribution of valves with minimal clumping therefore overcoming the problems associated with the base of the Loch Duart Marsh core (E.

Maddison, personal communication 2014). The detailed methodologies for diatom preparation, as well as the other laboratory methods outlined in this chapter, are presented in full in Appendix 1. Sample resolution was led by the stratigraphic record; transitions of initial interest were investigated at a high resolution of 4 cm to 8 cm whilst low resolution samples, taken every approximately 32 cm, filled in the gaps in diatom analysis. A minimum of 250 diatoms were counted per slide to obtain a statistically robust assemblage. Diatoms were counted systematically in a vertical transverse to avoid multiple counts of the same valves.

Diatoms were identified using Hartley et al. (1996) whilst their salinity preferences were determined using Haworth (1976), Robinson (1982) and Hustedt (1953) following which they were characterised using the halobian classification scheme, outlined in Table 4.1. This classification scheme was first outlined by Kolbe (1927) and later modified by Hustedt (1953) and Hemphill-Haley (1993). These specific habit tolerances of diatoms (Table 4.1) enables the marine, brackish and freshwater phases of basin isolation (Figure 4.2) to be determined therefore enabling the isolation contact to be precisely identified. C2 was used to illustrate changes in the counted diatom assemblages, and their salinity preferences, throughout the collected sediment cores (Juggins 2003). Diatom assemblages have been divided into local diatom assemblage zones, based on stratigraphically constrained cluster analysis, using the constrained incremental sums of squares (CONISS) program in Tilia (Grimm 1987).

Table 4.1: The halobian classification scheme of diatoms (Hustedt 1953).

Classification	Salinity range (‰)	Description
Polyhalobous	>30	Marine
Mesohalobous	0.2-30	Brackish
Oligohalobous-halophile	<0.2	Freshwater- stimulated at low salinity
Oligohalobous-indifferent	<0.2	Freshwater-tolerates low salinity
Halophobous	0	Salt-intolerant
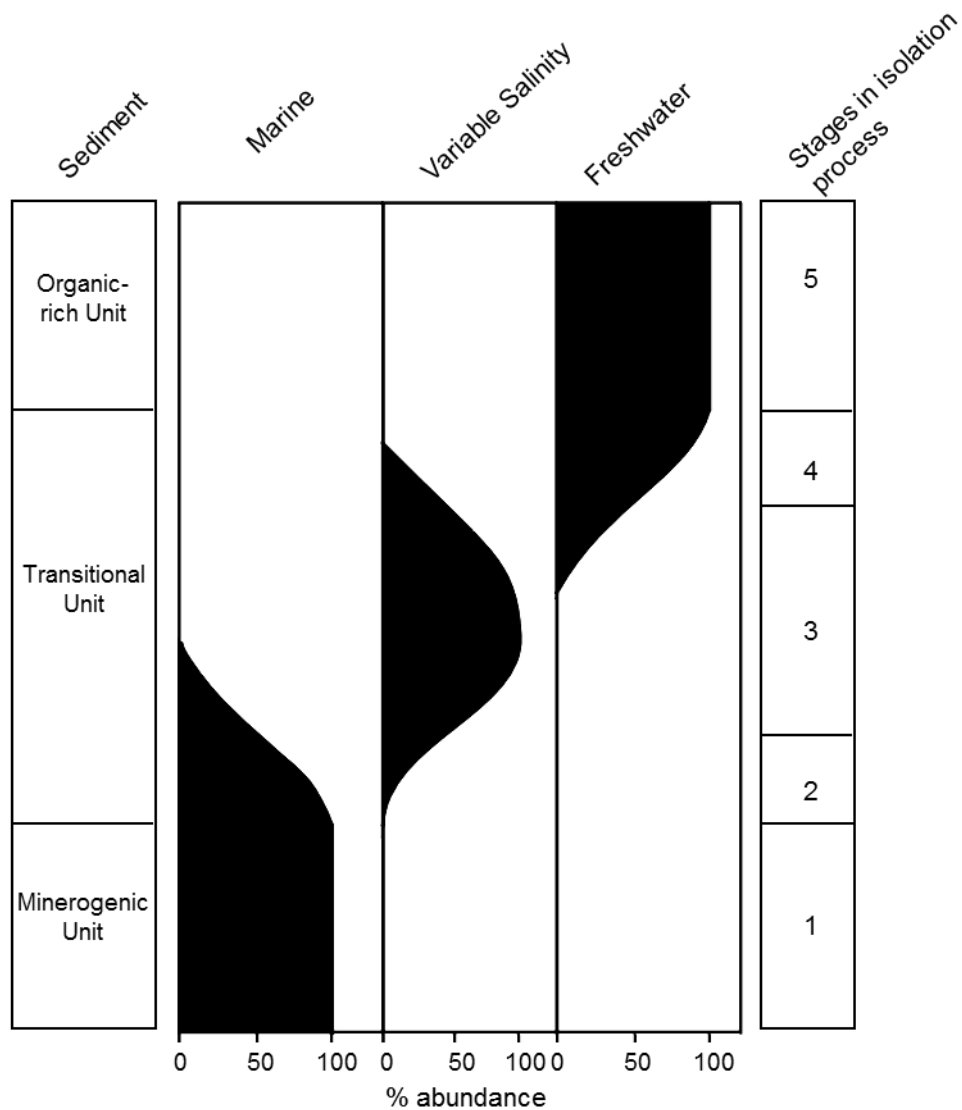
Figure 4.2: A conceptual model of the change in diatom assemblage during a RSL fall resulting in the isolation of the basin. The left column presents typical sediment types deposited during an isolation process. The right column relates to stages of the isolation process. During stage 1 the basin is inundated throughout the tidal cycle and is marine whilst by stage 5 the basin is isolated and a freshwater lake (Lloyd & Evans 2002). Adapted from Laidler (2002).

Pollen

Pollen analysis reconstructs vegetation using the pollen grains preserved in geological deposits (Faegri & Iversen 1989). This enables climatic change to be deduced due to the response of plants to Quaternary climatic shifts. Qualitative pollen analysis (J. Innes, personal communication 2014) generated a 'skeleton of radiocarbon dates'(Moore & Webb 1978), providing an overview of the relative age of the isolation and ingression contacts identified from diatom analysis. Pollen preparation followed the standard methodology outlined by Moore et al. (1991).

Particle-size Analysis

Sedimentary properties, such as particle-size and organic content, are diagnostic of the nature of the environment in which sediments were deposited (Veres 2002). The concentration of the sand, silt and clay fractions in the cores is indicative of the energy required for deposition (Briggs & Smithson 1987; Pye 1994). The dominance of sand particles will be indicative of a low energy environment as the velocity is not large enough to maintain the particles in suspension (Hjulstrom 1939).

Particle-size analysis for samples from Loch na Claise, Duart Bog and Loch Duart Marsh was carried out by Thomas (2014) and Dias (2014) using a Malvern Mastersizer 3000 at the University of Bristol whilst samples from Oldany were analysed using a Coulter Granulometer at Durham University. The full methodology is presented in Appendix 1 along with the hydrogen peroxide digestion method used to remove the aggregating effects of organic material (Kunze & Dixon 1987). The results were categorised into the percentage sand, silt and clay fraction for each sample using the Wentworth Scale (Wentworth 1922).

Organic Content

Organic matter is an important component of lake sediments which represents a range of outputs produced by organisms living within the lake and the surrounding catchment (Meyers & Teranes 2001). Organic matter originates from biota present in the past and the quantity and type present is an indication of the environmental conditions when the sediment was deposited; enabling changes in the local and regional ecosystems to be deciphered (Meyers & Teranes 2001).

Organic matter was determined using a loss on ignition method. The results for Loch na Claise, Duart Bog and Loch Duart Marsh were generated by Dias (2014) and Thomas (2014) at the University of Bristol. Despite being regarded as a crude indication of organic matter, loss on ignition is a good method if care is taken and the thermal properties of the material investigated are understood (Ball 1964; Boyle 2004). Samples taken from each of the cores were placed in a muffle furnace at 850°C for 30 minutes. The temperature used for this method however is important and debated; 850°C for 30 minutes or 375°C for 16 hours are commonly used (Keeling 1962; Ball 1964; Heiri et al. 2001). Hamilton (2013) compared the results generated by these two temperatures using sediment cores collected from Stoer, located less than 3 km south of Loch na Claise. The results produced using these temperatures were comparable however it highlighted that care must be taken when the sediment is composed of >60 % clay (Ball 1964; Dean 1974; Hamilton 2013). This variation in results produced by each temperature was likely due to the loss of structural

water from clay at the higher temperature (Ball 1964; Dean 1974). Dean (1974), however, noted that organic material is not completely ignited until 500°C.

4.3 Radiocarbon Dating

Radiocarbon chronology is based on AMS ^{14}C dating of bulk sediment samples taken from the organic unit adjacent to the isolation or ingression identified from the diatom assemblages. Bulk sediment samples are regarded as less reliable than a chronology based on plant macrofossils, due to the potential for non-representative sample ages. Older ages can result, for example, from the input of reworked sediment by physical processes, resulting in contamination by carbon from an older source, whilst differences in the ^{14}C residence times between the atmosphere and freshwater and marine reservoirs can also result in an age offset (Olsson 1991; Lowe & Walker 1997; Bjorck & Wohlfarth 2002; Ascough et al. 2011). Younger ages can result from the downward reworking of humic acids or rootlets (Balesdent 1987) whilst poor refrigeration can result in microbial growth and contamination with modern carbon (Colman et al. 1996). Utilising AMS dating methods for bulk sediments is however an improvement on conventional radiocarbon dating. Shennan et al. (2000) compared conventional and AMS radiocarbon dating methods for sites in Arisaig, Kentra and Applecross in north west Scotland, and illustrated that AMS methods resulted in slightly older ages for the sea-level index points due to the higher precision achieved by this method (Beta Analytic 2014). Research undertaken by Shennan et al. (2000) indicated that the impact of the marine reservoir effect in environments such as isolation basins is potentially minimal due to mixing. This was illustrated by an AMS ^{14}C date from bulk sediment (8178-7942 cal yr BP) and one from calcareous foraminifera (8175-7976 cal yr BP) producing nearly identical ages from the same Loch nan Corr sample (Lloyd 2000; Shennan et al. 2000). Another explanation for these similar ages however is the offset of the marine reservoir effect by the input of old carbon to the bulk sediment (Shennan et al. 2000; Shennan et al. 2006b). In contrast, comparison of AMS ^{14}C ages of paired samples from bulk peat and macrofossils, taken from salt marsh setting in Girdwood, Alaska, show significant discrepancies attributed to sediment reworking (Shennan et al. 2008). Qualitative pollen analysis (J. Innes, personal communication 2014) provided an estimated age for each dated contact from Duart Bog and Loch Duart Marsh. Comparison between this data and the AMS radiocarbon dates will enable erroneous ages to be identified.

The radiocarbon measurements produced by the ^{14}C CHRONO Centre for Climate, the Environment, and Chronology and Beta Analytic were calibrated using CALIB REV7.0 (Reimer et al. 2013) to account for variations in atmospheric carbon. This program produces a 1-sigma and 2-sigma calibrated age estimation and potential range for each

radiocarbon point. The radiocarbon dates are presented in Chapter 5 whilst additional information is outlined in Appendix 5.

Chapter 5: Results and Interpretation

This chapter presents the results for each site split into 5 sections; site survey, lithostratigraphy, biostratigraphy, chronology and finally a palaeoenvironmental interpretation. Site topography has been reconstructed, allowing the rock sill, regarded as the threshold of the isolation basin, to be identified. Core transects have been taken to investigate stratigraphy and the topography of the sites, including the rock sill. Determining the diatom assemblage for each sampled core allowed changes from freshwater to marine conditions to be documented, and therefore identification of isolation or ingression contacts. The diatom assemblages are supported by qualitative pollen analysis, to provide an estimated age. Detailed lithological analysis is provided by particle size and organic content analysis. Combining this multi-proxy approach enables a reconstruction of the palaeoenvironment to be built.

5.1 Loch na Claise

Loch na Claise is a large basin, comprising of a freshwater loch to the east, draining into Balchladich Bay, and an infilled portion to the west, nearer the present coastline (Figure 3.2). The Loch na Claise freshwater basin drains to the present coastline through a channel which has been subject to some realignment to improve drainage.

Site Survey

The topography and altitude of the rock sill was determined by surveying a transect along the channel, draining the Loch na Claise basin, from the present day beach (Figure 5.1). The altitude of the channel bedrock remained at c. 3 m for a distance of 200 m from the bridge (Figure 5.1.B), following which the bedrock reached a peak altitude at 3.50 m OD and decreased sharply towards the basin. The rock sill is 1.2 m above MHWST whilst the ground surface of the sampled core (4.1 m OD) is 0.6 m above the rock sill.
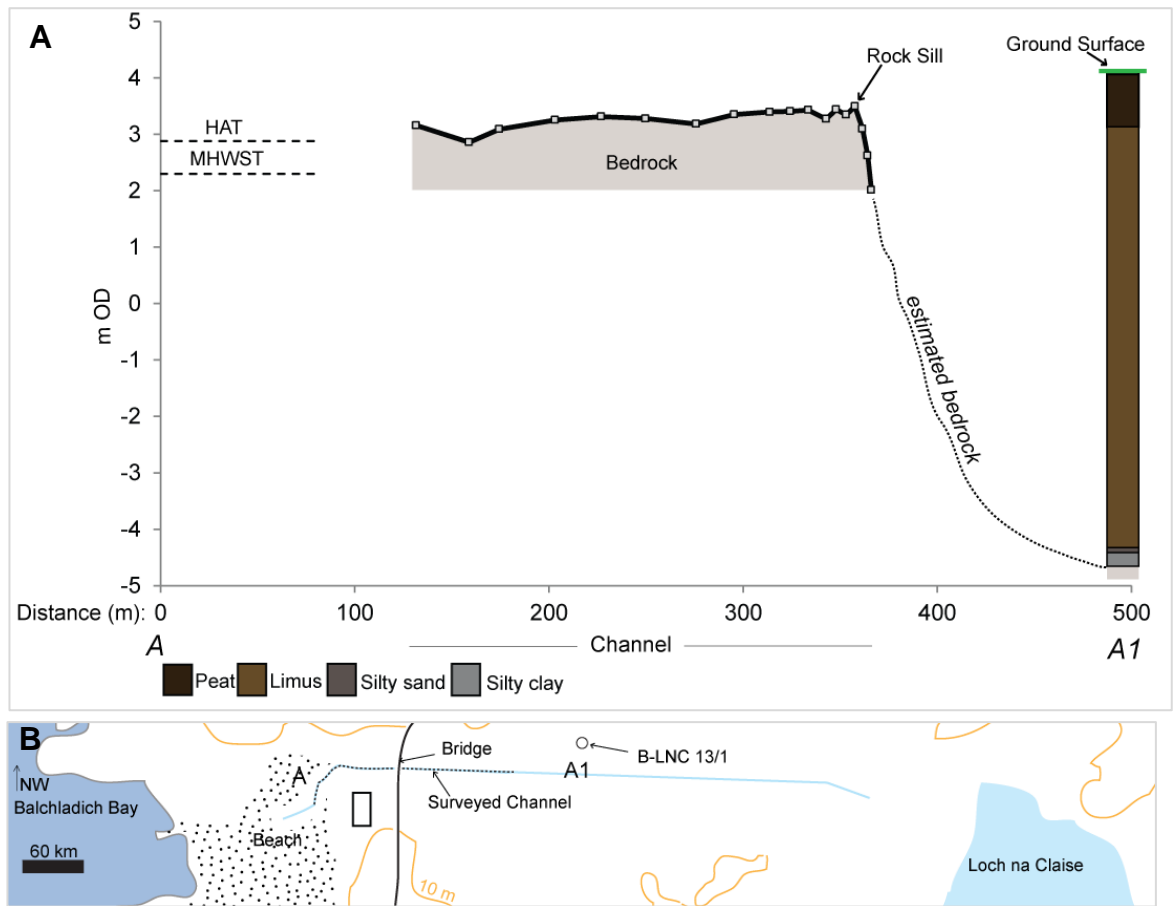
Figure 5.1: (A) Survey data for Loch na Claise illustrating the location and altitude (3.50 m OD) of the rock sill and the stratigraphy of the sampled core along with the upper sediment unit, which was not sampled. (B) Location of the transect, A to A1, in the context of the Loch na Claise basin.

Lithostratigraphy

The core sampled for analysis was collected from near the centre of the infilled portion of Loch na Claise (Figure 3.2). The up-core stratigraphy consists of 4 sediment units (Figure 5.2): silty clay (874 cm to 850 cm) overlain by a thin silty sand unit (850 cm to 845 cm) followed by limus (850 cm to 100 cm) and an upper peat unit (Figure 5.1). The section sampled for further analysis, 500 cm to 874 cm, does not include the overlying sediment units due to the homogeneity of the stratigraphy (Figure 5.1).

Samples for particle size analysis were taken at 8 cm intervals, with the sample resolution increasing to 4 cm intervals by 825 cm and 1 cm between 844 cm and 853 cm and at the base (n = 67 samples) (Dias 2014). The sample resolution increased with depth in accordance with changes in pollen flora (844 cm to 848 cm) and stratigraphy (845 cm to 874 cm).

Figure 5.2: Stratigraphy, particle size and loss on ignition results for the sampled core from Loch na Claise. Clay, silt and sand fractions are defined by Wentworth (1922). Particle size and loss on ignition results were generated at the University of Bristol by Dias (2014).

The lower section of this core (874 cm to 844 cm) is dominated by silt, which exceeds 70%, whilst the clay content reaches 20 %. A sharp transition occurs for each fraction between 849 cm and 844 cm, most notably the sand content increases by 60 % across this 5 cm transition. The upper section (844 cm to 500 cm) is dominated by silt and sand with limited clay content. Within the upper part of the core there are sections where silt is dominant, exceeding 50 % of the total fraction analysed, (e.g. 820 cm to 680 cm) and sections where sand is more dominant (e.g. 840 cm to 800 cm).

A total of 58 samples were analysed to determine changes in the percentage loss on ignition, as an indicator of trends in organic content (Figure 5.2) (Dias 2014). Organic content increases from a low of 3 % at 873 cm to 20 % at 857 cm. A rapid increase, from 10 % to 28 % organic content, occurs between 849 cm and 844 cm. Loss on ignition is constant throughout the upper section (844 cm to 500 cm) however a major fluctuation occurs at 591 cm with an increase of up to 42 % organic content.

Biostratigraphy

A total of 24 samples were analysed for diatoms with 224 species identified (all raw counts are presented in Appendix 2). Three zones can be identified based on stratigraphically constrained cluster analysis of the diatom flora (Figure 5.3), using CONISS (Grimm 1987). Efforts were made to classify the diatom species identified according to the halobian classification scheme. This however was not possible for all species due to limited spatial distribution of salinity measurements. These diatom species were identified as habiting freshwater environments however are categorised as 'unclassified' for each site, as shown in Figure 5.3.

Zone 1 (874 cm to 870.5 cm) is dominated by *Diploneis elliptica* and other freshwater species, but also contains a small peak of *Cocconeis scutellum* (4 %), a polyhalobous species, at 871 cm. Freshwater conditions remain dominant throughout with salt-intolerant species, such as *Tabellaria flocculosa*, representing less than 8% of the total count at the base of the core. Oligohalobian-indifferent species remain dominate in zone 2 (870.5 cm to 832 cm). *Fragilaria construens* exceeds 80 % of the total count at 869 cm however declines gradually throughout zone 2, reaching 14 % of the total count by 848 cm. In contrast, *Staurosirella pinnata* increases gradually from 3 % to 71 % in this zone. In zone 3 (832 cm to 500 cm) *Fragilaria construens* and *Staurosirella pinnata* account for minimal proportions of the total count whilst other freshwater species, such as *Fragilariforma virescens*, reach 20 % of the total count. Salt-intolerant species, such as *Tabellaria flocculosa*, increase to 10 % of the total count in this zone.
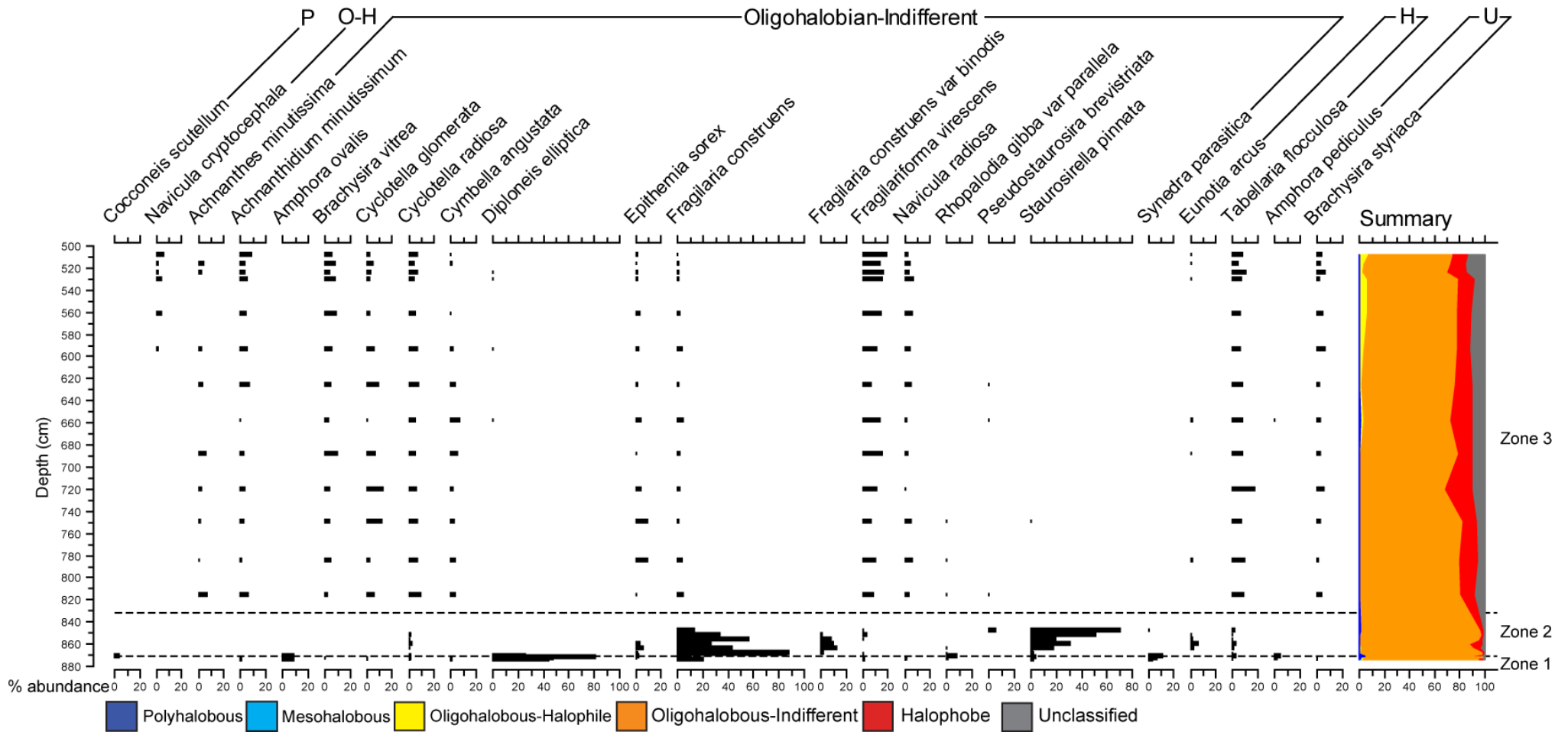
Figure 5.3: Diatom assemblage for Loch na Claise; flora shown exceed 5 % of the total valves counted, whilst Cocconeis scutellum is mentioned in the text. Diatoms are grouped by halobian classification (Hustedt 1953).

Chronology

Pollen flora were qualitatively analysed at 844 cm, 846 cm and 848 cm (J. Innes, personal communication 2014). Flora, such as *Juniperus* (juniper), *Empetrum* (crowberry) and a range of tundra herbs, indicating Late Glacial age were found at 846 cm and 848 cm. In contrast, at 844 cm, flora such as *Ulmus* (elm), *Tilia* (lime), *Corylus* (hazel), *Calluna* (heather) and *Pteridium* (bracken), indicating late Holocene age were found. The difference in taxa over 2 cm raises concern of a hiatus at the base of this core.

Palaeoenvironmental Interpretation

Oligohalobian-indifferent and halophobous species dominate the diatom flora indicating that freshwater conditions occur throughout with evidence for a minor marine-brackish influence towards the base of the core at 871 cm. These results indicate that the Loch na Claise basin was not inundated by the sea following deglaciation. The record produced however is confined to the Late Glacial and late Holocene periods due to the sediment hiatus (marked in Figure 5.4) identified from the pollen flora and supported by particle size analysis and loss on ignition. The hiatus explains the sharp increase in the clay and silt fractions as well as the sharp decline in organic content between 849 cm and 844 cm. Particle size analysis and loss on ignition data indicate that the sediment below 848 cm and that above represent very different environments; a freshwater environment lacking in organic material (874 cm to 844 cm) in comparison to one which is organic rich (844 cm to 500 cm), therefore supporting the interpretation of a hiatus. This sharp transition, however, is not evident from the diatom assemblage.

Figure 5.4: Summary diagram of results produced for Loch na Claise. Lithostratigraphy and diatom summary (see Figure 5.3 for key to halobian classification illustrated) are presented whilst the estimated age is based on pollen flora discussed above. The point marked 'hiatus', within zone 2, is discussed in the 'Palaeoenvironmental Interpretation' and is identified from the pollen flora and supported by the lithostratigraphy.

5.2 Oldany

Oldany is a large, sheltered infilled basin lying just below 10 m OD and located inland of the present coastline (Figure 3.3). The coring transect (Figure 5.5) began on the periphery of the basin and finished towards the centre, where the sampled core (core 4 identified in Figure 5.5) was taken.

Site Survey

The topography and altitude of the rock sill was identified by coring transects within the stream and the infilled sediment basin (Figure 5.5.B). Further coring along the stream, which runs parallel to the sediment basin, enabled the altitude and location of the rock sill to be identified at 8.10 m OD (Figure 5.5), c. 6 m above MHWST. Bedrock was reached at the base of cores 1 to 4 (Figure 5.5), demonstrating deepening with proximity to the centre of the basin.
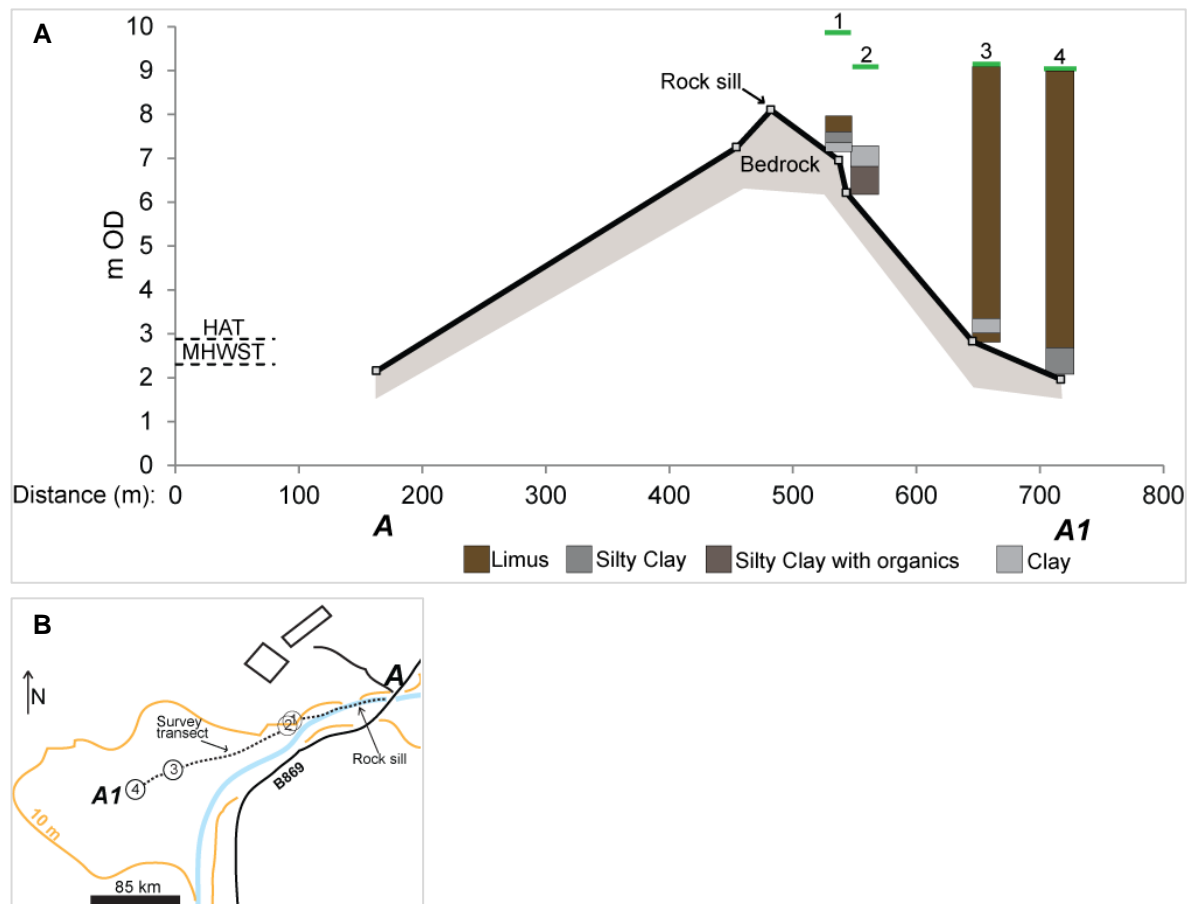
Figure 5.5: (A) The location, topography and altitude of the rock sill was determined from a transect within the stream and the infilled sediment basin. (B) The dashed line illustrates the transect investigated to determine the location and elevation of the sill at this basin.

Lithostratigraphy

The sampled core (core 4) is divided into two sediment units: a silty clay unit (720 cm to 650 cm) and an organic unit (650 cm to 605 cm). The sampled core, 605 cm to 712 cm, does not include the overlying 6 m due to the homogeneity of the stratigraphy (Figure 5.5).

Particle size was analysed in 7 samples taken from this core (Figure 5.6). The percentage clay fraction increases gradually from the base, peaking at 50 % (694 cm), following which it decreases to 7 % by 614 cm whilst the silt fraction remains constant following a sharp increase until 687 cm (73 %). The percentage sand remains below 20 % and almost constant throughout the core.

Loss on ignition was investigated at the same resolution as particle size. The organic content increases from 4 % (710 cm) to 45 % (614 cm), with a sharper increase in rate at 662 cm, as shown in Figure 5.6.

Biostratigraphy

A total of 7 samples were analysed and 88 diatom species identified from core 4 (Figure 5.7). The diatom assemblage is dominated by oligohalobian-indifferent species whilst halophobous species are also present. Stratigraphically constrained cluster analysis of the diatom flora led to the identification of 3 zones (Grimm 1987).

Zone 1 (712 cm to 686 cm) is dominated by oligohalobian-indifferent flora, particularly *Fragilaria construens* which exceeds 40 % of the total count, whilst halophobous species such as *Tabellaria flocculosa* are also present. Zone 2 (686 cm to 649 cm) is still dominated by oligohalobian-indifferent species whilst salt-intolerant species, such as *Tabellaria flocculosa*, remain. In contrast to zone 1, *Brachysira vitrea* and *Cyclotella glomerata* dominate the assemblage, each reaching 30 % of the total count in zone 2. Zone 3 (649 cm to 605 cm) contains *Brachysira vitrea* and *Cyclotella glomerata* whilst *Fragilariforma virescens* increases to 26 % of the total count.

Chronology

Due to the absence of marine influence in this core, and therefore its limited value for constraining the elevation of past sea level, pollen analysis was not done on this core.
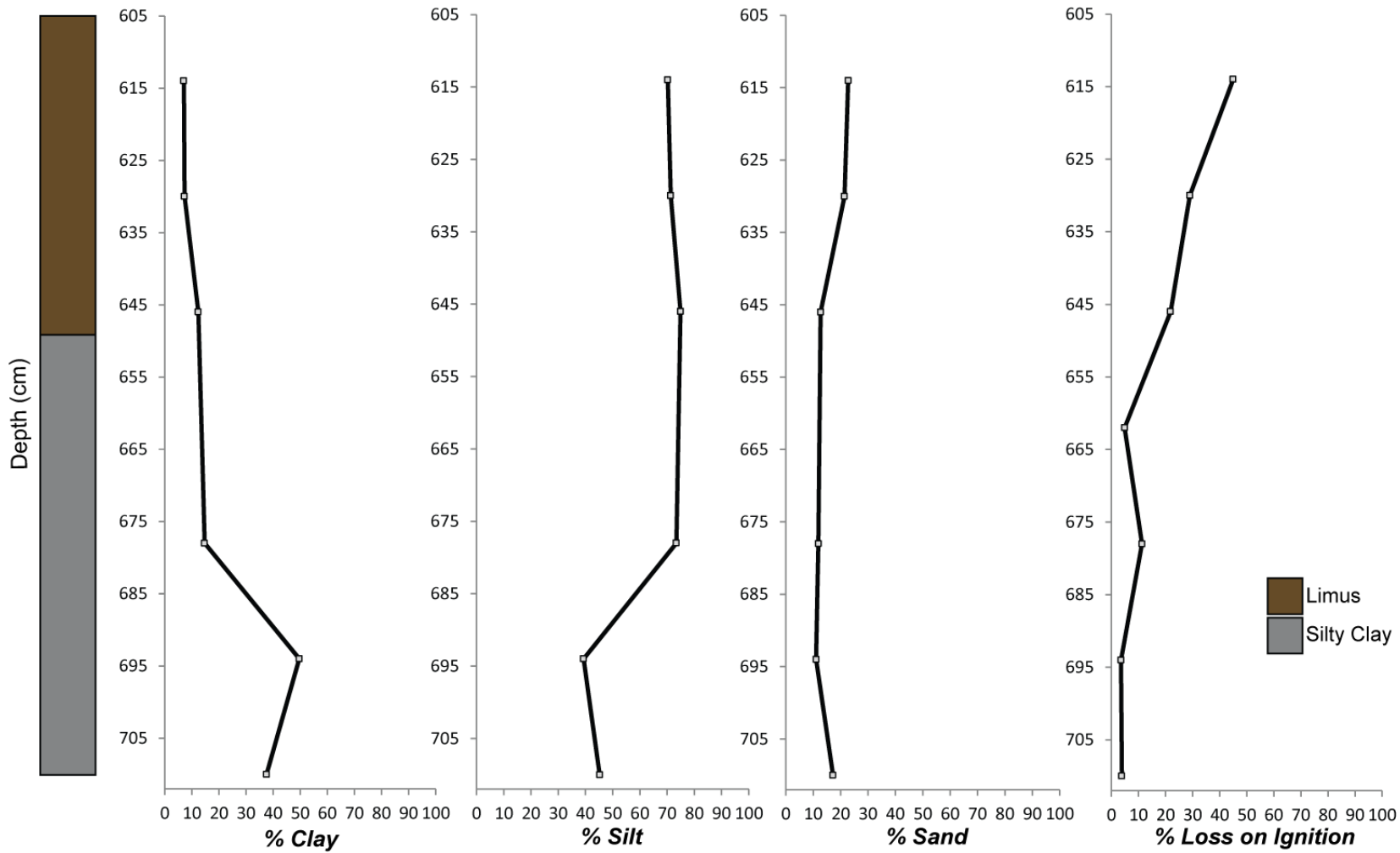
Figure 5.6: Stratigraphy, particle size and loss on ignition results for the sampled core, core 4, from Oldany. Clay, silt and sand fractions are defined by Wentworth (1922).
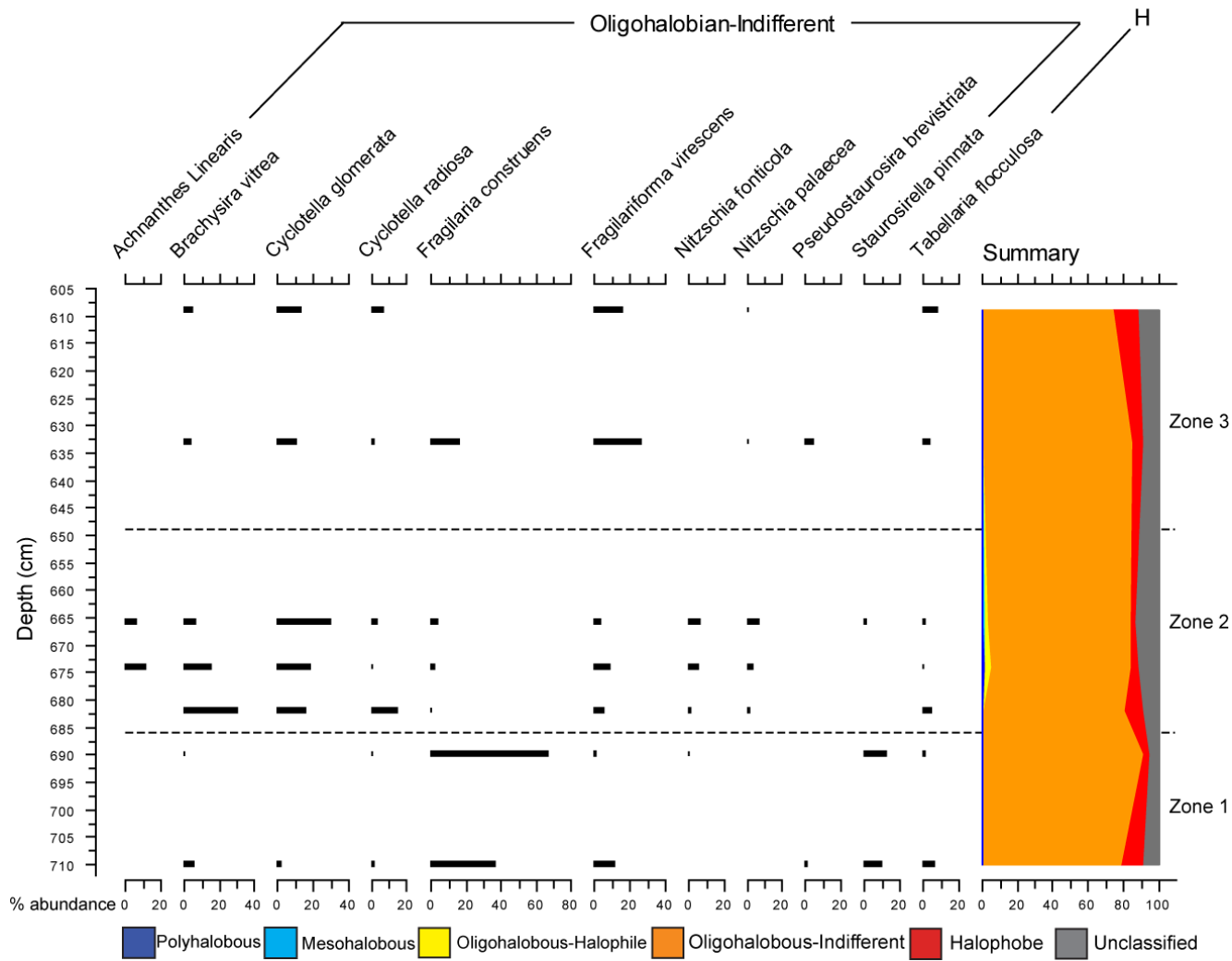
Figure 5.7: Diatom assemblage for Oldany; flora exceed 5 % of the total valves counted and are grouped using the halobian classification (Hustedt 1953).

Palaeoenvironmental Interpretation

Diatom flora illustrate that a freshwater environment persists in core 4, indicated by the dominance of oligohalobian-indifferent species and the occurrence of halophobous species throughout the assemblage. This result is unsurprising given that the sill altitude is 8.10 m OD, far exceeding the RSL highstands predicted for Coigach in the Assynt region (Figure 2.10); a mid-Holocene highstand is predicted below 2.5 m OD (Bradley et al. 2011).
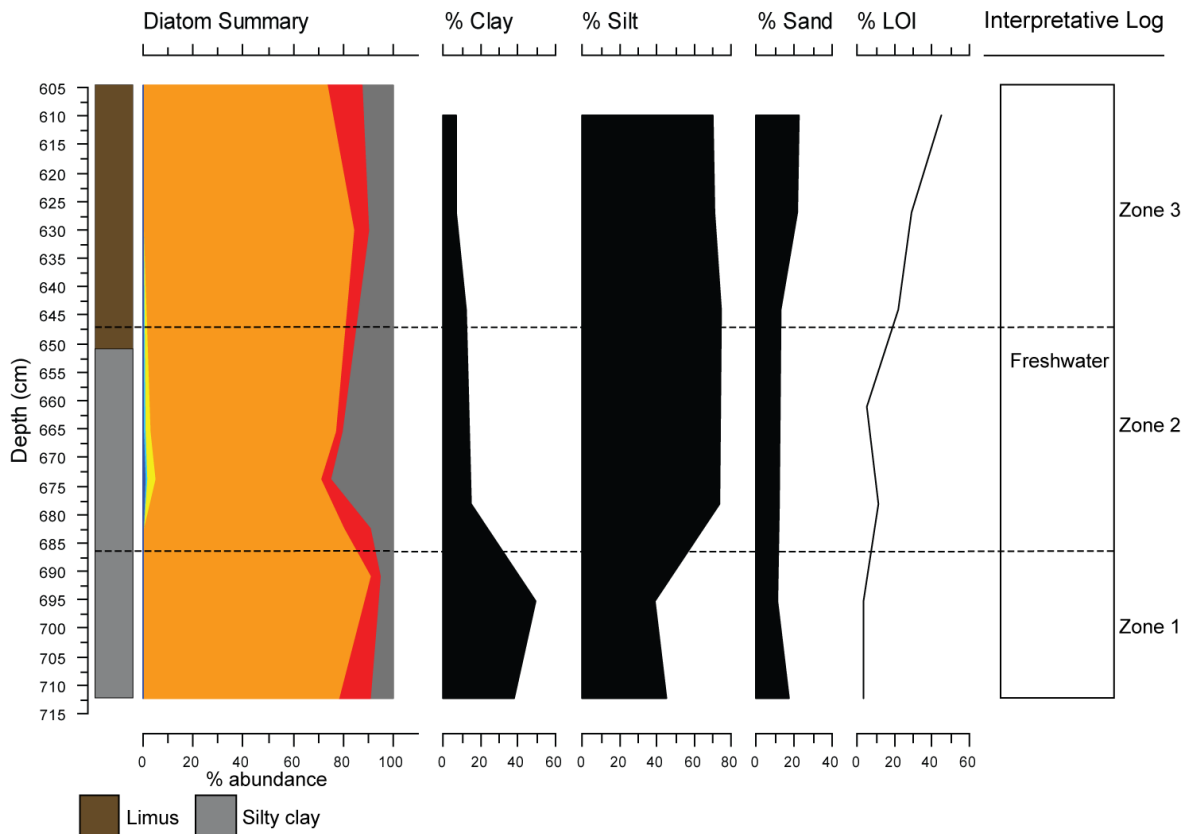
Figure 5.8: Summary diagram of results produced for core 4 from Oldany. Lithostratigraphy and diatom summary (see Figure 5.7 for key to halobian classification) are presented.

5.3 Duart Bog

Duart Bog is an infilled basin located on the western coastline of Loch Nedd and is encircled by deciduous woodland. The site is proximal to Loch Duart Marsh (section 5.4), which can be accessed through the woodland surrounding Duart Bog.

Site Survey

The topography and altitude of the rock sill was documented by coring north-east through the woodland to the beach (Figure 5.9.B). As a result, the highest point of the rock sill was identified at 4.77 m OD, 2.5 m above MHWST. Coring transects identified two topographic lows in this basin, as shown in Figure 5.9. The second topographic low was sampled (core 3) due to the sediment record being longer however both depressions reach a similar depth.
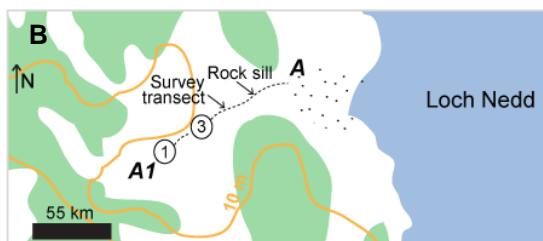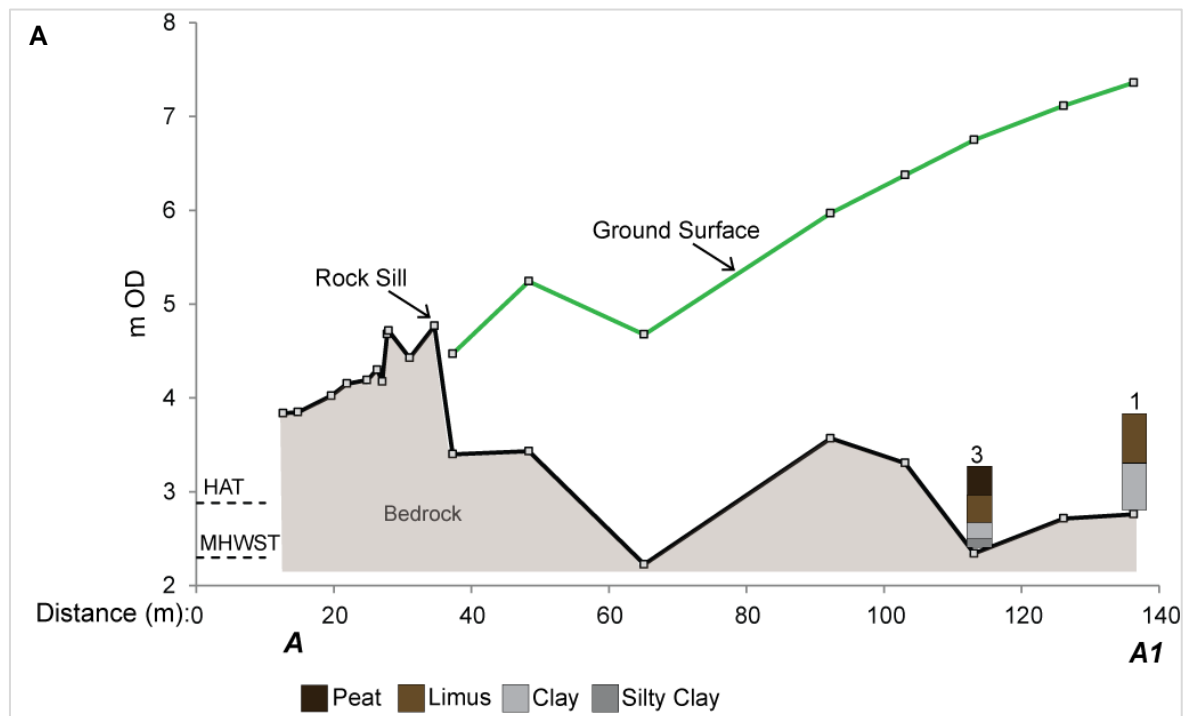
Figure 5.9: (A) The location, topography and altitude (4.77 m OD) of the rock sill was determined from a transect extending from the centre of the basin to the beach. (B) Location map of the transect in the context of Duart Bog.

Lithostratigraphy

The stratigraphy of core 3 (Figure 5.10) documents a transitional sediment sequence from clay to silty clay overlain by limus and an upper peat unit. These transitions were not documented in the sediment record for core 1 (Figure 5.9).

Particle size was analysed for 17 samples at a resolution of 8 cm, between 346 cm and 370 cm, which increased to 4 cm, between 386 cm and 430 cm, over the clay to limus transition (Figure 5.10) (Thomas 2014). The lower section of this core (430 cm to 390 cm) is dominated by silt which exceeds 60 % of the particle size whilst the sand fraction accounts for less than 15 %. The clay decreases gradually from a peak of 30 % to 13% within this section. In contrast, the sand fraction increases in the upper section (390 cm to 340 cm) of the core correlating with a decrease in silt whilst the percentage clay remains minimal at 5 %.

A total of 12 samples were collected to investigate changes in the percentage loss on ignition, as shown in Figure 5.10 (Thomas 2014). A sharp increase, from 3 % to 18 % organic content, happens between 430 cm and 422 cm following which a gradual increase to 92 % organic content occurs.

Biostratigraphy

Through core 3 15 diatom samples resulted in the identification of 114 diatoms species (Figure 5.11). The up-core assemblage is divided into three zones; a lower brackish zone (zone 1; 430 cm to 425.5 cm) followed by a transitional zone (zone 2; 425.5 cm to 387.5 cm) dominated by freshwater species and an upper freshwater zone (387.5 cm to 340 cm). Throughout the brackish zone, zone 1, *Diploneis didyma* and *Scolioneis tumida* are dominant, exceeding 20 % of the total count. *Fragilaria construens* and *Fragilariforma virescens*, oligohalobian-indifferent species, are also present in this zone, reaching up to 16 % and 30 % respectively. The progression into the transitional zone, zone 2, is marked by the disappearance of brackish influence. *Fragilaria construens* and *Fragilariforma virescens* remain abundant in zone 2A however decreasing to 0 % and 8 % respectively of the total count in zone 2B. *Staurosira elliptica* and *Staurosirella pinnata* are also dominant in zone 2A exceeding 30 % and 20 % respectively however these freshwater species were not present in zone 2B. Salt-intolerant species, such as *Tabellaria flocculosa*, are also present throughout zone 2A increasing to 11 % of the total count in zone 2B. The presence of salt-intolerant species increases greatly in the upper freshwater zone, zone 3, surpassing 30 % of the total count. *Tabellaria flocculosa* exceeds 20 % of the total count by 380 cm whilst other species such as *Tabellaria fennestrata* also increase in abundance.
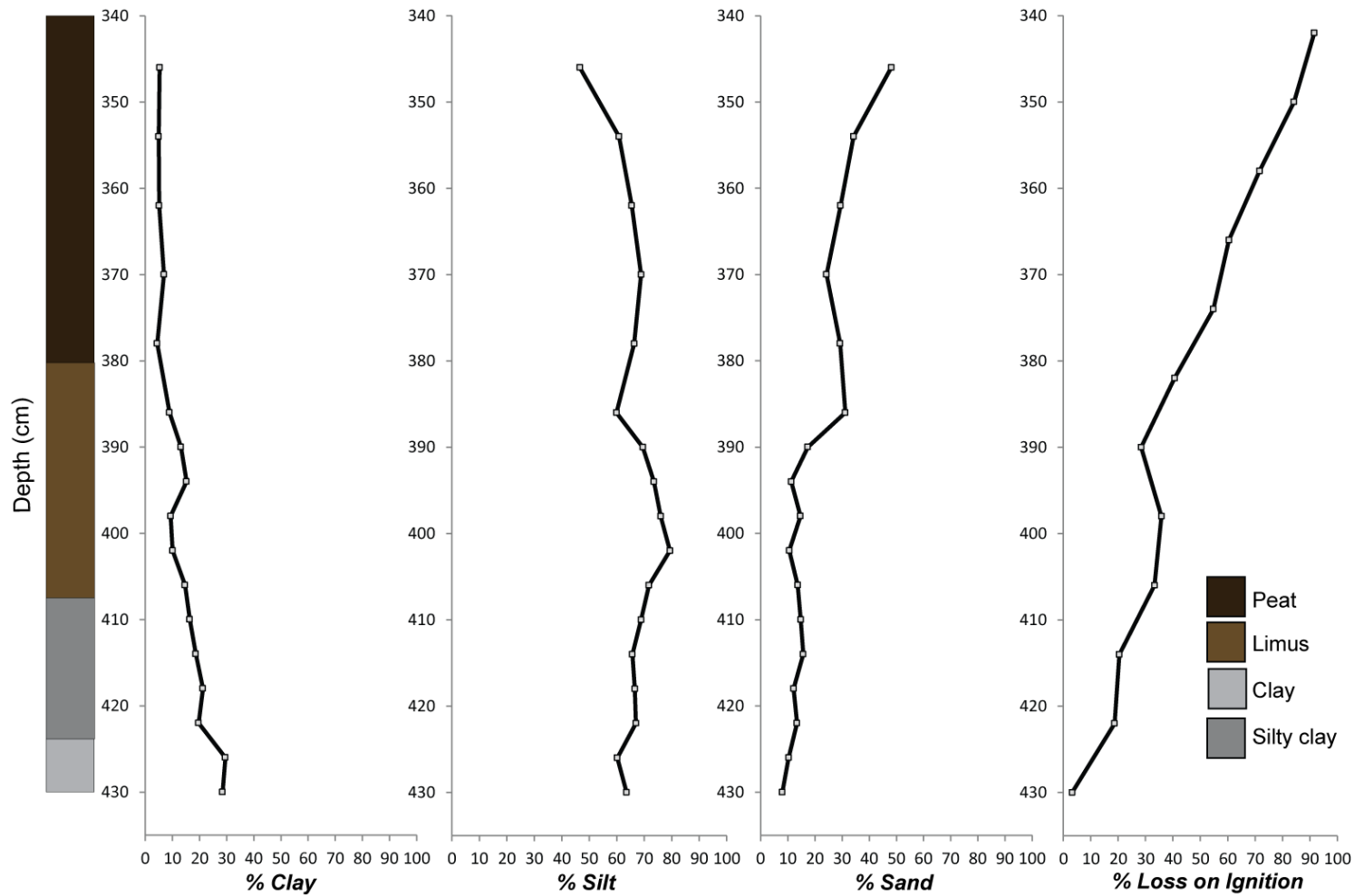
Figure 5.10: Stratigraphy, particle size and loss on ignition results for the sampled core, core 3, from Duart Bog. Clay, silt and sand fractions are defined by Wentworth (1922). Particle size and loss on ignition results were generated at the University of Bristol by Thomas (2014).
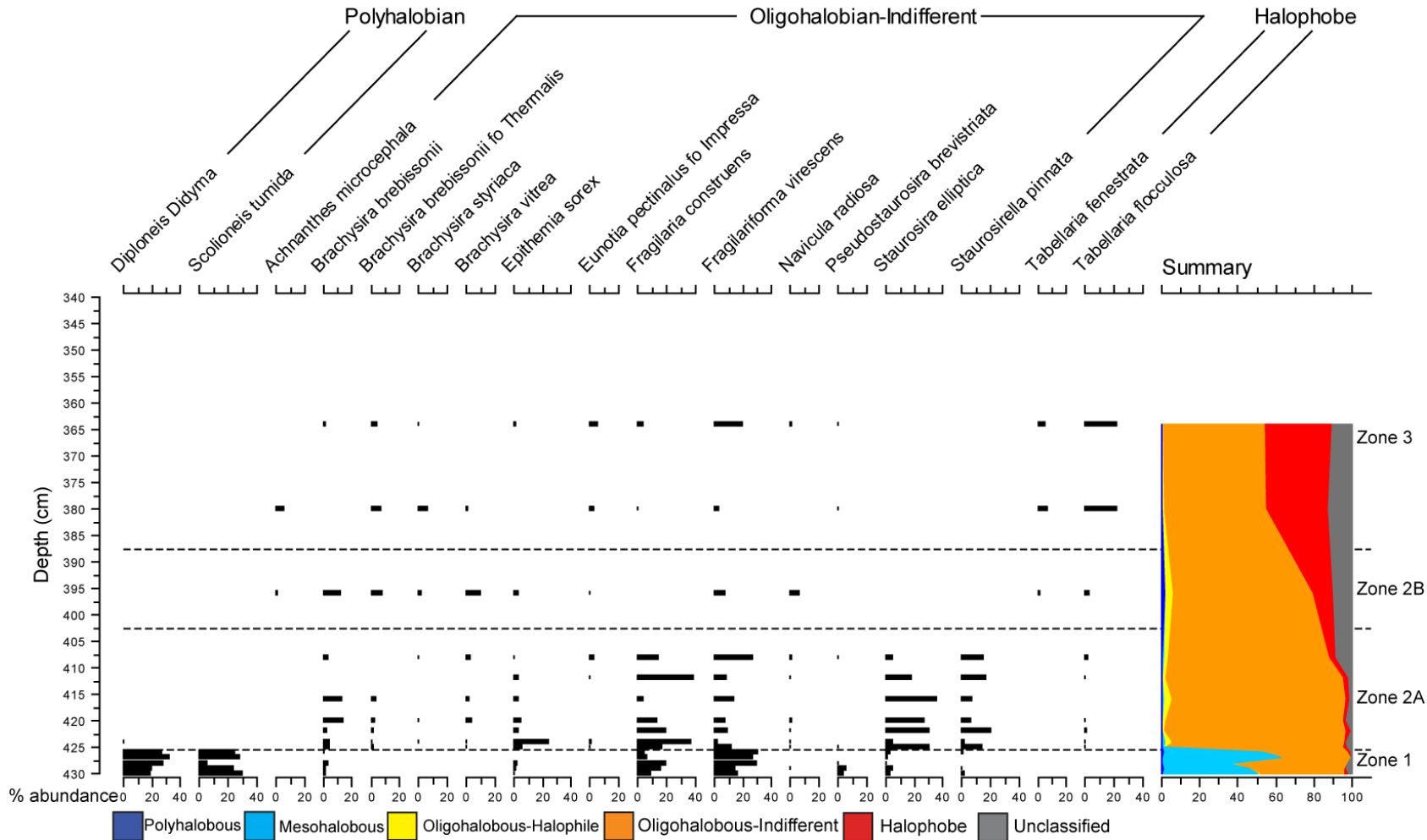
Figure 5.11: Diatom assemblage for core 3 from Duart Bog. The flora shown exceed 5 % of the total valves counted and are grouped using the halobian classification (Hustedt 1953).

Chronology

Pollen flora was qualitatively analysed in a sample taken from 415 cm (J. Innes, personal communication 2014). Flora such as *Empetrum* (crowberry) was abundant whilst low counts of *Artemisia* (mugwort) along with other aquatic plants and algae were also found (see Appendix 3 for all species identified from qualitative pollen analysis). This indicates that the sample represents a pond environment with heath and floating aquatic plants and algae. The pollen assemblage provides an estimated age linking to the end of the Loch Lomond Stadial, during the early stages of the transition to the Holocene, or prior to the Late Glacial Interstadial. A sample for AMS radiocarbon dating was taken from the sampled core at 425 cm in order to determine the age of the isolation contact identified from the diatom flora. The radiocarbon sample (DB13/3-425) returned a date of 10810 ± 41 ^{14}C yrs BP (12583-12833 cal. yrs BP). The radiocarbon dates produced for each isolation or ingression contact identified from the Duart Bog and Loch Duart Marsh sampled cores are compared with the estimated age, determined from qualitative pollen analysis, in Table 5.1.

Table 5.1: AMS radiocarbon dates produced for the isolation and ingression contacts determined from bio- and litho-stratigraphic analyses for the Duart Bog and Loch Duart Marsh sampled cores.

Sample ID	Laboratory ID	Sample Depth (cm)	Material Dated	Conventional age (^{14}C yr BP)	Calibrated age (cal. yr BP)	Estimated age (pollen)
DB 13/3-425	UBA-26502	425	Bulk	10810 ± 41	12583-12844	Late Glacial or Loch Lomond Stadial
LDM13/1-199	Beta-390107	199	Bulk	12670 ± 80	14612-15243	Late Glacial
LDM13/1-160	UBA-26501	160	Bulk	8887 ± 36	9888-10183	mid-early Holocene
LDM13/1-40	UBA-26500	40	Bulk	332 ± 34	421-456	late Holocene

Palaeoenvironmental Interpretation

The diatom flora are dominated by brackish species in zone 1 indicating that there was a marine influence into the basin, most likely with it connected to Loch Nedd. The diatom flora indicate a sharp reduction in marine influence at 425 cm following which the basin is isolated from the sea. This transition from brackish to freshwater conditions is supported by the lithostratigraphical data; reduction in the clay fraction and increasing loss on

ignition values across the transition from zone 1 to zone 2 indicates a transition to a low energy, organic rich environment. The pollen flora indicate that this regression dates to the end of the Loch Lomond Stadial or prior to the Late Glacial Interstadial. The basin has a sill altitude of 4.77 m OD; the regressive contact, dated to 12583-12844 cal. yr BP, will therefore provide a constraint on the RSL fall prior to the Loch Lomond Stadial.
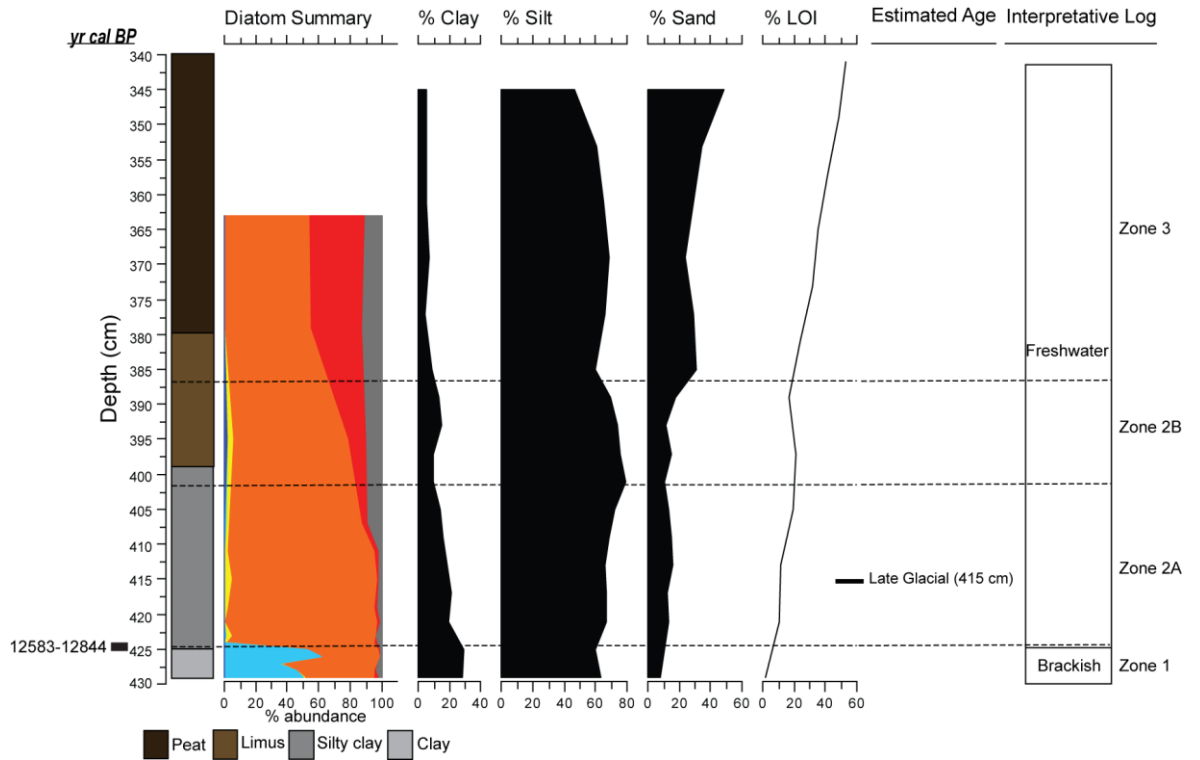
Figure 5.12: Summary diagram of results produced for Duart Bog (core 3). Lithostratigraphy and diatom summary (see Figure 5.11 for key to halobian classification) are presented whilst the estimated age is based on pollen flora discussed above.

5.4 Loch Duart Marsh

Loch Duart Marsh is a raised marsh connected to the adjacent tidal basin at high tide which in turn is connected to the sea by Loch Nedd, as shown in Figure 3.6.

Site Survey

Unlike the previous sites discussed, a bedrock sill, with overlying boulders at the mouth of the basin which contains Loch Duart Marsh, is exposed at present, at an altitude of 1.95 m OD (Figure 5.13). The sill is raised above the adjacent tidal basin by c. 70 cm. A transect, running north east from this tidal basin to Loch Nedd (Figure 5.13.B) illustrates the step of c. 1.5 m which occurs between Loch Nedd and the mouth of the tidal basin.

Lithostratigraphy

The sampled core is 220 cm deep consisting of 4 main units (Figure 5.14). The lower silty clay unit (220 cm to 200 cm) is overlain by an organic rich silty clay deposit (200 cm to 160 cm) where rootlets are abundant. This is replaced by a silty clay unit between 160 cm and 60 cm with a 10 cm thick shell layer (152 cm to 142 cm) occurring at the transition between the second and third units. The upper unit of this core comprises of the modern salt marsh.

The clay, silt and sand fractions in the Loch Duart Marsh core were analysed from 41 samples at a resolution of 8 cm until 200 cm, following which samples were analysed every 4 cm between 200 cm and 220 cm (Figure 5.14) (Thomas 2014). The lower section of the core (220 cm to 100 cm) is dominated by clay and silt whilst sand is absent. Within this section of the core there are parts where clay is dominant, exceeding 50 % (e.g. 220 cm to 216 cm and 168 cm to 100 cm) whilst others where silt is more dominant (e.g. 208 cm to 200 cm and 188 cm to 172 cm). The upper section (100 cm to 0 cm) is comparable to the lower section (220 cm to 100 cm) and is characterised by sharp shifts in the silt and clay fraction however peaks in the sand fraction also occur (44 cm and 28 cm). Silt is dominant at 92 cm and 76 cm whilst clay becomes the dominant fraction between 68 cm and 52 cm.

The percentage loss on ignition was analysed in 27 samples throughout the core and an overall increasing trend, from 4 % to 41 %, between 220 cm and the surface is shown in Figure 5.14 (Thomas 2014). This trend is punctuated by peaks in the organic content, most notably at 164 cm (31 %) and 28 cm (72 %).
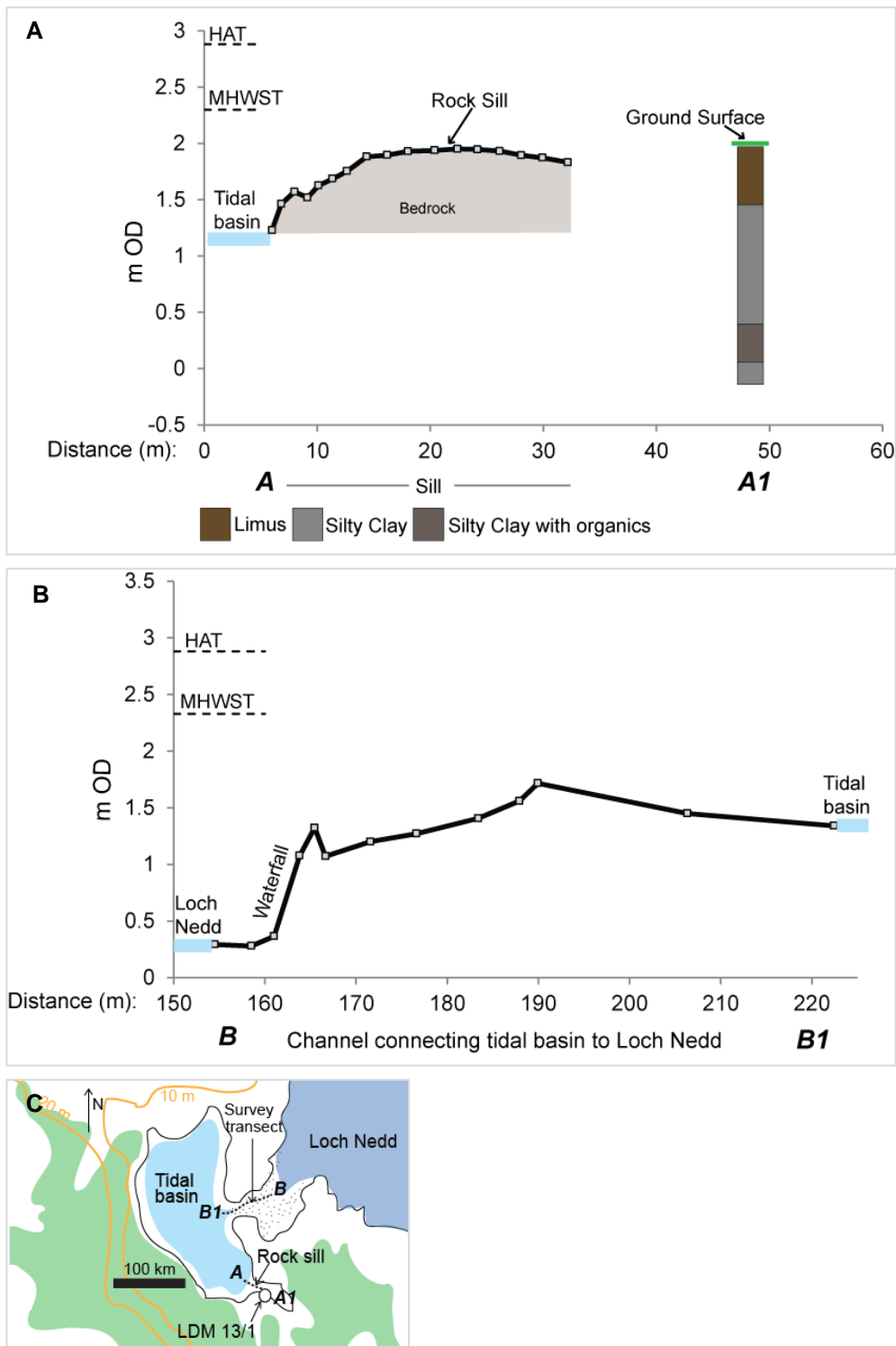
Figure 5.13: Survey data for Loch Duart Marsh illustrating (A) the elevation of the sill and its connection to the adjacent tidal basin along with the sampled core (B) the transect extending north east from the tidal basin to investigate the connection with Loch Nedd (C) location of the transects in relation to the sampled core.
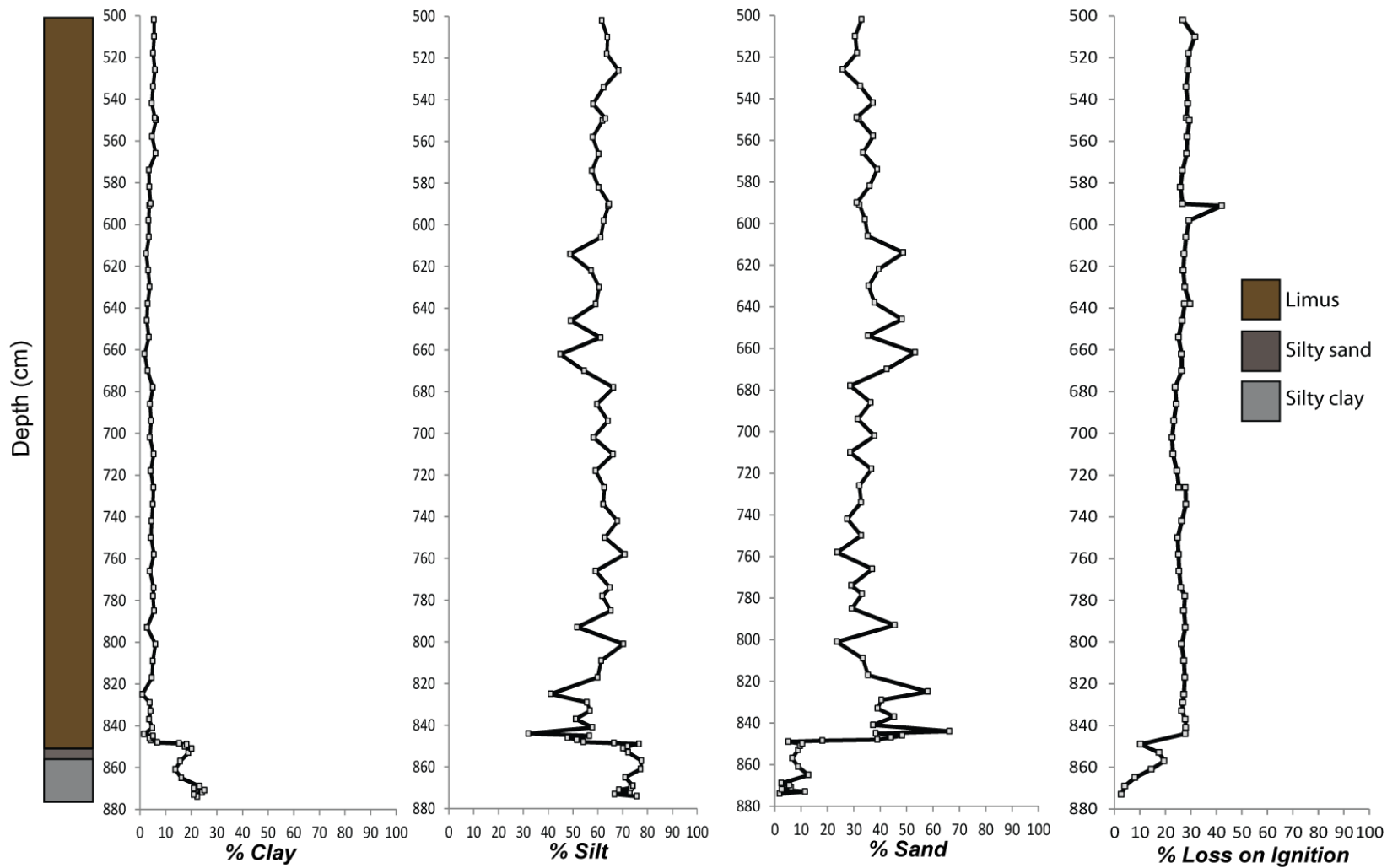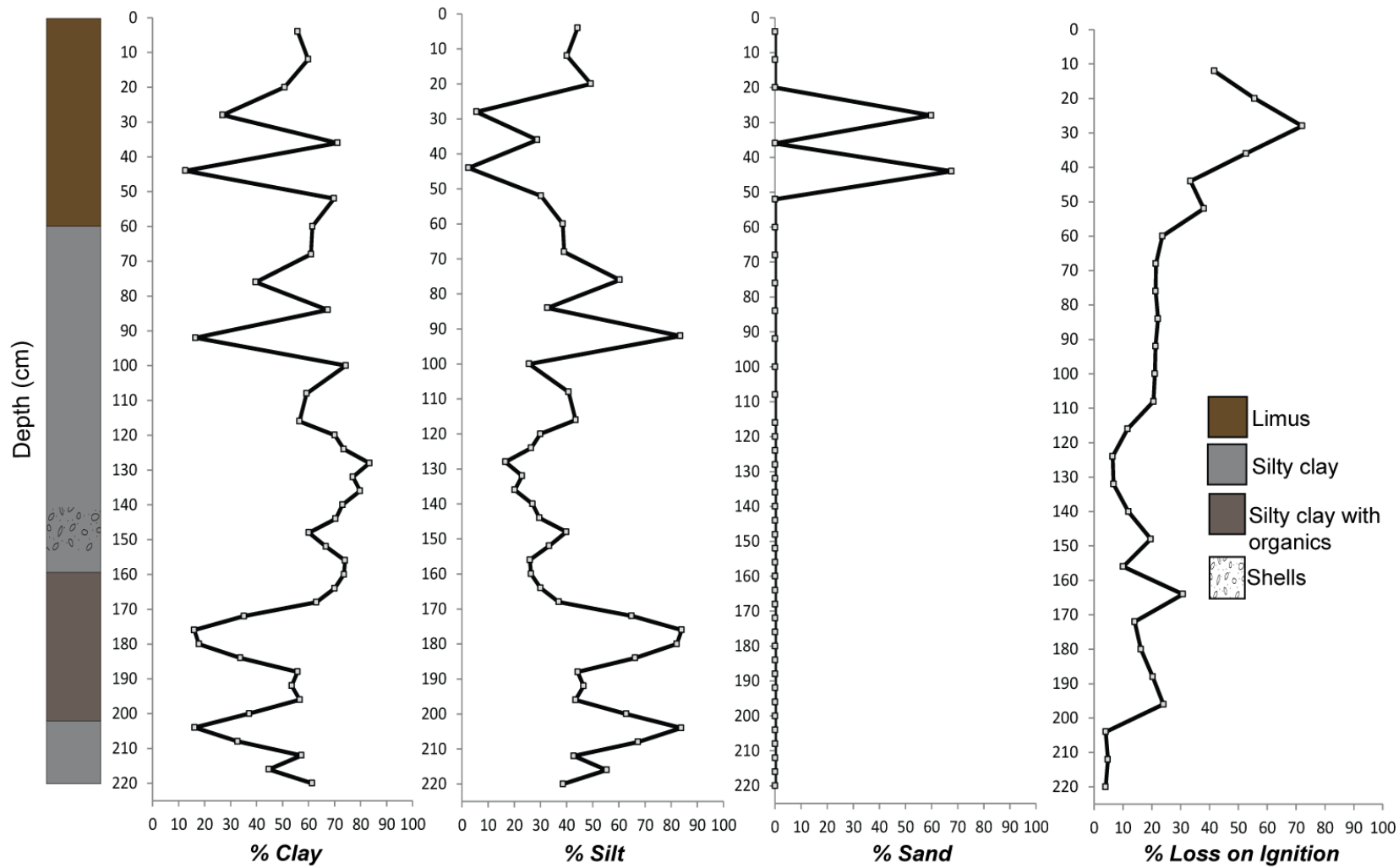
Figure 5.14: Stratigraphy, particle size and loss on ignition results for Loch Duart Marsh. Clay, silt and sand fractions are defined by Wentworth (1922).

Particle size and loss on ignition results were generated at the University of Bristol by Thomas (2014).

Biostratigraphy

A total of 27 samples were analysed and 166 diatoms species identified to determine the biostratigraphy of the Loch Duart Marsh core (Figure 5.15) which is divided into four zones: a lower marine zone (zone 1; 220 cm to 208 cm), an intermediate freshwater zone (zone 2; 208 cm to 157.5 cm) followed by an upper marine zone (zone 3; 157.5 cm to 55 cm) and finally the zone representing the modern marsh environment (zone 4; 55 cm to 0 cm).

Throughout the lower marine zone, zone 1, species such as *Paralia sulcata* and *Scolioneis tumida* dominate the assemblage whilst oligohalobian-indifferent species such as *Epithemia sorex* and *Brachysira brebbisoni* are also present in small amounts (<5 %). In zone 2, oligohalobian-indifferent species such as *Fragilaria construens*, *Epithemia sorex*, *Fragilaria virescens* and *Brachysira brebissonii* exceed 20% of the total count. *Fragilaria construens* decreases gradually throughout this zone from 57 % of the total count to less than 1 %. Salt-intolerant species, such as *Tabellaria floculosa*, also occur throughout however are not present at the upper and lower boundary of this zone.

In the upper marine zone, zone 3 *Opephora marina*, *Rhabdonema minutum* and *Paralia sulcata* exceed 20 % of the total count. Oligohalobian-indifferent species, such as *Fragilaria construens* and *Epithemia sorex*, which were abundant in the zone 2, now represent a minimal proportion of the total count. *Staurosirella pinnata* dominates the freshwater species in this zone, exceeding 30 % of the total count. Salt-intolerant species are nearly absent from this zone and represent less than 3 % of the total count at several points.

Zone 4 represents the modern day marsh environment at this site. Polyhalobous species, such as *Opephora marina* and *Paralia sulcata*, still occur in this zone however do not exceed 4 % of the total count. Oligohalobian-indifferent species, such as *Fragilaria virescens*, which were absent in zone 3 however present in zone 2, reoccur in zone 4. *Staurosira elliptica*, which had not been abundant in the lower zones, exceeds 40 % of the total count in zone 4.
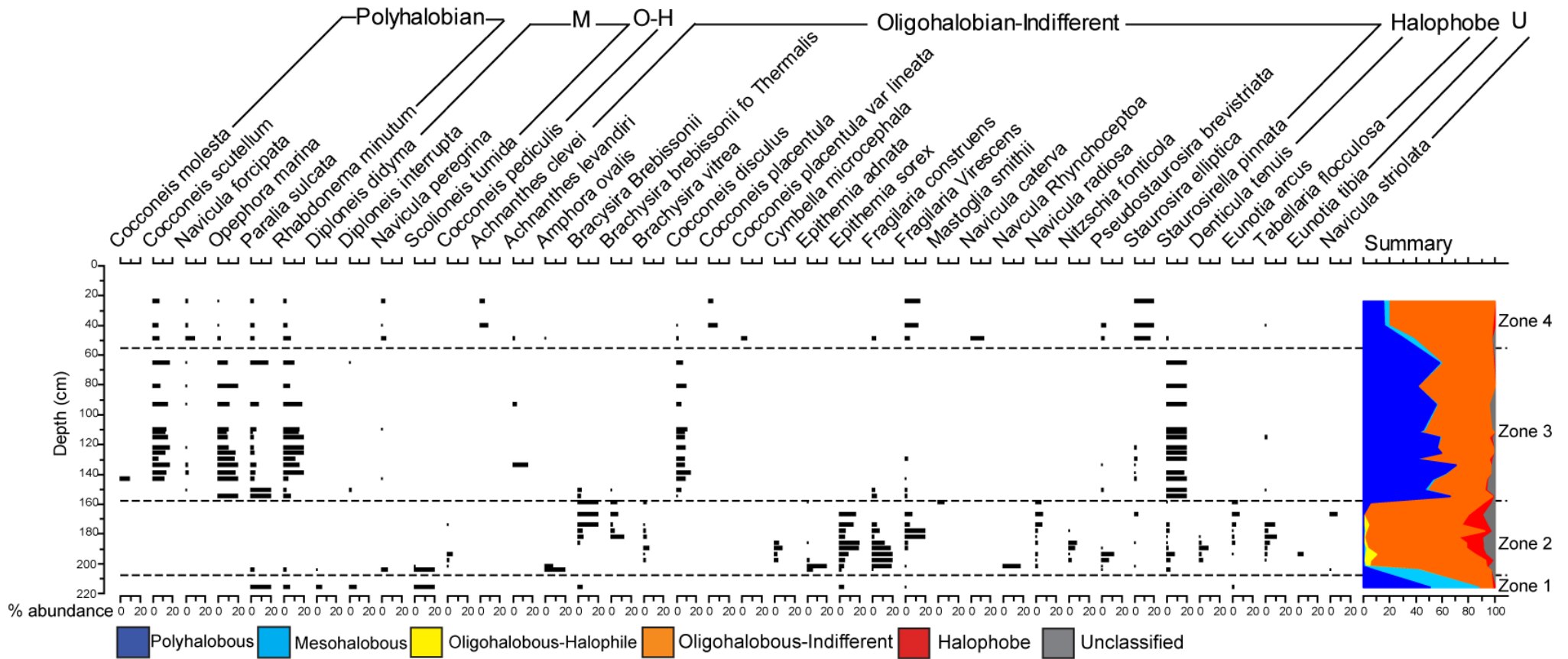
Figure 5.15: Diatom assemblage for Loch Duart Marsh, illustrating the transition from marine to freshwater conditions between zone 1 and 2 and zone 3 and 4. The diatom flora shown in the diagram exceed 5 % of the total valves counted and are grouped using the halobian classification (Hustedt 1953).

Chronology

Pollen flora were qualitatively analysed at 195 cm and 112 cm (J. Innes, personal communication 2014). *Empetrum* (crowberry), Cyperaceae (sedges), *Poaceae* (grasses) and *Artemisia* (mugwort) were found at 195 cm indicating an estimated Late Glacial age and an arctic, tundra environment indicative of a deep pond. In comparison, species such as *Betula* (birch) and *Alnus* (alder) were found at 112 cm indicating mid-Holocene age and a woodland environment however saltmarsh indicators were also present. Samples for AMS radiocarbon dating were taken at the isolation and ingression contact at 199 cm and 160 cm respectively as well as at 40 cm, where a reduction in marine influence is recorded by the diatom flora. The radiocarbon samples, outlined in Table 5.1, returned dates from the Late Glacial, early Holocene and late Holocene therefore supporting the estimated ages determined from pollen analysis.

Palaeoenvironmental Interpretation

The diatom flora indicate there was a marine influence into the basin at the base of the sequence with a decrease in marine conditions leading to isolation of the basin at 202 cm. This isolation dates to the Late Glacial (14612-15243 cal. yr BP) and is supported by pollen analysis. The basin remains isolated until a marine ingression, indicated by the diatom flora, at 160 cm. The pollen flora indicate this inundation dates to the early-mid Holocene and this is confirmed by the ^{14}C date, 9888-10183 cal. yr BP. The basin sill altitude is 1.95 m OD and this dated contact will therefore constrain the timing of the RSL rise above present during the early to mid-Holocene. Marine conditions persist until a reduction at 60 cm with the basin partially isolated by 40 cm. The ^{14}C date (307-479 cal. yr BP) and pollen flora illustrate that this transition dates to the Late Holocene therefore constraining the RSL fall to present following the mid-Holocene highstand. The lithostratigraphy supports the diatom assemblage results; increases in organic matter correspond with the isolation and partial isolation of the basin by 202 cm and 40 cm respectively whilst increases in the clay content correlate with periods of marine influence.

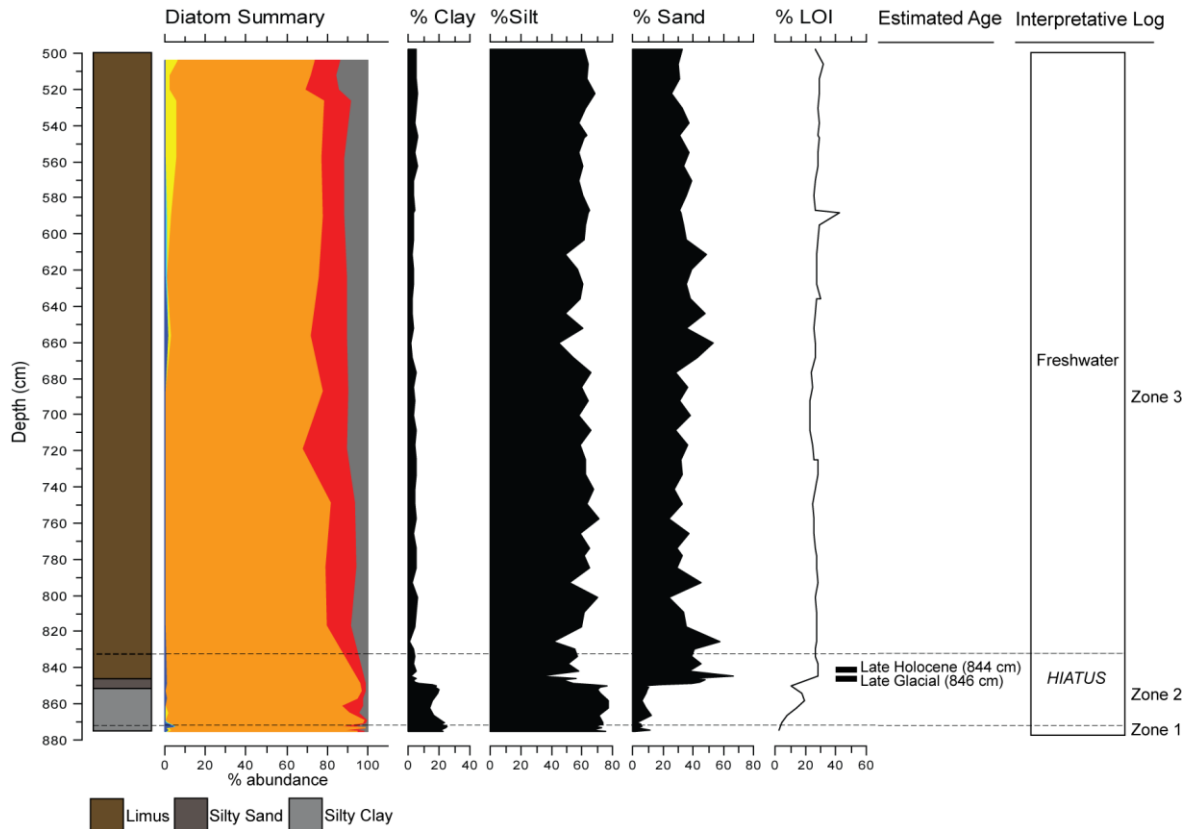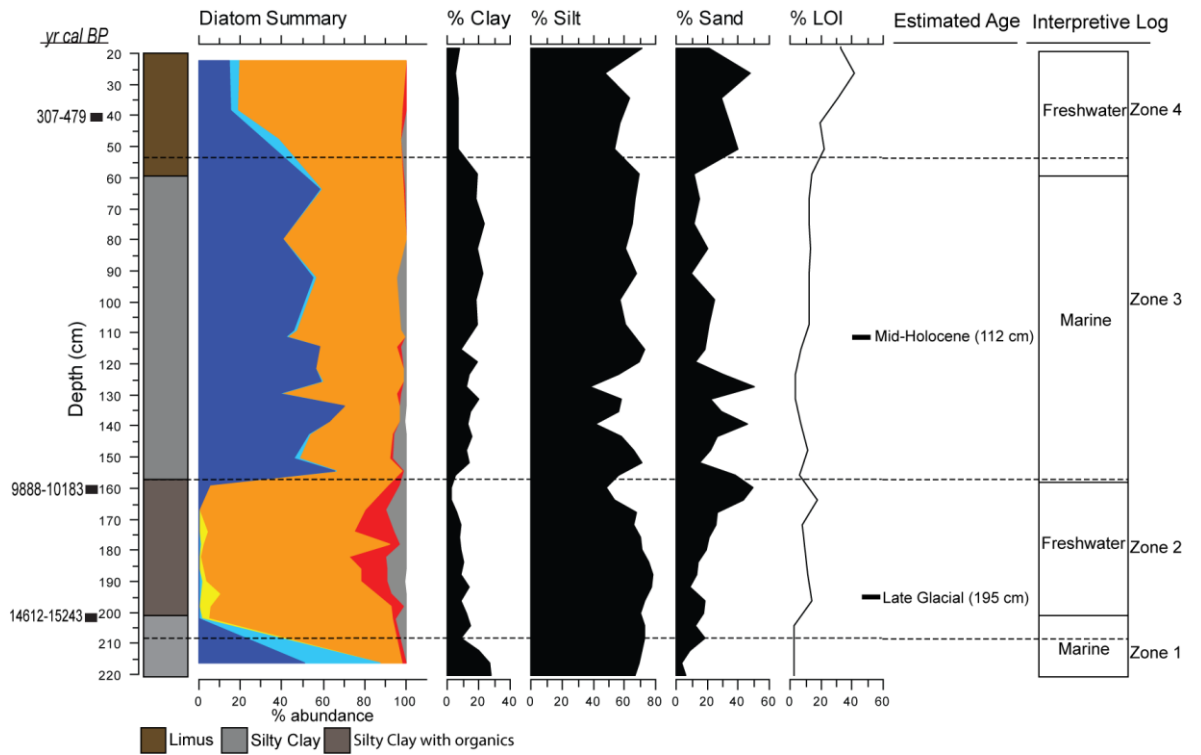*Figure 5.16: Summary diagram of results produced for Loch Duart Marsh. Lithostratigraphy and diatom summary (as per halobian classification illustrated in Figure 5.15) are presented whilst the estimated age is based on pollen flora discussed above.*

Chapter 6:Discussion

This chapter presents the sea-level index points generated for the Assynt region, based on the results presented in the previous chapter. The fit of these index points with the existing RSL data from Coigach, in this region, and the Bradley et al. (2011) GIA model is assessed. Following which, the implications of this research on the understanding of post-LGM RSL in the Assynt region, as well as elsewhere in north west Scotland, are discussed.

6.1 Reconstructions of RSL from Duart

The isolation contacts, identified within the bio- and litho-stratigraphy, at Duart Bog and Loch Duart Marsh are summarised in Figure 6.1. The isolation contact at Duart Bog (Figure 6.1.A; index point 1), identified by diatom flora, records a sharp decline in marine influence and transition to freshwater conditions at 425 cm dated to 12583-12844 cal yrs BP. The pollen flora (415 cm) estimated the age to be Loch Lomond Stadial or Late Glacial for basin isolation (425 cm). An isolation (index point 2), an ingression (index point 3) and a partial isolation (index point 4) contact are identified from the diatom assemblage and lithostratigraphy at Loch Duart Marsh. Ages for each were estimated, from pollen flora, to be Late Glacial (index point 2), early to mid-Holocene (index point 3) and Late Holocene (index point 4). These estimates were confirmed by ^{14}C dates, outlined in Figure 6.1. The location, age, elevation and tendency for each index point are defined in Table 6.1.
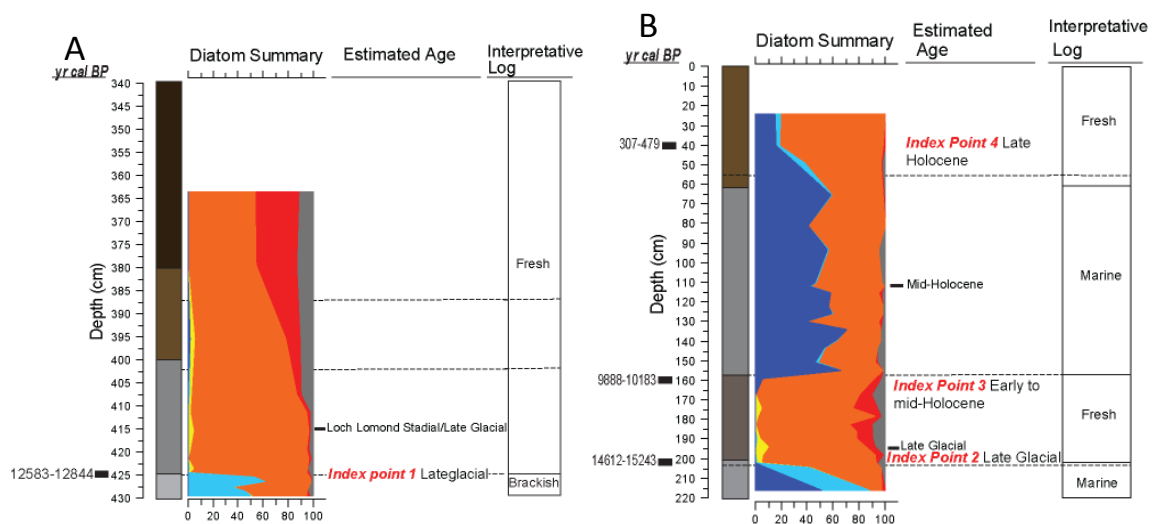
Figure 6.1: Summary of the diatom assemblage (see Figure 5.15 for key to halobian classification) for (A) Duart Bog and (B) Loch Duart Marsh. The isolation contacts identified and location of dated sea-level index points are also shown (see Figure 5.12 (Duart Bog) and Figure 5.16 (Loch Duart Marsh) for stratigraphy key).

Duart Bog

The indicative meaning, defined by the reference water level, and indicative range, the vertical range over which the dated contact could have formed, for each index point must be determined in order to calculate the elevation attribute (Devoy 1982; Heyworth & Kidson 1982; Shennan 1982). Bio- and litho-stratigraphic analysis of isolation basins have been used in many studies to precisely estimate the reference water level (e.g. Shennan et al. 1994; Zong & Tooley 1999; Long et al. 2011; Lloyd et al. 2013) using the isolation contacts determined by Kjemperud (1986). For example, the diatomological isolation contact is defined as the sediment-water interface when the water in the photic zone becomes fresh with a brackish influence remaining, indicating regular tidal connection in the basin, whilst the hydrological isolation contact represents the end of marine incursions (Kjemperud 1986). Shennan et al. (1994) infer that the hydrological isolation contact approximates to a reference water level of highest astronomical tide (HAT) whilst the diatomological isolation contact represents a lower reference water level, MHWST, since the basin is still regularly connected to the sea therefore representing an earlier stage during basin isolation. MHWST has been extensively used as the reference water level for the diatomological isolation contact in previous isolation basin studies (e.g. Shennan et al. 1995; Lloyd et al. 2009; Long et al. 2011). MHWST is used as the reference water level for the diatomological isolation contact identified at 425 cm for Duart Bog. The vertical range over which the index point 1 isolation contact formed is estimated to be between MHWST and HAT, therefore the indicative meaning is 2.10 ± 0.29 m (where the error is equivalent to half of the range of MHWST to HAT).

Loch Duart Marsh

Based on the discussion above, MHWST is selected as the reference water level for the diatomological isolation contact at 202 cm (index point 2) and also for the ingressive contact at 160 cm (index point 3), identified from the bio-and litho-stratigraphic analysis of the Loch Duart Marsh core.

A diatom transfer function is developed to produce a quantitative RSL reconstruction for the regressive salt marsh sequence identified in the upper 60 cm of the Loch Duart Marsh core. Sedimentation has infilled the Loch Duart Marsh basin resulting in the upper salt marsh sequence in the core. The regional 'coastal transition' model of modern diatom in north west Scotland, developed by Barlow et al. (2013), is used as it extends from Jura to Loch Laxford and Kyle of Tongue, therefore including Loch Duart Marsh. The diatom transfer function reconstructs palaeomarsh-surface elevation (PMSE) for each fossil salt marsh sample based on the relationship between the modern diatom assemblages in the regional 'coastal transition' model and elevation. PMSE is converted to RSL as follows:

$$RSL\ (m) = Depth\ (m\ OD) - PMSE\ (m\ OD) \qquad \textit{(Equation 6.1)}$$

The PMSE of a number of samples within the regressive saltmarsh sequence were reconstructed to provide context for the dated level. The modern analogue technique was used to assess the similarity between the salt marsh samples from Loch Duart Marsh and the modern samples (Barlow et al. 2013). The 5th percentile of minimum dissimilarity (minDC) was used as the boundary between a 'good' and 'close' modern analogue whilst the 20th percentile is the threshold for a 'poor' modern analogue (Watcham et al. 2013). Based on these percentile thresholds, the calibration of the fossil samples using the regional 'coastal transition' model produces reliable reconstructions for each salt marsh sample, with no sample exceeding the 5th minDC percentile. The diatom transfer function produced a reconstructed RSL of 0.16 m (± 0.35) for the dated sample from 40 cm. The output produced by the diatom transfer function for this regressive salt marsh sequence is presented in Appendix 4.

Limiting Data

The freshwater diatom assemblage for Oldany (Figure 5.7) illustrates that, based on the altitude of the rock sill (8.10 m OD) mean sea level (MSL) did not exceed 6 m, providing a limiting altitude for post-LGM RSL in Assynt.

Errors

The sample specific vertical error for each index point is shown in Table 6.2. The identification of the correct tidal datum as the reference water level and interpretation of the indicative meaning as well as the impact of changes in tidal range, sediment compaction and field levelling are examples of the individual sources which require consideration when calculating the total vertical error (E_t) as follows:

$$E_t = \sqrt{(e_1^2 + e_2^2 + e_3^2 + \cdots + e_n^2)} \qquad \text{(Equation 6.2)}$$

where $e_1 \ldots e_n$ are the individual sources of error (Preuss 1979; Shennan et al. 2000; Horton et al. 2000).

Changes in tidal amplitude, since the LGM, would have a significant impact on the interpretation of isolation basin records, due to the implications for determining the reference water level. Few studies account for changes in the tidal regime since the LGM leading to a potential over- or under-estimation of the vertical error associated with each index point. If tidal range was greater in the past, for example, the correction of the reference water level to MTL would be larger resulting in RSL above present being lower and overestimated. Changes in tidal range for north west Scotland have been modelled by Uehara et al. (2006) however the coarse resolution of these models reduces their application to regional sea-level reconstructions. Regional models of palaeo-tide level (e.g. Shennan & Horton 2002) have predicted changes in tidal range to be most significant within large estuaries whilst changes at the open coast are relatively small.

Neill et al. (2010) however predicted a 2.6 m reduction in MHWST at Arisaig between 16 ka BP and present using POLCOMS (Proudman Oceanographic Laboratory Coastal Ocean Modelling System). Applying the resulting palaeotidal correction reduced the misfit between RSL data (Shennan et al. 2005) and the Shennan et al. (2006a) GIA model predictions. Neill et al. (2010) illustrate, however, that the change in tidal level is minimal (c.0.6 m for MHWST) for sea-level index points dating between the Loch Lomond Stadial (12.9-11.7 ka) and Holocene. Changes in tidal amplitude following the LGM is therefore likely to have a minimal influence on index points 3 and 4 (dating from the Holocene), however it may result in an overestimate of RSL for index points 1 and 2 (pre-Loch Lomond Stadial dates).

Compaction reduces the vertical thickness of the sediment column due to physical and biochemical processes (Allen 2000; Brain et al. 2012). This post-depositional lowering of the original elevation of the sediment therefore impacts RSL reconstruction and can introduce significant errors, particularly for salt marsh based sea-level reconstructions and those associated with low energy intertidal environments (Greensmith & Tucker 1986; Shennan & Horton 2002; Edwards 2006; Long et al. 2006; Horton & Shennan 2009; Horton et al. 2013; Barlow et al. 2013). Most sediment utilised to generate sea-level index points have experienced a degree of post-depositional compaction as a result of loading by overlying sediment or water. Sediment compaction however does not need to be considered when utilising isolation basin records. The altitude of the isolation, or ingression, contact is determined from the elevation of the rock sill and the reference water level of the indicative meaning component, neither of which will be altered by post-deposition compaction (Shennan & Horton 2002; Edwards 2006). Index point 4 (Figure 6.1.B) however lies within the biostratigraphic zone representing the modern salt marsh environment (Figure 5.16) and therefore may be influenced by sediment compaction. Brain et al. (2012) use a numerical model to demonstrate that compaction is negligible, not exceeding 0.1 mm yr^{-1}, for records from shallow (< 0.5 m) uniform-lithology stratigraphies, or shallow near-surface salt-marsh deposits in regressive successions. Sediment compaction is therefore likely to have had a minimal impact on index point 4 however it is still quantified and included in the estimate of the vertical error (Table 6.2). Post-depositional lowering for index point 4 in this regressive salt marsh sequence does not exceed 39.1 mm since 391 cal yr BP, well within the uncertainties calculated by the transfer function.

Table 6.1: Sea-level index points for Duart.

Index point	Sample	¹⁴C age BP (± σ)	Calibrated age (yr cal BP)	Sill elevation (m OD)	Reference Water Level	Indicative Meaning (m)	Tendency	RSL change from present (m ± error)	
1	DB 13/3: 425	10810 ± 82	12583-12844	4.766	MHWST	2.1	-ve	2.67	0.59
2	LDM 13/1: 203	12670 ± 80	14612- 15243	1.95	MHWST	2.1	-ve	-0.15	0.59
3	LDM 13/1: 160	8887 ± 72	9888-10183	1.95	MHWST	2.1	+ve	-0.15	0.59
4	LDM 13/1: 40	332 ± 68	307-479	1.95	-	-	-ve	0.16	0.37

Table 6.2: Vertical error associated with each sea-level index point outlined in Table 6.1

Index point	Sample	Levelling Error (m)	Sill Elevation Error(m)	Indicative Range Error (m)	Sediment Compaction (m)	Transfer function (± 2σ) (m)	Total Error (m)
1	DB 13/3:425	0.10	-	0.58	-	-	0.59
2	LDM 13/1:203	0.10	0.05	0.58	-	-	0.59
3	LDM 13/1:160	0.10	0.05	0.58	-	-	0.59
4	LDM 13/1:40	0.10	0.00	-	0.04	0.35	0.37

6.2 Assynt RSL: Duart and Coigach

The sea-level index points from Duart help to constrain postglacial RSL for previously unstudied time periods, such as the Late Glacial and late Holocene. These sea-level index points add to the 8 existing index points from Coigach, located 25 km south-west of Duart, which reconstruct the RSL rise to the mid-Holocene highstand and associated fall (Figure 6.2). Index point 2 extends the RSL reconstruction to the Late Glacial whilst index point 4 constrains RSL above present during the late Holocene. The sea-level index points for Assynt, from both Duart and Coigach, record a sequence of fall-rise-fall and provide additional constraint on the RSL rise and fall prior to and following the mid-Holocene highstand. Raised shorelines in the Assynt region are identified at Achnahaird Bay, Coigach at c. 5.2 m OD (Shennan et al. 2000) and at Stoer Beach, Enard Bay at 6.47 m OD (Hamilton 2013). Shennan et al. (2000) assume that fossil shore platforms such as these formed between MTL and MHWST. Therefore these raised shorelines in Assynt represent a water level of 3.1-5.2 m at Achnahaird Bay and 4.37-6.47 m at Stoer Beach, allowing comparison with the RSL plot in Figure 6.2. This does not correspond with the reconstructed altitude of the Main Postglacial Shoreline (-2 m OD) or the Blairdrummond Shoreline (-2 m OD) determined by quadratic trend surfaces by Smith (2005) for Duart.
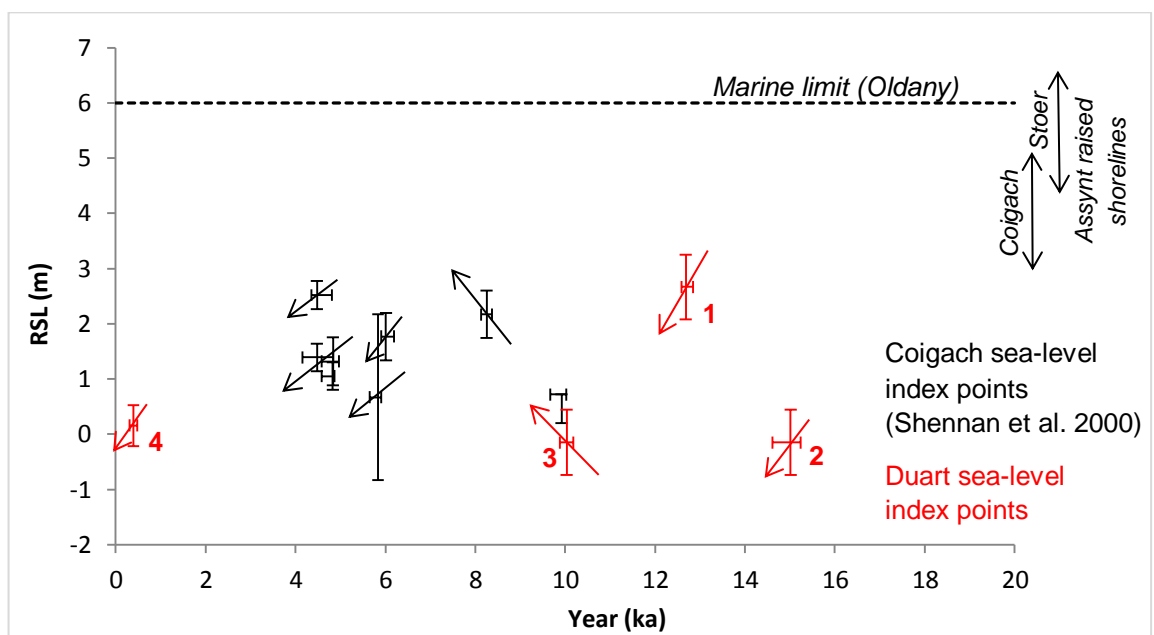
Figure 6.2: RSL reconstructions from the Assynt area. The red, numbered sea-level index points show the data outlined in Table 1. The arrows associated with each sea-level index point illustrate the tendency associated with it. The marine limit identified from Oldany agrees well with the raised shorelines identified from Achnahaird Bay and Stoer Beach.

RSL fall during the Late Glacial;

RSL during the Late Glacial is constrained by two new index points (index points 1 and 2), a new limiting point, and potentially, by the altitude of raised shorelines in the Assynt region. The isolation basin at Oldany records freshwater conditions throughout the record – no marine inundation is identified from the diatom assemblages. This, therefore, suggests the marine limit during the Late Glacial period was below 6 m. Index points 1 and 2 record RSL falling during the Late Glacial. Index point 2 records RSL at 0.15 ± 0.59 m below present, at 14612-15243 yr cal BP, an age which is supported by the pollen flora analysed from the core (Figure 6.1). Index point 1 records RSL falling below 2.47 ± 0.59 m between 12583 and 12844 yr cal BP, significantly later than suggested by index point 2. Given that the rock sill at Duart Bog, index point 1, (4.77 m OD) is 2.82 m higher than the rock sill at Loch Duart Marsh, index point 2, (1.95 m OD) if both basins are recording the same RSL fall, one would expect Duart Bog to record the regression earlier than Loch Duart Marsh. One possible explanation is that Duart Bog records a later additional marine ingression. For this to be the case however, Loch Duart Marsh ought to record this additional marine event during the Late Glacial Interstadial (i.e. between index point 2 and 3) as the basin sill is lower than that of Duart Bog however this does not occur. An alternative explanation is that the ^{14}C date of the isolation of Duart Bog is incorrect and influenced by younger carbon from the downward reworking of humic acids or rootlets, for example (Balesdent 1987). This interpretation is supported by the lithostratigraphic and qualititative pollen analysis produced for Duart Bog and Loch Duart Marsh. The AMS ^{14}C dates from Loch Duart Marsh are supported by the lithostratigraphic analysis (Figure 5.16); decreasing organic content, for example, between 196 cm and 172 cm to 14 %. Low organic content suggests decreased productivity between index point 2 (202 cm) and 3 (160 cm) possibly due to cooler climate. This is seen in dated cores from Loch Assynt (Boomer et al. 2012), Ardtoe (Shennan et al. 1996) and Skye (Selby et al. 2000) to be associated with the Loch Lomond Stadial. The AMS ^{14}C dates from Loch Duart Marsh are also supported by qualitative pollen analysis; Late Glacial pollen (195 cm) close to index point 2 (202 cm) and mid-Holocene pollen (112 cm) above index point 3 (160 cm). Qualitative pollen analysis at 415 cm for Duart Bog is dominated by *Empetrum* (crowberry) and aimed to provide an age estimate to support the AMS ^{14}C dated contact at 425 cm (Figure 6.1.A). Pollen analysis in the Assynt region, and elsewhere in northern Scotland, identified that *Empetrum* (crowberry) dominated pollen zones correspond to the Late Glacial Interstadial as well as the opening of the Holocene (Pennington et al. 1972). The *Empetrum* (crowberry) pollen zone in northern Scotland associated with the Late Glacial Interstadial, like the Duart Bog sample, is also dominated by sedge pollen. The evidence outlined above suggests the ^{14}C date for index point 1 is erroneously young however quantitative pollen analysis needs to be completed to support this interpretation. Additional AMS radiocarbon dating of macrofossils, if possible, would confirm this.

RSL rise to mid-Holocene highstand;

Sea-level index points from both Duart (index point 3) and Coigach provide constraint on the RSL rise prior to the mid-Holocene highstand between 9888-10183 yr cal BP and 8250-8370 yr cal BP. Both index points have a positive tendency documenting a RSL rise. Index point 3 records RSL rise from -0.15 ± 0.59 m at Loch Duart Marsh continuing to rise above 2.17 ± 0.43 m based on the isolation basin at Dubh Lochan, Coigach. A limiting altitude for the mid-Holocene highstand is determined at 2.6 m above present from Loch Raa, Coigach from freshwater diatom and pollen flora (Shennan et al. 2000). Duart Bog provides a further limiting point for the altitude of the mid-Holocene highstand, freshwater conditions persist following the marine regression identified near the base of the sequence (Figure 6.1), constraining the altitude below 2.47 ± 0.59 m.

RSL fall to present following the mid-Holocene highstand;

The trend of a negative sea-level tendancy (or RSL fall) extends into the late Holocene following the mid-Holocene highstand reconstructed for Coigach. Index point 4 records RSL falling below 0.16 ± 0.37 m, between 307 cal yr BP and 479 cal yr BP, to present in the upper regressive salt marsh sequence at Loch Duart Marsh. Recent research has developed continuous 2000 year records of RSL change from salt marshes at Loch Laxford and Kyle of Tongue, 18 km and 49 km north east of Duart respectively. These records, which aim to enhance understanding of sea level during the last few thousand years for the North Atlantic, indicate that RSL fall during the last 2000 years was long-term and gradual in north west Scotland (Barlow et al. 2014) fitting with the RSL reconstruction from Loch Duart Marsh.

6.3 Fit with GIA models

The Assynt sea-level index points have the potential to provide further constraint on model predictions of RSL for the area (Figure 6.3), such as those by the Bradley et al. (2011) model (hereafter referred to as the Bradley et al. model). Prior to the sea-level index points generated in this study, empirical constraint on the GIA in this region was poor with the exception of the mid-Holocene, as outlined in Chapter 2. The new RSL data presented here from the Late Glacial through to the late Holocene, as detailed above, highlights misfit between the Bradley et al. model predictions and RSL data for the deglacial period and early Holocene. This indicates the need to potentially refine the Earth and ice model selection for this region.

The predicted RSL fall during the LGM is now constrained by index point 2 from this study, as well as index point 1 however there are uncertainties associated with the age of this index point. Based on sea-level index point 2, the Bradley et al. model under predicts the elevation of RSL during the Late Glacial RSL by up to c.10 m. No marine signal is present in the core sampled from Oldany (6 m). This marine limit elevation fits reasonably

well with the Bradley et al. model prediction of c. 5 m, as well as the raised shoreline evidence from the Assynt region (Figure 6.3) (Shennan et al. 2000; Hamilton 2013). Although these geomorphological features are not dated, comparison with the index points indicates they are too high to be mid-Holocene in age and are therefore likely associated with Late Glacial sea level. Reconstructions, for both Duart (index point 3) and Coigach, lie above the Bradley et al. predictions for the RSL rise to the mid-Holocene highstand. Index points constraining the mid-Holocene highstand, from Coigach (Shennan et al. 2000), and the late Holocene RSL fall, from Duart (index point 4), reconstruct RSL close to that predicted by the Bradley et al. model.
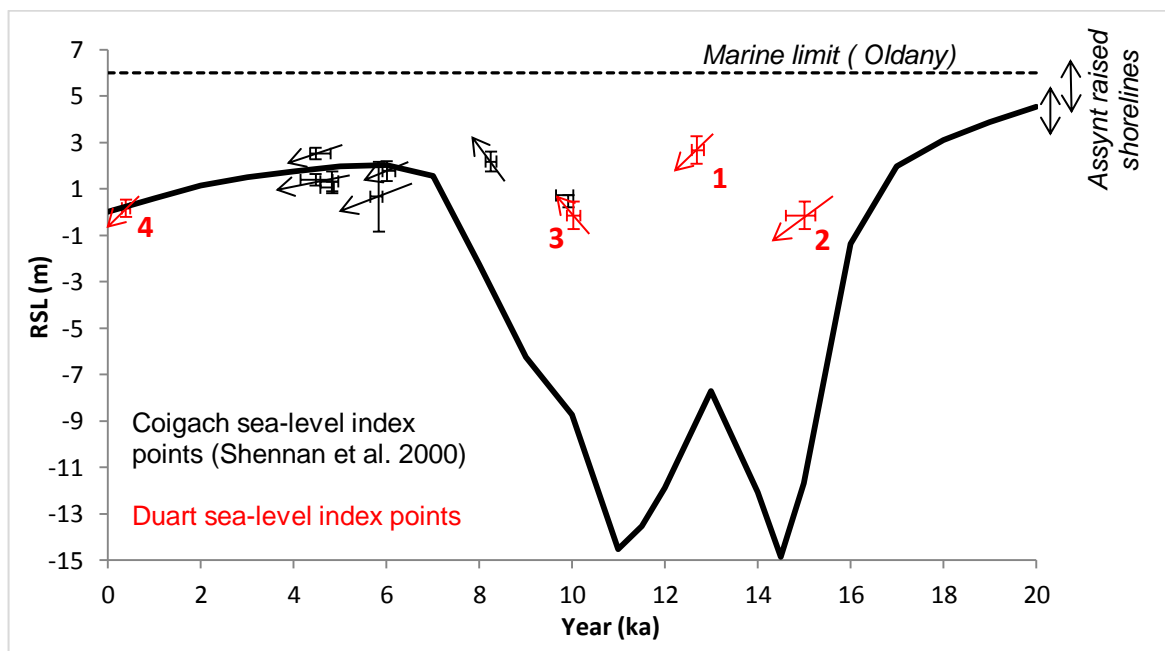
Figure 6.3: Bradley et al. (2011) model predictions for Assynt, including previous sea-level index points for the Assynt region from Coigach, shown in black, (Shennan et al. 2000) and the sea-level index points generated from Duart in this study in red. The arrows indicate the positive or negative tendency associated with each sea-level index point; increasing arrow indicates RSL increase for example. The marine limit and raised shorelines, from Coigach (Shennan et al. 2000) *and Stoer* (Hamilton 2013), *identified in the Assynt region fit well with the Bradley et al. predictions.*

The misfit between the RSL data, outlined in section 6.2, and the Bradley et al. model is contrasted with predictions from the Kuchar et al. (2012) GIA model. The Kuchar et al. (2012) model combined a three-dimensional thermomechanical ice sheet model (Hubbard et al. 2009), which predicted the thermal and dynamic evolution of the BIIS, with the Bradley et al. (2011) GIA model and is the first to adopt this approach for the British Isles. The Hubbard et al. (2009) ice model is driven by palaeoclimate data and is based on the physics of ice flow data therefore providing a test for the interpretation of trimline data (e.g. Ballantyne et al. 1998) as it is not constrained by geomorphological evidence. Comparison between the Bradley et al. model and that developed by Kuchar et al. (2012)

for Assynt wasn't possible due to the model output from the latter not being available at the time of submission.

6.4 RSL in north west Scotland and implications for models of BIIS

The sea-level index points produced in this study have led to the post-LGM RSL history for Assynt being extended to the Late Glacial which remains an understudied period throughout north west Scotland. Arisaig remains the only location in north west Scotland to have a long and detailed record of post-LGM RSL change prior to the Loch Lomond Stadial. It is therefore difficult to draw substantiated conclusions about regional RSL in north west Scotland due to the rather restricted temporal range of data form most sites, other than Arisaig, and the focus of RSL data on the Holocene.
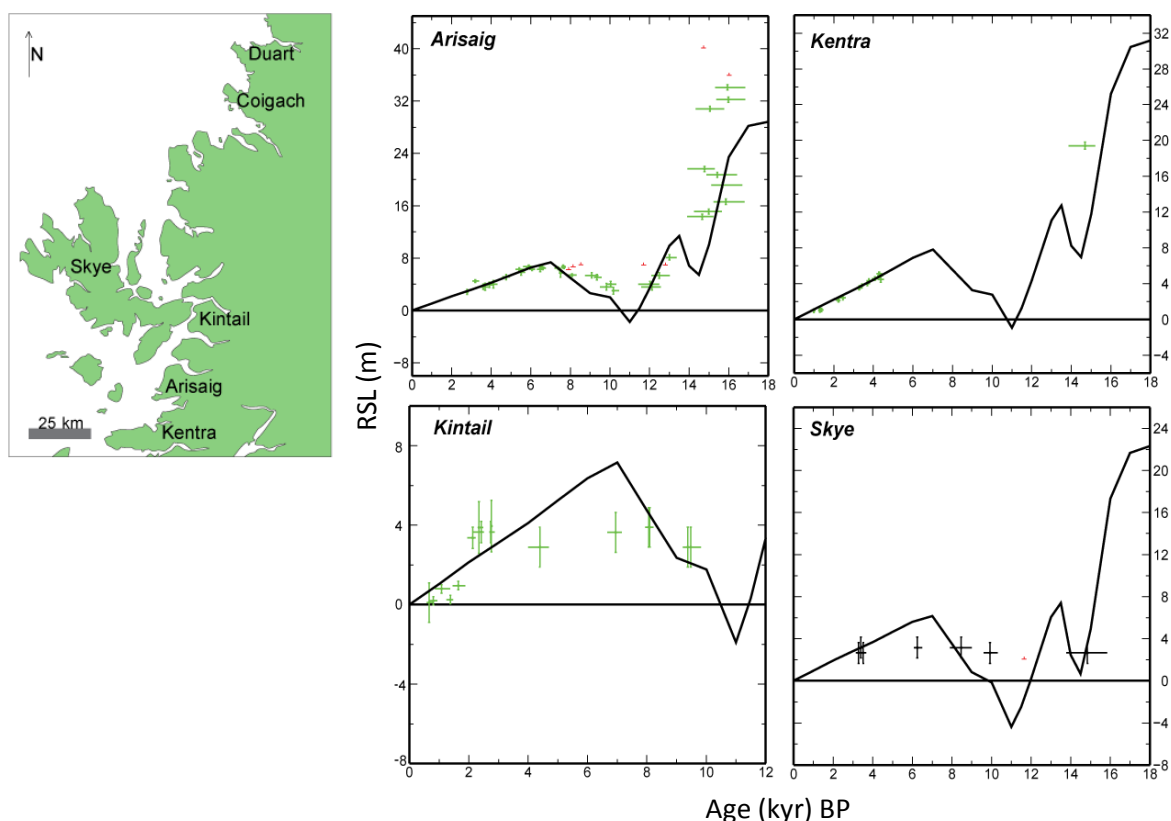
Figure 6.4: RSL reconstructions and predictions, based on the Bradley et al. model, for other sites located in north west Scotland (Adapted from Bradley et al. 2011). Inset is a map showing the location of these sites with respect to Duart and Coigach.

Index point 2 is reconstructed above the Bradley et al. model predictions (Figure 6.3) for the Late Glacial period. Neill et al. (2010) modelled the evolution of MHWST and MHWNT at Arisaig between 16 ka and present to determine the magnitude of change in the tidal amplitude following the LGM. As outlined earlier in this chapter, predicted MHWST at Arisaig decreased by c. 2 m during the Late Glacial period therefore resulting in sea-level index points, which had been reconstructed above the Shennan et al. (2006a) model, being lowered once the palaeo-tidal correction was applied. The misfit therefore between

index point 2 and the Bradley et al. model would be reduced if the tidal correction outlined by Neill et al. (2010) were applied. If the predicted palaeo-tidal correction for MHWST was applied to index point 2, since its associated reference water level is MHWST, then RSL would be reconstructed at 2.35 m below present between 14612 and 15243 yr cal BP. A degree of misfit (c. 8 m) would therefore still remain following the application of this palaeo-tidal correction.

The Bradley et al model, along with previous GIA models (e.g. Shennan et al., 2006a), predict that the long-term trend of RSL fall during the Late Glacial is interrupted by an oscillation in RSL, associated with meltwater pulse 1a (MWP-1a) which dates to c. 14.5 ka (Shennan 1999; Shennan et al. 2005). The MWP-1a oscillation is predicted to be recorded in the RSL record of sites located within the BIIS limit. Sites on the margins of the BIIS, where RSL fall, following deglaciation, was less should record a shift in tendency associated with MWP-1a rather than a reduced rate of RSL fall (Peltier 1998; Shennan 1999; Shennan et al. 2002). An oscillation in RSL, due to MWP-1a, is predicted for Assynt (Figure 6.3), due to the dominance of the non-local RSL signal predicted by the Bassett et al. (2005) global ice-model. The Bradley et al. model predicts a RSL highstand associated with MWP-1a for sites such as Arisaig, Skye and Kentra. There is however currently no RSL data supporting that MWP-1a was recorded in north-west Scotland. Sea-level index points from Arisaig, shown in Figure 6.4, illustrate a continual RSL fall, at a decreasing rate between 16 ka and 10 ka. Sea-level index points for Arisaig however do not constrain the RSL predictions between 14000 cal yr BP and 13000 cal yr BP, due to a gap in basins between 9.3 m and 15.5 m, therefore it is possible that MWP-1a falls within this gap in data (Shennan et al. 2005).

Sea-level index points are reconstructed above GIA model predictions of RSL during the early Holocene in the Assynt region (Figure 6.3) as well as other sites in north west Scotland, such as Arisaig, Skye and Kintail (Figure 6.4). This misfit in Scotland is attributed by Peltier (1998) to the earlier onset of Antarctic melt (Peltier et al. 2002; Shennan et al. 2002). It is widely believed that Antarctica was the main meltwater source during the mid-to-late Holocene (e.g. Peltier et al. 2002; Sugden et al. 2006) however the rate and magnitude of this contribution to global ice-equivalent (or "eustatic") sea level remains debated. The global ice model, developed by Bassett et al. (2005), is unconstrained by RSL data during the Holocene. Bradley et al. (2008) aimed to resolve this issue by developing a Holocene model of global ice-equivalent sea-level change using new far-field RSL datasets from China (Zong 2004) and the Malay-Thailand region (Horton et al. 2005). A range of Antarctic melt scenarios for the Holocene were modelled and tuned to these RSL datasets. It is noted however by Zong (2004) and Horton et al. (2005) that local processes, such as post-depositional lowering and tectonic movements, have likely altered the sea-level history for the mid-to late-Holocene, particularly in the

China dataset. The vertical errors associated with these local processes were not taken into account by Zong (2004) or Horton et al. (2005). This may have an impact on the Bradley et al. predictions of global ice-equivalent sea level which were tuned to the China and Malay-Thailand RSL datasets. Alternatively, this early Holocene misfit may represent the difficulty associated with modelling the spatial variability of post-LGM RSL change throughout the British Isles which is complicated by the Fennoscandian forebulge (Peltier 1998). In Scotland, post-LGM RSL is complicated further with proximity to the BIIS centre of ice loading. Modelling these complex RSL histories is therefore extremely difficult for north west Scotland; this early Holocene misfit may reflect this.

The timing and magnitude of the mid-Holocene highstand varies geographically due to the interplay of local isostasy and the fingerprint pattern of the eustatic component. Well constrained predictions of the mid-Holocene highstand are limited in north west Scotland, aside from the Assynt and Arisaig area, whilst in locations such as Kintail the misfit with model predictions is significant (Figure 6.4). The mid-Holocene highstand is well constrained for the Assynt region by index points from Coigach (Shennan et al. 2000) fitting well with the Bradley et al. model predictions. Data-model misfit is also minimal for the mid-Holocene highstand at Arisaig which is constrained to 6.74 m above present, in contrast with 2.6 m above present in the Assynt region due to differences in proximity to the former centre of ice loading, in the western Grampians. Global ice-melt is predicted (Bradley et al. 2008) to have continued through the late Holocene ceasing 2000 years ago, resulting in minimal misfit during the late Holocene for most sites in north-west Scotland, including Assynt.

The misfit, discussed above for sites throughout north west Scotland (Figure 6.4), is likely attributed to uncertainties associated with the global and local ice model used by the Bradley et al model. The suitability of the Earth model adopted for the British Isles is evident from the fit between the 16000 year Arisaig RSL record and model predictions (Figure 6.4). Regional uncertainties associated with the geomorphological constraint on the BIIS ice model, particularly its surface elevation and deglaciation chronology, may have significant implications for GIA models and resulting post-LGM RSL predictions.

Palaeo-trimlines, interpreted from high weathering limits in Scotland (e.g. McCarroll et al. 1995; Ballantyne et al. 1998), have been used to constrain the maximum surface elevation of the BIIS by the Bradley et al. model, like previous GIA models for the British Isles (e.g. Shennan et al. 2006a; Brooks et al. 2008). Recently, however, the palaeo-trimline data has been reinterpreted, based on cosmogenic-nuclide analysis of bedrock and erratics 'pairs', as representing englacial thermal boundaries therefore constraining the minimum, rather than maximum, surface elevation of this ice sheet (Ballantyne & Hall 2008; Ballantyne 2010; Fabel et al. 2012). This reassessment has significant implications

for the potential thickness and future modelling of the BIIS. Additional ice will result in greater glacial isostatic rebound following the LGM leading to higher sea level during the Holocene. The incorporation of the palaeo-trimline data into previous GIA modelling studies will have led to the elevation of RSL being underestimated in some parts of Scotland; the data presented in this thesis supports this.

The deglaciation chronology and timing of glacial readvances, as well as reconstructions of the BIIS extent, have been extensively supported by surface exposure dating using cosmogenic [10]Be. The primary uncertainty associated with determining exposure ages is the calculation of the [10]Be production rate which is affected by altitude and location whilst temporal variations also occur (Ballantyne & Stone 2012; Ballantyne et al. 2013). Scaling schemes were developed by Balco et al. (2008) to relate the isotope production rate to location and altitude and therefore the exposure age however the age produced is dependent on the chosen scaling scheme. For example, the 'Lm' scaling scheme produces ages approximately 1.5-4.5% younger than the 'Du' or 'De' scaling scheme. This results in significant uncertainties associated with the chronology of deglaciation therefore impacting GIA model inputs for the BIIS. The more advantageous approach, which overcomes the short-falls associated with these scaling schemes, is to adopt a locally determined [10]Be production rate (LPR) which produces more precise ages with significantly reduced uncertainty (Ballantyne 2012; Ballantyne & Stone 2012; Ballantyne et al. 2013). For example, Ballantyne (2012) recalibrated existing exposure ages using an LPR for sites extending from Orkney to Beinn Inverveigh in the Scottish Highlands. Prior to recalibration , 62 % of these published [10]Be exposure ages for ice retreat during the Loch Lomond Stadial were younger than 11.7 ka however following recalibration 73% were within the chronological limits of the Loch Lomond Stadial (12.9-11.7 ka) (Ballantyne 2012). The shift in age, illustrated by this example, through the use of a LPR, has significant implications for published [10]Be exposure ages documenting the timing of deglaciation prior to the Loch Lomond Stadial. The use of global [10]Be production rates, rather than locally determined rates, to obtain surface exposure ages can result in the onset of deglaciation occurring erroneously late. The incorporation of [10]Be exposure ages, which have not been recalibrated using a LPR, into GIA models has implications for predicted post-LGM RSL change as well the current understanding of the deglaciation chronology of the BIIS. Earlier onset of ice sheet retreat would have resulted in the Late Glacial RSL fall beginning sooner than currently predicted by GIA models.

6.5 Summary

The research undertaken in this study has extended the RSL record for Assynt and produced the first Late Glacial sea-level index points for the region. The index points, from Coigach and Duart, highlight variable fit with the Bradley et al. model. The interpretation of the Assynt RSL record, as well as that from other sites in north west Scotland, highlights

several potential problems associated with both the BIIS and global ice sheet model resulting from the geomorphological data and predictions of global ice-equivalent sea-level change respectively. Uncertainties with the geomorphological data are primarily associated with the use of trimline data to constrain the maximum surface elevation of the BIIS in GIA models (e.g. Ballantyne et al. 1998; Ballantyne 2010; Fabel et al. 2012). Additionally, the limited number of locally derived ^{10}Be production rates reduces the precision associated with calculating surface exposure ages therefore influencing the reliability of the deglaciation chronology determined for the BIIS (Ballantyne 2012; Ballantyne & Stone 2012; Ballantyne et al. 2013). Uncertainties associated with predictions of global ice-equivalent sea level relate to the debated distribution of the rate and magnitude of melt from Antarctica prior to and during the Holocene (e.g. Bassett et al. 2005).

Chapter 7: Conclusions

The aim of this research was to develop new sea-level index points for Assynt, which in turn may be used to refine GIA model predictions of post-LGM RSL change for this region. Sediment cores were collected from isolation basins, with sill altitudes ranging from 1.95 m OD to 8.10 m OD, to add to the existing body of RSL data from Coigach, which is restricted to the mid- to late-Holocene (Shennan et al. 2000). The bio- and litho-stratigraphy is presented for each of the basins investigated in Chapter 5. The diatom assemblages from Loch Duart Marsh and Duart Bog identified several clear transitions from marine to freshwater conditions as well as freshwater to marine. AMS radiocarbon dating of these isolation and ingression contacts led to new Late Glacial, early and late Holocene sea-level index points being developed therefore achieving part of the main aim of this thesis. No marine signal is present in the core sampled from Oldany. This site therefore acts as a limiting point for RSL reconstructions. Based on the altitude of the rock sill (8.10 m OD), MSL must have been below 6 m OD. The marine limit for the region must therefore lie below 6 m OD. This marine limit elevation fits reasonably well with the Bradley et al. model prediction of c. 5 m RSL, as well as the raised shoreline evidence from the Assynt region (Shennan et al. 2000; Hamilton 2013). Although these geomorphological features are not dated, comparison with the index points indicates they are too high to be mid-Holocene in age and are likely associated with Late Glacial sea level. The record produced from Loch na Claise (3.50 m OD) is confined to the Late Glacial and late Holocene due to the occurrence of a large sediment hiatus. The sea-level index points for Assynt, from both Duart (this thesis) and Coigach (Shennan et al. 2000), produce a post-LGM RSL record extending from the Late Glacial through to the late Holocene documenting a pattern of RSL fall-rise-fall (Figure 6.2).

The hypothesis set out at the start of this thesis, was that RSL in Assynt during the Late Glacial and early Holocene is higher than predicted by the Bradley et al. model. The RSL data, from Coigach and Duart, fits well with the GIA model predictions of RSL during the mid- to late-Holocene. The model however, under-predict RSL during the Late Glacial and early Holocene when compared to the new sea-level index points presented here (Figure 6.3). For the Late Glacial and early to mid-part of the Holocene it is not possible to reject the hypothesis as the Bradley et al. GIA model under predicts the recorded RSL change. This indicates that the Earth and ice model selected may need refining. RSL reconstructions from elsewhere in north west Scotland, such as Arisaig, Skye and Kintail, have a similar misfit with the Bradley et al. model during the early Holocene. These misfits are most likely due to uncertainties associated with the global and local ice-model. These uncertainties have been attributed to the geomorphological data constraining the BIIS model as well as the predictions of global ice-equivalent sea-level change used by the

global ice sheet model. The rate and magnitude of the contribution of Antarctic melt to global ice-equivalent sea level following the LGM remains debated (e.g. Sugden et al. 2006). These uncertainties may, in part, explain the data-model misfit observed throughout north west Scotland during the early Holocene. This misfit cannot be resolved by altering the BIIS model, constrained by geomorphological data, alone according to Shennan et al. (2002) who attribute the solution to altering the globally significant far-field parameters. However, recent reassessment of trimline data has led to the argument that it has been misinterpreted as the maximum surface elevation of the BIIS (e.g. Ballantyne & Hall 2008; Ballantyne 2010). Similarly use of global ^{10}Be production rates, rather than locally determined rates, to obtain surface exposure ages has also been shown to produce ages which are too young. This geomorphological data is used by GIA models, such as Bradley et al (2011), to constrain the BIIS. These uncertainties associated with the geomorphological data are likely to result in a reconstruction of the BIIS which is too thin and retreating too late. The index points produced in this thesis supports this hypothesis. The Bradley et al. model underestimates RSL during the Late Glacial and early Holocene in Assynt, suggesting more ice and therefore more rebound is needed in the region, whilst the timing of the Late Glacial RSL fall and early Holocene RSL rise is predicted too late.

In a future study, it would be beneficial to further investigate isolation basins at higher elevations within the Assynt region, such as those at a similar altitude to the basin at Oldany, and elsewhere in north west Scotland to see if further constraint can be applied to the Late Glacial part of the sequence. Additional sea-level index points, at or below the limiting point at Oldany, are needed to help constrain the marine limit in this region. There is also a need for more index points from lower altitudes to attempt to constrain the sea level lowstand at the Late Glacial to Holocene transition. Future developments resolving the uncertainties associated with the geomorphological data, such as research being undertaken by BRITICE-CHRONO, may result in a much thicker ice-sheet being reconstructed for Scotland which retreated earlier than currently predicted. If this is proven to be the case then post-LGM RSL would have been higher resulting in basins at altitudes higher than currently investigated being inundated during early deglaciation.

Appendices

Appendix 1

A1_1 Methodology for standard diatom preparation (Palmer & Abbott 1986; Battarbee 1986)

A sample weighing approximately 0.5 cc was placed into a polypropylene tube and 20 ml of hydrogen peroxide (400 ml of 30 % weight of volume hydrogen peroxide topped up to 2 litres with de-ionized water) was added in order to digest organic material. The organic material was removed to ensure optimum visibility when identifying the microfossils. These test tubes were covered with tin foil and placed overnight in a waterbath to enable digestion to occur. The samples were removed from the waterbath once the solution had turned clear and therefore digestion was complete. Samples were then centrifuged, at 4000 rpm for 4 minutes, and decanted to remove the hydrogen peroxide, following which they were topped up to 25 ml with distilled water.

Microscope slides were prepared by pipetting drops of the sample onto cover slips after drops of distilled water had been added. When the cover slips were dry, slides were labelled and drops of Naphrax added to each, to mount the cover slips. The cover slips were inverted and placed on top of the Naphrax and the slides were then placed on the hot plate. The slides remained on the hot plate until the toluene solvent was removed from the Naphrax.

A1_2 Alternative methodology for diatom preparation (Scherer 1994)

Preparation of the sediment for quantitative diatom assemblage analysis followed the settling technique of Scherer (1994), as adapted by C.S. Allen (E. Maddison, personal communication 2014). This method was used to determine absolute diatom concentration (diatoms valves per gram of dry sediment) and relative abundances of species within the total diatom assemblage. This settling procedure results in slides with an even distribution of valves with minimal clumping.

Approximately 0.005-0.01g of oven dried sample was weighed using a Mettler AE240 balance, placed in a glass vial (20 ml) and half filled with distilled water. Approximately 3 ml of hydrogen peroxide (30%) was added to oxidize organics and disaggregate particles and 1 ml of hydrochloric acid (50%) was added to remove any carbonate in the vial. The vials were left on a hotplate on a low setting for 6 hours. After oxidation 10 ml of dispersing agent (e.g. sodium hexametasulphate, prepared from 2 grammes of powder per 500 ml distilled water) was added and left for 1 hour. The vial containing the sample was then placed in an ultrasonic bath for 1-3 seconds to fully disaggregate the sample. The contents of the vial were then emptied into a clean 1 litre flat bottomed beaker filled

with distilled water. At the bottom of each beaker was a petri dish to which a slide was attached, and two cover slips were attached to this slide with a glue stick (or bluetack). The beaker was covered and after a period of four hours of settling the beaker was slowly drained (over a 12 hour period) from underneath the petri dish by a pipette held in place through a small hole in the petri dish. After allowing the cover slips to air dry, permanent slides were made using Norland Optical Adhesive (Refractive Index 1.56) and were cured with UV light.

Figure5.2
(a) Schematic of apparatus used in the preparationofquantitativelight microscope slides.Nine beakers are setup to produce 18 slides (two per sample).
(b)Photographof apparatusin(a).
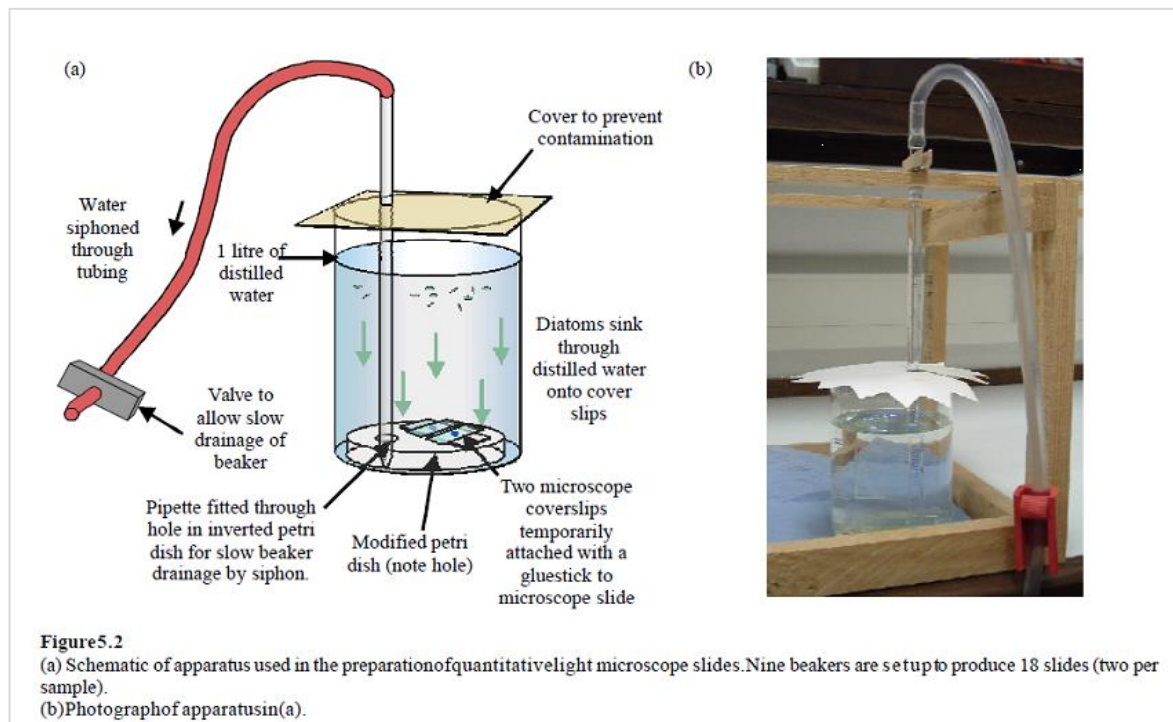
A1_3 Methodology for pollen preparation

Pollen preparation followed the standard methodology outlined by Moore et al. (1991). Following the removal of a 1 cm^3 sample, 20 ml of potassium hydroxide was added to the sample in a polypropylene tube and placed for 30 minutes in the water bath, were it was stirred occasionally. The sample was decanted through a 180 micron sieve and the residue was washed with distilled water and centrifuged at 4000 rpm for 4 minutes; this process was repeated until the supernatant liquid was unstained.

Hydrofluoric acid was added, to digest any siliceous material present, and the sample heated in boiling water until the sediment dispenses and stratified sediment appears. On completion, the sample was stirred, centrifuged and the supernatant decanted. Hydrochloric acid (10% solution) is then added and heated in boiling water for 3-5 minutes. Following this, it is centrifuged, decanted, washed with distilled water and then stirred, centrifuged and decanted once more.

After the sample has been transferred into small, narrow plastic tubes a number of procedures to evacuate unaltered lignin and cellulose must be implemented. Once 20 ml of glacial acetic acid has been added, the sample is stirred, centrifuged and decanted. A

20 ml mixture of acetylation (1 sulphuric acid: 9 acetic anhydride) is then added and stirred well and heated in boiling water for 1 minute. It is topped up with glacial acetic acid, centrifuged and the supernatant decanted, this is then repeated. Distilled water is then added, stirred, centrifuged and decanted twice.

The pollen is then stained by firstly washing the sample twice with ethanol, to remove the water, after which it is centrifuged and decanted. The samples are transferred into sample vials, centrifuged and decanted once 2 ml of tertiary butyl alcohol and 2 drops of safran in have been added. Silicone fluid, at the same volume as the sample, is added and the mixture is stirred and the vial plugged with cotton wool. The vials are left for several hours to allow the remaining tertiary butyl alcohol to evaporate.

Finally, the pollen slides are created by firstly adding several drops of silicon fluid onto each slide. After mixing the sample in the vial with a wooden stirrer, a small amount is extracted using the stirrer and mixed with the silicon fluid on the microscope slide. Following which, a coverslip is placed onto the microscope slide for analysis.

A1_4 Methodology for particle size analysis

Once the organic material was digested, the sample was centrifuged, the supernatant decanted and 20ml of distilled water added. Following which, 2ml of sodium hexametaphosphate solution (33 grams SHMP, 7g sodium carbonate, topped up to 1 litre with distilled water) was added to prevent clumping.

Pre-treated samples were sieved at 2mm to remove larger grains. Grains were added to a beaker of distilled water and placed in the Mastersizer/Coulter. The measurement was taken once the obscurity was between 10% and 15%, and not altering by more than one decimal place.

A1_5 Methodology for loss on ignition

A sample, weighing a minimum of 0.5 g, was dried overnight at 105°C and the dried weight recorded once removed from oven. The sample was then placed in the muffle furnace for 30 minutes at 850°C following which it was removed and placed in a desiccator to cool and prevent the influence of moisture. Once cool, the weight of the ash was recorded on a Mettler AE240 balance and the loss on ignition value calculated as a percentage of the weight of the oven dry soil.

Appendix 2

A2_1 Raw diatom counts for Loch na Claise

Diatom Species	Depth (cm): Group	508	516	524	530	561	593	626	658	688	720	749	784	816	848	852	856	860	864	868	869	871	872	873	874
Amphora turgida	P	0	0	0	0	0	0	0	0	0	0	0	0	0	0	0	1	0	0	0	0	0	0	0	0
Cocconeis scutellum	P	0	0	0	0	0	0	0	0	0	0	0	0	0	0	0	0	0	0	0	0	12	0	0	0
Navicula crucifera	P	0	0	0	0	0	0	0	0	0	0	0	0	0	0	0	0	0	0	0	0	0	0	1	0
Navicula directa var subtillis	P	0	0	0	0	0	0	0	0	0	0	0	0	0	0	0	0	0	0	0	0	0	0	2	0
Navicula distans	P	0	0	0	0	0	0	0	0	0	0	0	0	0	0	0	0	0	0	0	0	0	0	0	0
Navicula forcipata	P	0	0	0	0	0	0	0	3	0	0	0	0	0	0	0	0	0	0	0	0	0	0	0	0
Pleurosigma normanii	P	0	0	0	0	0	0	0	0	0	0	0	0	0	2	0	0	0	0	0	0	0	0	0	0
Achnanthes delicatula	M	0	0	0	0	0	0	0	0	0	0	0	0	0	0	0	0	0	0	0	0	0	0	0	1
Achnanthes lemmermannii	M	0	0	0	0	0	0	1	0	0	0	0	0	0	0	0	0	0	0	0	0	0	0	0	0
Amphora coffeaeformis	M	0	0	0	0	0	0	0	0	0	0	0	0	0	0	0	0	0	0	0	0	0	0	0	0
Amphora exigua	M	0	0	0	0	0	0	0	0	0	0	0	0	0	0	0	0	0	0	0	0	0	0	0	0
Caloneis Westii	M	0	0	0	0	0	0	0	0	0	0	0	0	0	0	0	0	0	0	0	0	0	0	0	0
Diploneis didyma	M	0	0	0	0	0	0	0	0	0	0	0	0	0	0	0	0	0	0	0	0	1	0	0	0
Navicula digitoradiata	M	0	0	0	0	0	0	0	0	0	0	0	0	0	0	0	0	0	0	0	0	0	0	0	0
Navicula gregaria	M	0	0	0	0	0	0	0	0	0	0	0	0	0	0	0	0	0	0	0	0	0	0	0	0
Navicula halophila	M	0	0	0	0	0	0	0	0	0	0	0	0	0	0	0	0	0	0	0	0	0	0	0	0
Navicula peregrina	M	0	0	0	0	0	1	0	0	0	0	0	0	0	0	0	0	0	0	0	1	0	0	0	0
Navicula phyllepta	M	0	0	0	0	0	0	0	0	0	0	0	0	0	0	0	0	0	0	0	0	0	0	0	0
Navicula Salinarum	M	0	0	0	0	0	0	0	0	0	0	0	0	0	0	0	0	0	0	0	0	0	0	0	1
Nitzschia sigma	M	0	0	0	0	0	0	0	0	0	0	0	0	0	0	0	0	0	0	0	0	0	0	0	0
Nitzschia vitrea	M	0	0	0	0	0	0	0	0	0	0	0	0	0	0	0	0	0	0	0	0	0	0	0	0
Opephora Schulzii	M	0	0	0	0	0	0	0	0	0	0	0	0	0	0	0	0	0	0	0	0	0	0	0	0
Amphora veneta	O-H	0	0	0	0	0	0	0	2	0	0	0	0	0	0	0	0	0	0	0	0	0	0	1	0
Cocconeis pediculus	O-H	0	0	0	0	0	0	0	0	0	0	0	0	0	0	0	0	0	3	0	2	0	0	0	0
Cyclotella pseudostelligera	O-H	0	0	0	0	0	0	0	1	0	0	0	0	0	0	0	0	0	0	0	0	0	0	0	0
Cymbella caespitosa	O-H	0	0	0	1	2	2	0	1	0	0	0	0	0	0	0	0	0	0	0	0	0	0	0	0
Navicula cari	O-H	0	0	0	0	0	0	0	0	0	0	0	0	0	0	0	0	0	0	0	0	0	0	0	0
Navicula cari var cincta	O-H	0	0	0	0	0	0	0	0	0	0	0	0	0	0	0	0	0	0	0	0	0	0	0	0

Species		1	2	3	4	5	6	7	8	9	10	11	12	13	14	15	16	17	18	19	20	21	22	23	24
Navicula Cincta	O-H	0	0	0	0	0	0	0	0	0	0	0	0	0	0	0	0	0	0	0	0	0	0	2	1
Navicula Cryptocephala	O-H	17	6	5	12	12	4	1	0	0	0	0	0	0	0	0	0	0	0	0	0	0	0	0	0
Nitzschia Frustulum	O-H	0	0	0	0	0	0	0	0	0	0	0	0	0	0	0	0	0	0	0	0	0	0	0	0
Rhopalodia gibberula	O-H	0	0	0	0	0	0	0	0	0	0	0	0	0	0	0	0	0	0	0	0	0	1	0	0
Achnanthes exilis	O-I	0	0	0	0	0	0	0	0	0	0	0	0	0	0	0	0	10	2	0	0	0	0	0	0
Achnanthes laterostrata	O-I	2	0	0	0	0	0	0	0	0	0	0	0	0	0	0	0	0	0	0	0	0	0	0	0
Achnanthes linearis	O-I	0	7	0	0	0	4	0	9	3	3	5	0	6	0	0	0	0	0	0	0	0	0	0	0
Achnanthes minutissima	O-I	0	12	8	0	0	7	12	0	16	7	4	3	17	0	0	0	0	0	0	0	0	0	0	0
Achnanthes saxonixa	O-I	0	0	0	0	0	0	0	0	0	0	0	0	0	0	0	0	0	0	0	0	0	0	0	0
Achnanthidium biasolettianum	O-I	0	0	0	0	0	0	0	0	0	0	0	0	0	0	0	0	0	0	0	0	0	0	0	0
Achnanthidium minutissimum	O-I	26	12	11	15	15	16	22	2	9	11	10	5	16	0	0	0	0	0	0	0	0	0	0	5
Amphora ovalis	O-I	0	0	0		0	0	0	0	0	0	0	0	0	0	0	0	0	0	0	0	26	0	19	24
Brachysira vitrea	O-I	17	24	11	22	25	17	16	9	26	12	11	15	7	0	0	0	1	0	0	0	0	0	2	1
Caloneis limosa	O-I	0	0	0	0	0	0	0	1	0	0	0	0	0	0	0	0	0	0	0	0	0	0	0	0
Caloneis silicula	O-I	0	0	0	0	0	0	0	0	0	0	1	2	0	0	0	0	0	0	0	0	0	0	0	0
Cocconeis placentula	O-I	0	0	2	1	2	2	1	0	0	1	1	0	1	0	0	0	0	0	0	0	0	0	0	0
Cyclotella glomerata	O-I	7	14	10	7	8	18	29	3	18	37	34	8	15	0	0	0	1	0	0	0	0	0	3	2
Cyclotella kuetzingiana var planetophora	O-I	0	0	0	0	0	0	0	0	0	0	0	0	0	0	0	0	0	0	0	0	0	0	0	0
Cyclotella kuetzingiana var radiosa	O-I	0	0	0	0	0	0	0	0	0	0	0	0	0	0	0	0	0	0	0	0	0	0	0	0
Cyclotella radiosa	O-I	20	13	19	11	14	20	25	15	13	17	20	19	24	0	4	4	9	3	1	0	4	0	4	3
Cymbella affinis	O-I	0	1	0	1	0	0	1	1	0	1	0	0	1	0	0	1	1	0	1	2	2	1	1	0
Cymbella angustata	O-I	2	5	0	0	3	6	12	19	15	8	10	13	10	0	0	0	0	0	0	0	0	0	0	4
Cymbella cornuta	O-I	0	0	0	0	0	0	0	0	0	0	0	0	0	0	0	0	0	0	0	0	0	0	0	0
Cymbella helvetica	O-I	0	1	1	0	0	0	3	1	1	0	0	0	1	0	0	2	0	0	0	1	0	0	0	0
Cymbella lunata	O-I	5	1	2	10	0	0	2	3	2	0	4	3	1	0	0	0	0	0	0	0	0	0	0	1
Cymbella microcephala	O-I	9	11	8	8	8	7	13	4	11	4	8	8	12	0	0	0	0	0	0	1	0	0	0	0
Cymbella naviculiformis	O-I	0	0	0	0	0	0	0	0	0	0	0	0	0	2	0	0	0	0	0	0	0	0	0	0
Cymbopleura subaequalis	O-I	0	0	2	3	7	3	2	0	1	0	1	3	0	0	0	0	0	0	0	0	0	0	0	0
Denticula kuetzingii	O-I	1	1	1	1	1	1	0	3	0	0	1	3	4	0	0	3	10	4	1	2	1	0	1	0
Diploneis Elliptica	O-I	1	0	2	2	0	3	1	3	1	0	0	0	1	0	0	0	0	0	0	0	73	61	121	111
Diploneis ovalis	O-I	0	0	2	0	0	0	0	0	0	1	1	1	3	0	0	0	0	0	0	0	0	0	0	1
Encyonema minutum	O-I	0	0	0	0	0	0	0	0	0	0	0	0	0	0	0	0	0	0	0	0	0	0	2	0
Epithemia adnata	O-I	0	1	0	2	1	0	0	0	0	0	1	0	0	0	0	0	0	0	0	0	2	0	0	0

Species		1	2	3	4	5	6	7	8	9	10	11	12	13	14	15	16	17	18	19	20	21	22	23	24
Epithemia sorex	O-I	5	3	6	4	10	7	5	11	3	11	26	28	3	0	0	0	11	19	2	4	8	0	3	1
Epithemia adnata var porcellus	O-I	0	0	0	0	0	0	0	1	0	0	0	0	0	0	0	0	0	0	0	0	9	0	0	1
Epithemis turgida	O-I	0	0	0	0	0	0	0	0	0	0	0	0	0	0	0	0	3	0	0	0	0	0	0	0
Eucocconeis flexella	O-I	7	4	7	2	3	4	6	2	6	8	8	7	4	1	0	0	0	0	7	2	1	0	3	1
Eunotia curvata	O-I	0	0	0	0	0	0	1	0	0	0	0	0	0	0	0	0	0	0	0	0	0	0	0	0
Eunotia pectinalis	O-I	0	0	0	0	0	0	0	0	0	0	0	0	0	0	0	0	0	0	0	0	0	0	0	0
Eunotia pectinalis fo Impressa	O-I	2	3	4	1	2	4	3	2	1	1	1	4	1	0	0	0	0	0	0	0	0	0	1	2
Fragilaria construens	O-I	2	4	4	5	8	11	5	13	6	7	4	11	12	39	98	167	78	123	236	238	31	8	18	52
Fragilaria construens var binodis	O-I	0	0	0	0	0	0	0	0	0	0	0	0	0	0	6	25	29	37	7	0	0	0	0	0
Fragilaria vaucheriae	O-I	0	0	0	0	0	2	0	0	0	0	0	0	1	0	0	0	0	0	0	0	0	0	0	0
Fragilariforma virescens	O-I	56	39	47	42	42	32	22	37	41	31	19	30	23	2	11	2	0	0	0	2	3	0	0	4
Gomphonema accum. var corronation	O-I	0	0	0	1	0	0	0	1	0	0	0	0	0	0	0	1	4	0	0	1	2	0	0	0
Gomphonema angustatum	O-I	2	5	4	4	4	7	3	5	4	1	2	4	2	1	0	0	0	0	0	1	1	0	0	0
Gomphonema angustum	O-I	0	0	0	1	0	0	0	0	0	0	0	0	0	0	0	0	0	0	0	0	0	0	0	1
Gomphonema gracile	O-I	0	0	0	0	1	0	1	0	0	1	2	0	0	0	0	0	0	0	0	0	0	0	0	0
Gomphonema olivaceum	O-I	0	0	2	0	0	0	0	1	0	0	0	0	1	0	0	0	0	0	0	0	0	0	0	0
Gomphonema olivaceum var calcareum	O-I	0	0	0	0	0	0	0	0	0	0	0	2	0	0	0	0	0	0	0	0	0	0	0	0
Gomphonema truncatum	O-I	0	0	0	0	0	0	0	0	0	0	0	0	0	0	0	0	0	0	0	0	1	0	0	0
Gyrosigma acuminatum	O-I	0	0	0	0	0	0	0	1	0	0	0	0	0	0	0	0	0	0	0	0	0	0	0	0
Mastogloia smithii	O-I	0	0	2	4	5	1	5	6	2	5	7	12	6	0	0	0	0	0	0	0	0	0	0	0
Mastogloia elliptica var dansei	O-I	1	0	0	0	0	0	0	0	0	0	0	0	0	0	0	0	0	0	0	0	0	0	2	0
Mastogloia smithii var amphicephala	O-I	0	1	0	2	3	1	0	0	2	1	3	3	3	0	0	0	0	0	0	1	0	0	0	0
Navicula begeri	O-I	0	0	0	0	0	0	0	0	0	0	0	0	0	0	0	0	0	0	0	0	0	0	0	0
Navicula brookmannii	O-I	0	0	0	0	0	0	0	0	0	0	0	0	0	0	0	0	0	0	0	0	0	0	0	0
Navicula pupula	O-I	1	1	3	2	2	1	0	3	1	1	0	0	1	0	0	0	0	0	0	0	0	0	0	0
Navicula pusilla	O-I	0	0	0	0	0	0	4	0	2	0	0	1	0	0	0	0	0	0	0	0	0	0	0	0
navicula radiosa	O-I	8	13	10	18	17	13	16	4	7	2	15	18	8	0	1	0	0	1	0	0	0	0	4	3
Navicula rhynchocephala	O-I	0	0	0	0	0	0	0	0	0	0	0	0	0	0	0	0	0	0	0	0	0	0	0	0

Species																									
Navicula tripunctata	O-I	3	0	0	0	0	0	0	0	0	0	0	0	0	0	0	0	0	0	0	0	0	0	0	0
Navicula tuscula	O-I	0	0	0	0	0	0	0	1	0	0	0	0	0	0	0	0	0	0	0	0	0	0	0	0
Nitzschia amphibia	O-I	0	0	0	0	0	0	0	0	0	0	0	0	0	0	0	0	0	0	0	0	0	0	0	0
Nitzschia dissipata	O-I	0	0	0	0	0	0	0	0	0	0	0	0	0	0	0	0	0	0	0	0	0	0	0	0
Nitzschia fonticola	O-I	4	6	1	4	0	1	1	4	1	1	0	2	1	0	0	0	0	0	0	0	0	0	0	0
Nitzschia palea	O-I	0	1	1	1	4	1	1	1	2	0	1	0	1	0	0	0	0	0	0	0	0	0	0	0
Nitzschia pseudofonticola	O-I	0	0	0	0	0	0	0	0	0	2	0	0	0	0	0	0	0	0	0	0	0	0	0	0
Pinnularia abaujensis	O-I	0	0	2	2	0	0	1	4	0	0	2	0	0	0	0	0	0	0	0	0	0	0	0	0
Pinnularia biceps	O-I	0	0	0	0	0	0	0	0	0	0	0	0	0	0	0	0	0	0	0	0	0	0	0	0
Pinnularia brebissonii	O-I	1	0	0	0	0	0	0	0	0	0	0	0	0	1	0	0	0	0	0	0	0	0	0	0
pinnularia mesolepta	O-I	0	0	0	0	0	2	0	0	1	2	1	0	2	0	0	0	0	0	0	0	0	0	0	0
Pinnularia microstauron	O-I	1	2	3	5	4	7	3	0	2	0	1	7	0	0	1	1	1	0	0	0	0	0	0	1
Pinnularia major	O-I	0	0	0	1	0	1	0	0	2	0	1	0	0	1	0	0	0	0	0	0	0	0	0	0
Pinnularia viridis	O-I	0	0	0	1	0	0	1	0	0	0	0	0	0	0	0	0	0	0	0	0	0	0	0	0
Placoneis elginensis	O-I	0	0	0	0	0	0	0	0	0	1	0	0	0	0	0	0	0	0	0	0	1	0	0	0
Pseudostaurosira brevistriata	O-I	0	0	0	0	1	0	3	3	0	0	1	1	3	16	0	0	0	0	0	0	0	0	0	0
Rhopalodia gibba	O-I	0	0	0	1	0	0	0	0	0	0	0	0	0	0	0	0	0	0	0	0	1	0	0	0
Rhopalodia gibba var parallela	O-I	1	0	0	0	0	0	0	0	0	0	2	3	2	0	0	1	1	3	1	3	25	0	4	0
Stauroneis anceps fo gracilis	O-I	0	0	0	0	0	0	2	0	0	0	0	0	0	0	0	0	0	0	0	0	0	0	0	0
Stauroneis phoenicenteron	O-I	0	0	1	2	1	0	1	1	0	1	0	1	0	0	0	0	0	0	0	0	0	0	0	0
Stauroneis smithii	O-I	0	0	0	0	0	0	0	0	0	0	0	0	0	0	0	0	0	0	0	0	0	0	0	0
Staurosirella lapponica	O-I	0	0	0	0	0	0	0	0	0	0	0	0	0	0	3	11	3	5	0	0	0	0	0	0
Staurosirella pinnata	O-I	0	0	1	1	1	1	0	0	0	0	3	0	1	193	148	59	90	51	4	7	0	3	1	7
Surirella linearis	O-I	0	0	1	0	0	0	0	1	0	0	0	1	0	0	0	0	0	0	0	0	0	0	0	0
Synedra Parasitica	O-I	0	0	0	0	0	0	0	0	0	0	0	0	0	3	0	0	0	0	0	0	33	0	19	9
Synedra Ulna	O-I	0	0	0	0	0	0	0	0	0	0	0	0	0	0	0	0	0	0	0	0	0	0	0	0
Achnanthes pusilla	H	0	0	0	0	0	0	0	0	0	0	0	0	0	0	0	0	0	0	0	0	0	0	0	0
Amphora normanii	H	0	0	0	0	0	0	0	0	0	0	0	0	0	0	0	0	0	0	0	0	0	0	12	3
Cavinula cocconeiformis	H	0	0	0	0	0	0	0	3	0	0	0	0	0	0	0	0	0	0	0	0	0	0	0	0
Cyclotella antiqua	H	0	0	0	0	1	0	0	0	0	0	0	0	0	2	0	0	0	2	2	1	10	0	2	2
Cymbella amphicephala	H	0	0	0	0	0	0	0	0	0	0	0	0	0	0	0	0	0	0	0	0	0	0	0	0
Cymbella hebridica	H	0	0	0	1	1	1	4	3	1	1	2	1	1	0	1	1	1	0	0	0	4	0	0	1
Cymbella parva	H	0	0	0	0	0	0	0	0	0	0	0	0	0	0	0	0	0	0	0	0	0	0	0	0
Cymbella perpusilla	H	4	0	1	0	0	0	0	0	0	0	0	0	0	0	0	0	0	0	0	0	0	0	0	0
Denticula tenuis	H	0	0	0	0	0	0	0	0	1	0	1	0	1	0	0	0	0	0	0	1	0	0	0	0

Species																									
Encyonema perpusilla	H	0	0	0	0	0	0	0	0	0	0	0	0	0	0	0	0	0	0	0	0	0	0	1	0
Eunotia arcus	H	2	3	1	3	1	0	1	4	2	0	1	4	1	0	2	5	19	7	1	0	0	0	0	1
Eunotia exigua	H	0	0	0	0	0	0	1	0	0	0	0	0	0	0	0	0	0	0	0	0	0	0	0	0
Eunotia fallax	H	0	1	0	0	0	0	0	0	0	0	1	0	0	0	0	0	0	0	0	0	0	0	0	0
Eunotia praerupta	H	0	0	0	0	0	0	0	0	0	0	0	0	0	0	0	0	0	0	0	0	0	0	0	0
Frustulia rhomboides	H	1	6	7	4	4	3	3	5	0	0	1	3	0	0	0	0	0	0	0	0	0	0	0	0
Navicula cocconeiformis	H	1	2	0	0	0	0	0	0	0	0	0	0	0	0	0	0	0	0	0	0	0	0	0	0
Navicula Laevissima	H	0	1	0	0	0	0	0	1	0	0	0	0	0	0	0	0	0	0	0	0	0	0	0	0
navicula subtilissima	H	0	0	0	0	0	0	0	0	0	0	0	0	0	0	0	0	0	0	0	0	0	0	0	0
Nitzschia gracilis	H	0	0	0	0	0	0	0	0	0	0	0	0	0	0	0	0	0	0	0	0	0	0	0	0
Pinnularia appendiculata	H	0	1	0	0	0	0	0	0	0	0	0	0	0	0	0	0	0	0	0	0	0	0	1	0
Pinnularia stomatophora	H	0	0	0	0	0	0	0	0	0	0	0	0	0	0	0	0	0	0	0	0	0	0	0	0
Surirella robusta	H	0	0	0	0	0	0	0	0	0	0	0	0	0	0	0	0	0	0	0	0	0	0	0	0
Tabellaria fenestrata	H	3	5	4	4	4	7	4	6	4	8	4	5	2	0	0	0	0	0	0	0	0	1	0	0
Tabellaria flocculosa	H	24	15	31	21	19	18	27	23	23	49	21	29	24	6	2	2	10	5	1	2	9	0	3	2
Achnanthidium thermale	U	4	8	3	0	9	1	1	0	6	3	0	0	1	0	0	0	0	0	0	0	0	0	0	0
Psammothdium laurenbergianum	U	0	0	0	0	0	0	0	0	0	0	0	0	0	0	0	0	0	0	0	0	0	0	0	0
Planothidium conspicum	U	0	0	0	0	0	0	0	0	0	0	0	0	0	0	0	0	0	0	0	0	0	0	0	0
Amphora copulata	U	0	0	0	1	0	1	1	3	0	0	0	1	0	0	0	0	0	0	0	3	3	0	0	0
Amphora eximia	U	0	0	0	0	0	0	0	0	0	0	0	0	0	0	0	0	0	0	1	0	0	0	0	0
Halamphora subholsatica	U	0	0	0	0	0	0	0	0	0	0	0	0	0	0	0	0	0	0	0	0	0	0	0	0
Amphora pediculus	U	0	0	0	0	0	0	0	3	0	0	0	0	0	0	0	0	0	0	0	0	0	15	0	6
Aneumastus tusculus var capitata	U	0	0	0	0	0	0	0	0	0	0	0	0	0	0	0	0	0	0	2	0	0	0	0	0
Brachysira brebissonii	U	0	0	0	0	0	0	1	0	0	0	1	1	0	0	0	2	0	0	0	0	0	0	1	0
Brachysira brebissonii fo Thermalis	U	5	7	3	3	5	1	3	1	3	1	1	4	0	0	0	0	0	0	0	0	0	0	2	0
Brachysira styriaca	U	13	9	18	6	13	19	7	8	10	17	10	5	11	0	0	0	0	0	0	0	0	0	2	3
Caloneis alpestris	U	0	0	0	0	0	0	1	0	0	0	0	2	0	0	0	0	0	0	0	0	0	0	0	0
Caloneis bacillaris	U	0	0	0	0	0	0	1	1	0	0	0	0	0	0	0	0	0	0	0	0	0	0	0	0
Caloneis borealis	U	0	0	0	0	0	0	0	0	0	0	0	0	0	0	0	0	0	0	0	0	0	0	0	0
Caloneis lepidula	U	0	0	0	0	0	0	1	2	0	0	0	0	0	0	0	0	0	0	0	0	0	0	0	0
Caloneis undulata	U	0	0	0	0	0	0	0	0	0	0	1	1	0	0	0	0	0	0	0	0	0	0	0	0
Cavinula cocconeiformis	U	0	0	0	0	0	0	0	0	0	0	0	0	0	0	0	1	0	0	0	0	0	0	0	0
Cyclotella atomus	U	0	0	0	0	0	0	0	0	0	0	0	0	0	0	0	0	0	0	0	0	0	0	0	0

Cyclotella distinguenda	U	0	0	0	0	0	0	0	0	0	0	0	0	0	0	0	1	0	0	0	0	0	0	0	0
Cyclotella woltereckii	U	0	0	0	0	0	0	0	0	0	0	0	0	0	0	0	0	0	0	0	0	0	0	0	0
Cymbella amphioxys	U	0	0	0	0	0	0	0	0	0	0	0	0	0	0	0	0	0	0	0	0	0	0	0	0
Delicata delicatula	U	1	2	0	0	3	0	1	0	1	1	0	2	0	0	0	0	0	0	0	0	0	0	0	0
Cymbella descripta	U	0	0	0	0	0	0	0	0	0	0	0	0	0	0	0	0	0	0	0	0	0	0	0	0
Cymbella excisiformis	U	0	0	0	0	0	0	0	0	0	0	0	0	0	0	0	0	0	0	0	0	0	0	0	0
Encyonema gaeumanni	U	0	0	3	0	0	0	0	0	0	0	0	0	0	0	0	0	0	0	0	0	0	0	0	0
Cymbella laevis	U	1	0	0	0	0	0	0	0	0	0	0	0	0	1	2	1	0	0	0	0	0	0	0	0
Cymbella ovalis	U	0	0	0	0	0	0	0	0	0	0	0	0	0	0	0	0	0	0	0	0	0	0	0	0
Cymbella Paucistriata	U	0	0	0	0	0	0	0	0	0	0	0	0	0	0	0	0	0	0	0	0	0	0	0	0
Navicymbula pusilla	U	0	0	0	0	0	0	0	0	0	0	0	0	0	0	0	0	0	0	0	0	0	0	0	0
Encyonema silesiacum	U	0	0	2	0	1	0	0	0	2	0	1	0	0	0	0	0	0	0	0	0	0	0	0	0
Eunotia naegeli	U	0	1	0	0	0	0	0	0	0	0	1	0	0	0	0	0	0	0	0	0	0	0	0	0
Eunotia subtillissima	U	0	1	0	0	0	0	0	0	0	0	0	0	0	0	0	0	0	0	0	0	0	0	0	0
Eunotia sudetica	U	0	0	0	0	0	0	0	0	0	0	0	0	0	0	0	0	0	0	0	0	0	0	0	0
Eunotia quaternaria	U	0	0	0	0	0	0	0	0	0	0	0	0	0	0	0	0	0	0	0	0	0	0	0	0
Fragilaria crotonensis	U	1	2	0	0	0	0	0	0	0	0	0	0	0	0	0	0	0	0	0	0	0	1	0	0
Gomphonema auritum	U	0	0	0	0	0	0	1	0	0	0	0	0	0	0	0	0	0	0	0	0	0	0	0	0
Gomphonema dichotomum	U	0	0	0	1	0	0	0	0	0	0	0	0	0	0	0	0	0	0	0	0	0	0	0	0
Gomphonema hebridense	U	0	0	0	0	0	0	0	1	0	2	0	0	0	0	0	0	0	0	0	0	0	0	0	0
Gomphonema rhombicum	U	0	0	0	0	0	0	0	0	0	0	0	0	1	0	0	0	0	0	0	0	0	0	0	0
Navicula Angusta	U	0	0	0	0	0	0	0	0	0	0	0	0	0	0	0	0	0	0	0	0	0	0	0	0
Navicula Capitoradiata	U	0	0	0	0	0	0	0	0	0	0	0	0	0	0	0	0	0	0	0	0	0	0	0	0
Navicula detenta	U	0	0	0	0	0	0	0	0	0	0	0	0	0	0	0	0	0	0	0	0	0	0	0	0
Navicula glacialis	U	0	0	0	0	0	0	0	0	0	0	1	0	0	0	0	0	0	0	0	0	0	0	0	0
Navicula gottlandica	U	0	0	0	0	0	0	0	0	0	0	0	0	0	0	0	0	0	0	0	0	0	0	0	0
Navicula hemiptera	U	0	0	0	0	0	0	0	1	0	0	0	0	0	0	0	0	0	0	0	0	0	0	0	0
Fallacia hudsonis	U	0	0	0	0	0	0	0	0	0	0	0	0	0	0	0	0	0	0	0	0	0	1	0	0
Navicula ilopangoensis	U	0	0	0	0	0	0	0	0	0	0	0	0	0	0	0	0	0	0	0	0	0	0	0	0
Navicula salinicola	U	0	0	0	0	0	0	0	0	0	0	0	0	0	0	0	0	0	0	0	0	0	0	0	0
Navicula margalithii	U	0	0	0	0	0	0	0	0	0	0	0	0	0	0	0	0	0	0	0	0	0	0	0	0
Navicula pseudobryophila	U	0	0	0	0	0	0	0	0	0	0	0	0	0	0	0	0	0	0	0	0	0	0	0	0
Geissleria similis	U	0	0	0	0	0	0	0	0	0	0	0	0	0	0	0	0	0	0	0	0	0	0	0	0
Navicula Striolata	U	0	0	0	0	0	4	1	0	0	0	0	0	1	0	0	0	0	1	0	0	0	0	2	0
Navicula subinflatoides	U	0	0	0	0	0	0	0	0	0	0	0	0	0	0	0	0	0	0	0	0	0	0	0	0
Navicula toulae	U	0	0	0	0	0	0	0	1	0	0	0	0	0	0	0	0	0	0	0	0	0	0	0	0
Nitzschia Amphiplectans	U	0	0	0	0	0	0	0	0	0	0	0	0	0	0	0	0	0	0	0	0	0	0	0	0

Species		1	2	3	4	5	6	7	8	9	10	11	12	13	14	15	16	17	18	19	20	21	22	23	24
Nitzschia bryophila	U	0	0	0	0	0	0	0	0	0	0	0	0	0	0	0	0	0	0	0	0	0	0	0	0
Nitzschia capitellata	U	0	0	0	0	0	0	0	0	0	0	0	0	0	0	0	0	0	0	0	0	0	0	0	0
Nitzschia heufleriana	U	0	0	0	0	0	0	0	0	0	0	0	0	0	0	0	0	0	0	0	0	0	0	0	0
Nitzschia ovalis	U	0	0	0	0	0	0	0	0	0	0	0	0	0	0	0	0	0	0	0	0	0	0	0	0
Nitzschia paleacea	U	2	1	3	6	0	3	10	0	1	1	1	2	5	0	0	0	0	0	0	0	0	0	0	0
Nitzschia pumila	U	0	1	0	2	0	0	0	0	0	0	0	0	0	0	0	0	0	0	0	0	0	0	0	0
Nitzschia pura	U	0	0	0	0	0	0	0	0	0	0	0	0	0	0	0	0	0	0	0	0	0	0	0	0
Nitzschia sociabilis	U	1	1	5	0	0	0	3	1	0	1	0	0	0	0	0	0	0	0	0	0	0	0	1	0
Nitzschia supralittorea	U	2	3	2	2	0	2	0	0	0	0	0	0	0	0	0	0	0	0	0	0	0	0	0	0
Pinnularia bipectinalis	U	0	0	0	0	0	0	0	0	0	0	0	0	0	0	0	0	0	0	0	0	0	0	0	0
Pinnularia Dactylus	U	0	0	0	0	0	0	0	0	0	0	0	0	0	0	0	0	0	0	0	0	0	0	0	0
Pinnularia divergentissima	U	0	0	0	0	0	0	0	0	0	0	0	0	0	0	0	0	0	0	0	0	0	0	0	0
Pinnularia episcopalis	U	0	0	0	0	0	0	0	0	0	0	0	0	0	0	0	0	0	0	0	0	0	0	0	0
Pinnularia hemoptera	U	0	0	0	0	0	0	0	0	0	1	0	0	0	0	0	0	0	0	0	0	0	0	0	0
Pinnularia obscura	U	0	0	0	0	0	0	0	0	0	0	0	0	0	0	0	0	0	0	0	0	0	0	2	0
Pinnularia Rectangulata	U	0	0	0	0	0	0	0	0	0	0	0	0	0	0	0	0	0	0	0	0	0	0	0	0
Pinnularia subrostrata	U	0	0	0	0	0	0	0	1	0	0	0	0	0	0	0	0	0	0	0	0	0	0	0	0
Pinnularia transversa	U	0	0	0	0	0	0	0	0	1	0	0	0	0	0	0	0	0	0	0	0	0	0	0	0
Rhopalodia rupestris	U	1	0	0	0	0	1	0	0	0	0	0	0	0	0	0	0	0	0	0	0	0	0	0	0
Stauroneis agresti	U	0	0	0	0	0	0	0	0	0	0	0	0	0	0	0	0	0	0	0	0	0	0	0	0
Stauroneis alpina	U	0	0	0	0	0	0	0	0	0	0	0	0	0	0	0	0	2	0	0	0	1	0	0	0
Stauroneis kriegeri	U	0	0	0	1	0	0	0	0	0	0	0	0	0	0	0	3	0	0	0	0	0	0	0	0
Stauroneis lauenbergianna	U	0	0	0	0	0	0	0	0	0	0	0	0	0	0	0	0	0	0	0	0	0	0	0	0
Stauroneis muriella	U	0	0	0	0	0	0	0	0	0	0	0	0	0	0	0	0	8	6	1	0	0	0	0	0
Stauroneis rossii	U	0	0	0	0	0	0	0	0	0	0	0	0	0	0	0	0	0	0	0	0	0	0	0	0
Stauroneis tackei	U	0	0	0	0	0	0	0	0	0	0	0	0	0	0	0	0	0	0	0	0	0	0	0	1
Pseudotaurosira elliptica	U	0	0	0	0	0	0	0	1	2	1	0	0	0	0	0	0	0	0	0	0	0	0	1	0
Staurosirella leptostauron	U	0	0	0	0	0	0	0	0	0	0	0	0	0	1	2	0	0	1	0	0	0	0	0	0
Synedra nana	U	0	0	0	0	0	0	0	0	0	0	0	0	0	0	0	0	0	0	0	0	0	0	0	0
Navicula caroliniania	U	7	6	0	0	0	0	0	3	0	0	0	0	0	0	0	0	0	0	0	0	0	0	0	0
Total # of species:		274	267	266	255	267	268	297	254	256	264	259	276	243	270	283	294	287	280	266	275	281	75	250	250

Appendix 2

A2_2 Raw diatom counts for Oldany

Diatom Species	Depth (cm): Group	609	633	666	674	682	690	710
Nitzschia archibaldii	P	0	0	0	2	0	0	0
Achnanthes lemmermannii	M	0	0	2	1	0	0	0
Cocconeis pediculus	O-H	0	0	1	1	0	0	0
Cyclotella pseudostelligera	O-H	0	0	1	0	0	0	0
Navicula avenacea	O-H	0	0	0	1	0	0	0
Navicula cincta	O-H	0	0	3	0	0	0	0
Navicula cryptocephala	O-H	0	0	1	7	0	0	0
Achnanthes exilis	O-I	0	0	0	0	1	0	0
Achnanthes kryophila	O-I	0	0	3	0	0	0	0
Achnanthes Linearis	O-I	1	1	18	33	0	0	0
Achnanthes microcephala	O-I	7	10	2	0	4	3	0
Achnanthes minutissima	O-I	2	6	1	0	0	0	2
Brachysira vitrea*	O-I	14	11	20	43	80	2	16
Caloneis bacillum	O-I	0	1	0	0	0	0	0
Caloneis silicula	O-I	1	0	0	0	0	0	0
Cocconeis placentula	O-I	3	1	0	0	0	0	0
Cyclotella glomerata*	O-I	34	30	83	49	42	1	6
Cyclotella radiosa	O-I	18	4	9	3	39	3	4
Cymbella angustata	O-I	4	4	1	0	0	0	0
Cymbella affinis	O-I	1	0	0	5	2	3	0
Cymbella cymbiformis car nonpunctata	O-I	1	0	0	0	0	0	0
Cymbella helvetica	O-I	1	0	0	0	0	0	1
Cymbellla leptoceros	O-I	0	0	0	0	0	0	3
Cymbella microcephala	O-I	4	3	9	4	0	0	1
Cymbella subaequalis	O-I	1	0	0	0	0	0	0
Diploneis elliptica	O-I	2	0	0	0	0	0	0
Diploneis ovalis	O-I	5	0	0	0	0	0	1
Epithemia sorex	O-I	9	0	0	0	1	5	5
Eucoconeis flexuosa	O-I	2	0	0	0	0	0	0

Eunotia flexuosa	O-I	0	1	0	0	0	0	0
Eunotia pectinalis fo impressa	O-I	0	3	0	0	0	0	2
Fragilaria construens	O-I	0	44	12	6	2	187	98
Fragilariforma virescens	O-I	40	69	13	25	16	4	32
Gomphonema acuminatum var. coronatum	O-I	2	0	0	0	1	0	0
Gomphonema angustatum	O-I	5	2	0	1	3	0	1
Gomphonema gracile	O-I	2	1	0	0	0	0	0
Mastogloia smithii	O-I	0	0	1	0	0	0	0
Navicula pupula	O-I	1	0	0	0	0	0	0
Navicula radiosa	O-I	5	2	1	3	1	4	0
Navicula rhynchocephala	O-I	0	0	0	0	1	0	0
Nitzschia amphibia	O-I	0	0	5	9	0	0	0
Nitzschia fonticola	O-I	1	1	20	15	4	2	0
Nitzschia palaecea	O-I	3	3	19	9	5	1	0
Nitzschia palea	O-I	1	0	0	0	0	0	0
Pinnularia abaujensis	O-I	1	0	0	0	0	0	0
Pinnularia major	O-I	1	0	0	0	0	0	0
Pinnularia mesolepta	O-I	5	0	0	1	0	0	0
Pinnularia microstauron	O-I	2	0	0	0	0	0	0
Pseudostaurosira brevistriata	O-I	1	13	0	0	0	0	4
Rhopalodia gibba var parallela	O-I	0	0	0	0	0	0	1
Stauroneis phoenicenteron	O-I	1	0	0	1	0	0	2
Staurosirella pinnata	O-I	0	1	4	0	1	35	28
Synedra parasitica	O-I	1	7	0	0	0	0	0
Synedra parasitica var subconstricta	O-I	1	2	0	0	0	0	0
Cyclotella antiqua	H	0	0	0	1	3	0	2
Cymbella hebridica	H	1	0	1	1	0	0	2
Denticula tenuis	H	4	1	1	5	3	2	2
Eunotia arcus	H	6	2	0	1	1	1	9
Frustulia rhomboides	H	1	0	0	0	0	0	0
Pinnularia appendiculata	H	0	0	0	1	0	0	0
Pinnularia subcapitata	H	1	0	0	0	0	0	0
Tabularia fennostrata	H	1	1	1	0	6	3	1
Tabularia flocculosa	H	21	11	4	2	14	5	18
Achnanthidium thermale	U	4	5	1	1	0	1	4
Achnanthes minutissima var jacki	U	0	0	2	0	0	0	0
Achnanthes ploenesis	U	0	0	0	1	0	0	0

Brachysira brebissonii	U	4	2	5	11	1	0	1
Brachysira brebissonii fo thermalis	U	4	1	1	0	4	0	5
Brachysira styriaca	U	12	9	9	0	10	0	5
Caloneis borealis	U	1	0	0	0	0	0	0
Cyclotella comensis	U	0	0	1	0	4	0	0
Cymbella delicatula	U	0	2	0	0	0	0	4
Cymbella descripta	U	0	0	1	0	0	0	0
Cymbella gracile	U	4	3	0	3	0	0	0
Cymbella laevis	U	0	0	0	0	1	0	0
Cymbella perpusilla	U	0	0	0	1	0	0	0
Denticula kuetzingii	U	0	1	1	0	0	9	0
Gomphonema sphaerophorum	U	0	0	1	0	0	0	0
Nitzschia disjuncta	U	0	0	1	0	0	0	0
Navicula pseudobryophila	U	0	0	0	0	1	0	0
Navicula styriaca	U	0	0	0	6	0	0	0
Nitzschia pumila	U	0	0	0	1	0	0	0
Nitzschia sociablis	U	1	2	12	7	2	0	2
Nitzschia stryriaca	U	0	0	0	0	0	1	0
Nitzschia supralittorea	U	0	0	2	1	1	0	0
Stauroneis alpina	U	0	0	0	0	0	1	0
Staurosira elliptica	U	0	0	1	0	0	0	3
Tabularia fasciculata	U	0	0	0	0	0	3	0
Total # of species:		248	260	274	262	254	276	265

Appendix 2

A2_3 Raw diatom counts for Duart Bog

Diatom Species	Depth (cm):	364	380	396	408	412	416	420	422	424	425	426	427	428	429	430
	Group															
Amphora bacillaris	P	0	0	4	0	0	0	0	0	0	0	0	0	0	0	0
Caloneis Crassa	P	0	0	0	0	0	0	0	0	0	0	1	0	0	0	0
Cocconeis Scrutellum	P	0	0	0	0	0	0	0	0	0	0	0	0	0	1	0
Diploneis Didyma	M	0	0	0	0	0	0	0	0	3	1	70	84	70	55	49
Diploneis interrupta	M	0	0	0	0	0	0	0	0	0	0	0	2	0	0	1
Navicula digitoradiata	M	0	0	0	0	0	1	0	0	0	0	0	0	0	1	0
Navicula gregaria	M	0	0	0	1	0	0	0	0	0	0	0	0	0	0	0
Navicula halophila	M	0	0	0	1	0	0	0	0	0	0	0	0	0	0	0
Scolioneis tumida	M	0	0	0	0	0	0	0	0	0	0	64	74	16	64	78
Amphora veneta	O-H	0	0	0	0	0	4	0	0	0	0	0	0	0	0	0
Cocconeis pediculus	O-H	0	0	0	0	0	0	0	0	0	0	0	0	0	0	1
Cyclotella antiqua	O-H	0	0	0	1	4	1	1	1	6	1	0	0	1	0	0
Cymbella microcephala	O-H	0	1	9	0	0	5	3	0	1	0	0	0	0	0	0
Navicula cari	O-H	0	0	0	2	0	0	0	0	0	0	0	0	0	0	0
Navicula cari var cincta	O-H	0	0	0	0	0	0	0	0	0	0	0	0	1	0	0
Navicula cryptocephala	O-H	0	0	1	0	0	0	0	0	0	0	0	0	0	0	0
Rhopalodia gibberula	O-H	0	0	0	2	0	0	0	0	0	0	0	0	0	0	0
Achnanthes exilis	O-I	0	5	0	1	0	0	1	0	0	0	0	0	0	0	0
Achnanthes microcephala	O-I	1	15	5	0	0	0	0	0	0	0	0	0	0	0	0
Amphora ovalis	O-I	0	1	0	0	0	0	0	0	0	0	0	0	2	0	0
Brachysira brebissonii	O-I	5	1	34	9	0	33	36	8	10	11	2	0	8	6	5
Brachysira brebissonii fo Thermalis	O-I	11	18	21	0	0	8	6	6	2	4	0	0	0	0	1
Brachysira styriaca	O-I	3	17	6	3	1	1	2	0	1	0	0	0	0	0	0
Brachysira vitrea	O-I	0	5	28	8	0	6	11	1	1	3	0	0	0	0	1
Cocconeis placentula	O-I	2	1	1	0	0	0	0	0	0	0	0	0	0	0	0
Cyclotella radiosa	O-I	1	7	11	2	2	4	7	4	11	3	0	0	0	2	2
Cymbella affinis	O-I	0	6	12	0	0	3	3	1	1	1	0	0	2	0	1
Cymbella angustata	O-I	0	2	4	1	0	0	0	0	0	0	0	0	0	1	2
Cymbella aspera	O-I	0	1	0	0	0	0	0	0	0	0	0	0	0	0	0

Cymbella cistula	O-I	1	0	1	0	0	0	0	0	1	0	0	0	0	0	0
Cymbella cistula var maculata	O-I	0	0	0	0	0	1	0	0	0	0	0	0	0	0	0
Cymbella cornuta	O-I	0	1	0	0	0	1	0	0	0	0	0	0	0	0	0
Cymbella helvetica	O-I	2	1	0	0	0	2	1	0	0	0	0	0	0	0	0
Cymbella naviculiformis	O-I	0	0	0	1	0	0	0	0	0	0	0	0	0	0	0
Cymbella prostrata	O-I	0	0	4	0	0	0	0	0	0	0	0	0	0	0	0
Diploneis elliptica	O-I	1	1	0	0	0	0	0	0	0	0	0	0	0	0	0
Diploneis ovalis	O-I	8	9	0	0	0	0	0	0	0	0	0	0	0	0	0
Epithemia adnata	O-I	1	0	2	0	0	0	0	0	0	0	0	0	0	0	1
Epithemia adnata var porcellus	O-I	0	0	0	3	1	0	0	0	0	0	0	0	1	0	0
Epithemia sorex	O-I	4	0	9	2	8	9	14	9	57	16	1	0	6	4	3
Eunotia pectinalus fo Impressa	O-I	15	8	3	9	2	0	1	1	4	2	0	0	0	1	0
Fragilaria construens	O-I	11	2	0	37	100	11	35	56	86	45	14	18	50	43	25
Fragilariforma virescens	O-I	51	8	22	69	22	36	19	27	7	34	80	71	75	39	42
Gomphonema angustatum	O-I	3	1	0	0	0	0	1	3	1	0	0	0	1	0	0
Gomphonema truncatum var capitatum	O-I	0	0	0	1	0	0	0	0	0	0	0	0	0	0	0
Gomphonema acuminatum var coronatum	O-I	1	3	0	0	0	0	0	0	0	0	0	0	0	0	0
Gomphonema acuminatum var pusillum	O-I	0	0	0	0	1	0	0	0	0	0	0	0	0	0	0
Gomphonema subtile	O-I	0	0	0	0	0	0	1	0	0	0	0	0	0	0	0
Mastogloia elliptica var dansei	O-I	6	6	0	0	0	0	0	0	0	0	0	0	0	0	0
Mastogloia smithii	O-I	0	1	3	0	0	0	0	0	0	0	0	0	0	0	0
Navicula pupula	O-I	0	0	0	0	0	0	0	1	0	3	0	0	0	0	1
navicula radiosa	O-I	5	0	19	4	3	1	5	3	2	2	0	0	0	2	0
Navicula rhynchocephala	O-I	0	0	0	0	0	2	0	0	0	0	0	0	0	0	0
Navicula tripunctata	O-I	0	0	0	1	0	0	0	0	0	0	0	0	0	0	0
Navicula tuscula	O-I	0	0	0	0	0	0	1	0	0	0	0	0	0	0	0
Nitzschia fonticola	O-I	0	0	1	0	4	0	1	0	4	3	1	0	1	0	0
Nitzschia palea	O-I	0	0	0	0	0	0	0	0	1	0	0	0	0	0	0
Pinnularia abaujensis	O-I	0	0	1	0	1	0	0	0	0	0	0	0	0	0	0
Pinnularia cuneata var. reducta	O-I	0	0	0	0	0	0	0	0	1	0	0	0	0	0	0
Pinnularia major	O-I	0	0	0	1	1	0	0	0	0	0	0	0	1	1	0
pinnularia mesolepta	O-I	0	0	0	0	0	0	0	0	0	0	0	0	1	0	0
Pinnularia microstauron	O-I	1	4	0	1	1	1	1	0	0	0	0	0	0	0	0
Pinnularia viridis	O-I	0	0	0	1	0	0	0	0	0	0	0	0	0	0	0
Pseudostaurosira brevistriata	O-I	2	2	0	3	0	0	0	1	0	2	1	1	3	17	12
Rhopalodia Gibba var parallela	O-I	1	0	2	0	0	0	0	2	0	0	0	0	0	1	0
Stauroneis phoenicenteron	O-I	1	1	1	1	0	0	0	0	2	0	0	0	0	0	0

Species	Cat															
Staurosira elliptica	O-I	0	1	1	14	48	90	68	86	12	81	8	4	2	13	10
Staurosirella pinnata	O-I	0	0	0	39	44	19	17	57	6	38	5	1	1	2	7
Surirella biseriata	O-I	0	1	0	0	0	0	0	0	0	0	0	0	0	0	0
Cymbella hebridica	H	3	1	4	0	0	0	0	1	0	0	2	0	0	1	3
Cymbella perpusilla	H	0	0	0	0	0	1	0	0	0	0	0	0	0	0	0
Denticula tenuis	H	2	0	3	1	2	1	2	0	0	1	1	0	0	0	0
Eunotia arcus	H	1	0	6	0	0	0	0	0	0	2	0	0	0	0	0
Eunotia exigua	H	0	0	4	0	0	0	0	1	0	0	0	0	0	0	0
Eunotia fallax	H	1	0	0	0	0	0	0	0	0	0	0	0	0	0	0
Eunotia praerupta	H	11	0	0	0	0	0	0	0	0	0	0	0	0	0	0
Frustulia Rhomboides	H	0	0	0	0	0	0	0	0	0	0	0	0	0	0	2
Pinnularia subsolaris	H	0	4	0	0	0	0	0	0	0	0	0	0	0	0	0
Stauroneis anceps	H	1	0	0	0	0	1	0	0	0	0	0	0	0	0	0
Tabellaria fenestrata	H	13	18	4	1	1	0	0	0	0	0	0	0	0	0	0
Tabellaria flocculosa	H	57	55	8	7	3	1	2	4	1	3	0	0	0	0	0
Achnanthes gibberula	U	1	0	1	0	0	0	0	0	0	0	0	0	0	0	0
Amphora copulata	U	0	0	0	0	0	0	0	0	0	0	1	2	0	5	4
Cymbella alpina	U	0	0	0	0	0	0	0	0	0	0	0	0	0	1	0
Cymbella delicatula	U	0	0	1	0	0	2	4	0	1	0	0	0	0	0	0
Cymbella descripta	U	0	0	0	0	0	0	0	0	0	2	0	0	0	1	0
Cymbella gracile	U	1	6	0	0	0	0	0	0	0	0	0	0	0	0	0
Cymbella hybrida	U	0	0	0	1	0	0	0	0	0	0	0	0	0	0	0
Cymbella laevis	U	0	0	1	0	0	0	0	0	0	0	0	0	0	0	0
Cymbella minuta fo latens	U	0	0	0	0	0	0	0	0	0	0	0	0	0	0	2
Cymbella silesiaca	U	0	0	2	1	0	0	0	0	0	0	0	0	2	0	0
Denticula kuetzingii	U	5	0	7	0	0	0	0	3	0	1	1	0	1	4	1
Epithemia goeppertiana	U	0	0	0	0	0	0	0	0	1	0	0	0	0	0	0
Eucocconeis	U	9	6	9	0	0	0	1	1	1	0	0	0	2	0	0
Eunotia naegelii	U	2	3	0	0	0	0	0	0	0	0	0	0	0	0	0
Eunotia septentrinalis	U	2	0	0	0	0	0	0	0	0	0	0	0	0	0	0
Fragilaria crotonensis	U	4	9	0	0	1	0	0	0	0	0	0	0	0	0	0
Gomphonema angustum	U	1	1	0	0	0	0	0	0	0	0	0	0	0	0	0
Gomphonema minutum	U	0	0	0	0	0	0	0	0	0	0	0	0	2	0	0
Navicula leptostriata	U	0	0	5	0	0	1	2	0	0	0	0	0	0	0	0
Navicula Striolata	U	0	0	0	2	0	1	1	0	4	1	2	1	0	0	0
Nitzschia bryophila	U	0	0	0	1	2	1	0	0	0	0	0	0	0	0	0
Nitschia frequens	U	1	0	0	0	0	0	0	0	0	0	0	0	0	0	0

Nitzschia paleacea	U	0	0	0	0	0	0	0	0	1	2	0	0	0	0	0
Nitzschia sociabilis	U	0	0	0	0	1	0	1	0	0	1	0	0	0	0	0
Nitzschia supralittorea	U	0	0	1	1	0	0	0	0	0	0	0	0	0	0	0
Stauroneis wislouchii	U	0	0	0	1	0	0	0	0	0	0	0	0	0	0	0
Staurosirella leptostauron	U	2	0	0	0	0	0	0	0	0	0	0	0	0	0	0
Synedra var subconstricta	U	0	0	0	4	0	0	0	0	0	0	0	0	0	0	0
Tabularia fasciculata	U	0	0	0	4	1	0	0	0	1	0	0	0	1	0	0
Achnanthes linearis	U	0	6	0	0	0	0	0	0	0	0	0	0	0	0	0
Gomphonema dichotomum	U	0	0	0	4	2	0	0	0	0	0	0	0	0	0	0
Total # of species:		254	239	261	246	256	248	248	277	230	263	254	258	250	265	254

Appendix 2

A2_4 Raw diatom counts for Loch Duart Marsh

Diatom Species	Depth (cm): Group	24	40	49	65	81	93	110	112	115	122	126	130	134	139	143	151	155	159	174	178	182	186	190	194	198	202	204	216
Amphora bacillaris	P	0	0	0	0	0	0	0	0	0	0	0	0	0	0	0	0	0	12	0	0	0	0	0	0	0	0	0	0
Amphora ostrearia	P	0	0	0	0	0	0	0	0	0	0	0	0	0	0	1	0	0	0	0	0	0	0	0	0	0	0	0	0
Cocconeis costata	P	0	0	5	0	1	1	2	10	5	5	8	7	8	2	6	0	1	0	0	0	0	0	0	0	0	0	0	0
Cocconeis distans	P	0	0	0	0	0	0	0	0	0	0	0	0	0	5	0	0	0	0	0	0	0	0	0	0	0	0	0	0
Cocconeis molesta	P	0	0	0	0	0	0	0	0	0	0	0	0	0	1	27	0	0	0	0	0	0	0	0	0	0	0	0	0
Cocconeis peltoides	P	0	0	1	0	0	0	0	0	0	0	0	0	0	0	0	0	0	0	0	0	0	0	0	0	0	0	0	0
Cocconeis scutellum	P	16	13	16	44	18	38	35	33	40	45	33	14	28	37	32	1	1	0	0	0	0	0	0	0	0	0	0	0
Cocconeis stauroneif-ormis	P	0	0	0	0	0	0	0	0	0	0	3	0	1	0	0	0	0	0	0	0	0	0	0	0	0	0	0	0
Diploneis smithii	P	0	0	0	1	0	0	0	0	0	0	0	0	0	1	0	0	0	0	0	0	0	0	0	0	0	0	0	0
Mastogloia exigua	P	0	0	1	0	0	0	0	0	0	0	0	0	0	0	0	0	0	0	0	0	0	0	0	0	0	0	0	0
Navicula abrupta	P	0	0	0	7	4	3	2	1	2	4	3	4	4	0	1	0	0	0	0	0	0	0	0	0	0	0	0	0
Navicula cancellata	P	1	0	0	0	0	0	0	0	0	0	0	0	0	0	0	1	0	0	0	0	0	0	0	0	0	0	0	0
Navicula forcipata	P	5	5	23	3	2	2	0	1	0	3	0	0	3	7	1	2	0	0	0	0	0	0	0	0	0	0	0	0

Species	Type																													
Navicula humerosa	P	0	0	0	0	0	0	0	0	0	0	0	0	0	0	0	0	0	0	0	0	0	0	0	0	0	0	1	0
Navicula pennata	P	0	0	1	0	0	0	0	0	0	0	0	0	0	0	0	0	0	0	0	0	0	0	0	0	0	0	0	0
Opephora marina	P	3	3	6	25	66	29	27	23	24	27	46	43	38	47	54	0	59	0	0	0	0	0	0	0	0	0	0	0
Paralia sulcata	P	7	9	8	45	1	20	13	4	7	7	10	1	8	11	10	115	100	1	0	0	0	0	0	0	0	0	4	44
Rhabdonema minutum	P	7	8	17	26	15	45	42	39	69	56	55	30	25	61	11	6	18	1	0	0	0	0	0	0	0	0	3	6
Achnanthes delicatula	M	0	0	0	0	0	0	0	0	0	0	0	0	0	0	0	0	0	0	0	0	0	2	1	0	0	0	0	0
Amphora coffeaeformis	M	0	0	0	0	0	0	0	0	0	0	0	0	0	0	0	0	0	0	0	0	0	1	0	0	0	0	0	0
Caloneis westii	M	0	0	0	0	0	0	0	0	0	0	0	0	0	0	1	0	0	0	0	0	0	0	0	0	0	0	0	0
Diploneis didyma	M	0	0	0	0	0	0	0	0	0	0	1	0	0	0	0	0	0	0	0	0	0	0	0	0	0	0	1	5
Diploneis interrupta	M	0	0	0	3	0	1	0	0	0	0	0	1	0	0	0	5	1	0	0	0	0	0	0	0	0	1	0	7
Gyrosigma balticum	M	0	0	0	0	0	0	0	0	0	0	0	0	0	0	0	1	0	0	0	0	0	0	0	0	0	0	0	0
Navicula digitoradiata	M	0	0	0	0	0	0	0	0	0	0	0	0	0	0	1	0	0	0	0	0	0	0	0	0	0	0	0	0
Navicula halophila	M	0	0	0	0	0	0	0	0	0	0	0	0	0	0	0	0	0	0	0	0	1	0	0	0	0	0	0	0
Navicula peregrina	M	10	2	11	0	0	1	3	1	1	0	0	0	0	0	2	0	0	0	0	0	0	0	0	0	0	0	6	0
Navicula salinarum	M	0	6	6	0	0	0	0	0	0	0	0	0	0	0	0	0	0	0	0	0	0	0	0	0	0	0	0	0
Scolioneis tumida	M	0	0	0	0	0	0	0	0	0	0	0	0	0	0	0	0	0	0	0	0	0	0	0	0	0	2	28	24
Surirella brightwelli	M	1	0	0	0	0	0	0	0	0	0	0	0	0	0	0	0	0	0	0	0	0	0	0	0	0	0	0	0

Taxon		1	2	3	4	5	6	7	8	9	10	11	12	13	14	15	16	17	18	19	20	21	22	23	24	25	26	27	28
Surirella ovalis	M	0	0	1	0	0	0	0	0	0	0	0	0	0	0	0	0	0	0	0	0	0	0	0	0	0	0	0	0
Amphora veneta	O-H	0	0	0	0	0	0	0	0	0	0	0	0	0	1	0	0	0	0	0	0	0	0	1	0	0	0	0	0
Cocconeis pediculis	O-H	0	0	0	0	0	0	0	0	0	0	0	0	0	0	0	0	0	0	3	1	0	0	0	14	4	2	0	0
Cyclotella antiqua	O-H	0	0	0	0	0	0	0	0	0	0	0	0	0	0	0	0	0	0	8	3	1	6	5	12	9	7	1	0
Navicula cari	O-H	1	0	0	0	0	0	0	0	0	0	0	0	0	0	0	0	0	0	0	0	0	0	0	0	0	0	0	0
Achnanthes clevei	O-I	12	21	0	0	0	0	0	0	0	0	0	0	0	0	0	0	0	0	0	0	0	0	0	0	0	0	0	0
Achnanthes exilis	O-I	0	0	0	0	0	0	0	0	0	0	0	0	0	0	0	0	0	0	0	0	0	0	0	3	0	0	0	0
Achnanthes laterostrata	O-I	0	2	0	0	0	0	0	0	0	0	0	0	0	0	0	0	0	0	0	0	0	0	0	0	0	0	0	0
Achnanthes levandiri	O-I	0	0	4	0	0	9	0	0	0	0	0	0	25	0	0	0	0	0	0	0	0	0	0	0	0	0	0	0
Achnanthes minutissima microcephala	O-I	0	0	0	0	0	0	0	0	0	0	0	0	0	0	0	0	0	0	0	0	0	2	6	3	4	0	0	0
Achnanthes minutissima var jacki	O-I	0	0	0	0	0	0	0	0	0	0	0	0	0	0	0	0	0	0	0	0	1	0	1	0	0	0	0	0
Amphora ovalis	O-I	1	0	2	0	1	0	0	1	0	0	0	0	0	1	0	0	0	0	0	0	0	0	0	0	0	19	38	0
Bracysira Brebissonii	O-I	0	0	0	0	0	0	0	0	0	0	0	0	0	0	0	9	7	123	61	11	14	6	0	0	0	0	0	4
Brachysira brebissonii fo Thermalis	O-I	0	0	0	0	0	0	0	0	0	0	0	0	0	0	0	2	0	15	5	10	34	0	0	0	0	0	0	0
Brachysira styriaca	O-I	0	0	0	0	0	0	0	0	0	0	0	0	0	0	0	1	0	3	3	0	0	0	0	0	0	0	0	0
Brachysira vitrea	O-I	0	0	0	0	0	0	0	0	0	0	0	0	0	1	0	1	0	8	3	4	8	0	14	2	4	0	0	0
Cocconeis disculus	O-I	1	2	4	16	26	11	30	22	21	23	0	22	14	39	25	13	2	0	0	0	0	0	0	0	0	0	0	0

Taxon		1	2	3	4	5	6	7	8	9	10	11	12	13	14	15	16	17	18	19	20	21	22	23	24	25	26	27	28
Cocconeis placentula	O-I	11	22	0	0	0	0	0	0	0	0	0	1	0	0	0	0	0	0	0	0	0	0	0	0	0	0	0	0
Cocconeis placentula var euglypta	O-I	0	0	2	0	0	0	0	0	0	0	0	0	0	0	0	0	0	0	0	0	0	0	0	0	0	0	0	0
Cocconeis placentula var lineata	O-I	0	0	14	0	0	0	0	0	0	0	0	0	0	0	0	0	0	0	0	0	0	0	0	0	0	0	0	0
Cyclotella radiosa	O-I	0	0	0	0	0	0	0	0	0	0	0	0	0	0	0	3	2	9	4	2	4	4	8	1	1	0	1	0
Cymbella affinis	O-I	0	0	0	0	0	0	0	0	0	0	0	0	0	0	0	1	0	4	9	0	1	11	10	2	0	0	2	1
Cymbella angustata	O-I	0	0	0	0	0	0	0	0	0	0	0	0	0	0	0	0	0	0	2	0	0	1	1	0	0	0	0	0
Cymbella cesatii	O-I	0	0	0	0	0	0	0	0	0	0	0	0	0	0	0	2	0	0	0	0	0	0	0	0	0	0	0	0
Cymbella cistula var maculata	O-I	0		0	0	0	0	0	0	0	0	0	0	0	0	0	0	0	0	0	0	0	0	0	1	0	0	0	0
Cymbella helvetica	O-I	0	0	0	0	0	0	0	0	0	0	0	0	0	0	0	0	0	8	3	1	4	2	2	0	1	0	0	0
Cymbella lunata	O-I	0	0	0	0	0	0	0	0	0	0	0	0	0	0	0	0	0	2	1	0	0	0	0	0	0	0	0	0
Cymbella microcephala	O-I	0	0	0	0	0	0	0	0	0	0	0	0	0	0	0	0	1	1	0	0	0	12	21	8	8	0	0	0
Cymbella subaequalis	O-I	0	0	0	0	0	0	0	0	0	0	0	0	0	0	0	0	0	1	0	0	0	0	0	0	0	0	0	0
Diploneis ovalis	O-I	0	0	1	0	0	0	1	0	0	0	0	0	0	0	0	0	0	0	0	0	0	0	0	0	0	0	0	0
Diploneis elliptica	O-I	1	0	0	1	0	0	0	1	0	0	0	1	0	0	0	0	0	0	0	0	0	0	0	0	1	1	0	0
Epithemia adnata	O-I	0	0	0	0	0	0	0	0	0	0	0	0	0	0	0	1	0	2	0	0	0	2	0	1	4	85	6	0
Epithemia adnata var porcellus	O-I	0	0	0	0	0	0	0	0	0	0	0	0	0	0	0	0	0	0	3	0	0	0	0	0	0	0	1	0

Species		C1	C2	C3	C4	C5	C6	C7	C8	C9	C10	C11	C12	C13	C14	C15	C16	C17	C18	C19	C20	C21	C22	C23	C24	C25	C26	C27	C28
Epithemia sorex	O-I	0	0	0	0	0	0	0	0	0	0	0	0	0	0	0	1	1	1	38	17	15	92	51	25	13	10	2	4
Eunotia pectinalis fo impressa	O-I	1	0	0	0	0	0	0	0	0	0	0	0	0	0	0	0	0	2	1	0	0	0	1	0	3	0	0	0
Fragilaria construens	O-I	0	0	9	0	0	0	0	0	0	0	0	1	0	0	0	7	12	1	13	18	4	34	47	105	150	49	1	0
Fragilaria virescens	O-I	40	31	10	0	0	0	1	1	0	0	0	6	0	0	2	4	5	1	11	167	100	7	6	1	0	2	0	1
Fragilaria vaucheriae	O-I	0	6	2	0	0	0	0	1	0	0	0	2	0	0	0	0	0	0	0	0	0	0	0	0	1	0	0	0
Gomphonema acuinatum	O-I	0	0	0	0	0	0	0	0	0	0	0	0	0	0	0	0	0	0	0	0	0	1	0	0	0	0	0	0
Gomphonema acuminatum var coronatum	O-I	0	0	0	0	0	0	0	0	0	0	0	0	0	0	0	0	0	0	2	0	0	0	0	0	0	0	0	0
Gomphonema angustatum	O-I	0	0	0	0	1	1	0	0	0	0	0	0	0	1	0	1	0	2	2	1	1	2	0	0	1	0	0	0
Gomphonema angustum	O-I	1	0	3	0	0	3	0	0	1	0	0	3	0	1	0	0	0	0	0	0	0	0	0	0	0	1	0	0
Gomphonema gracile	O-I	0	0	0	0	0	0	0	0	0	0	0	0	0	0	0	0	0	0	0	0	0	0	1	0	2	1	0	0
Gomphonema olivaceum	O-I	0	0	0	0	0	0	0	0	0	0	0	0	0	0	1	0	0	0	0	0	0	0	0	0	0	1	0	0
Gomphonema parvulum	O-I	0	0	0	0	0	0	0	0	0	0	0	0	0	0	0	0	0	0	0	0	0	0	0	0	0	1	0	0
Mastoglia smithii	O-I	0	0	0	0	0	0	0	0	0	0	0	0	0	0	0	0	0	16	0	0	0	0	0	0	0	0	0	0
Mastogloia elliptica var dansei	O-I	0	0	0	0	0	0	0	0	0	0	0	0	0	0	0	0	0	0	1	0	0	0	1	0	0	0	0	0
Mastogloia smithii	O-I	0	0	0	0	0	0	0	0	0	0	0	0	0	0	0	0	0	1	2	0	0	0	0	0	0	0	0	0
Navicula caterva	O-I	0	0	34	0	0	0	0	0	0	0	0	0	0	0	0	0	0	0	0	0	0	0	0	0	0	0	0	0
Navicula cuspidata	O-I	0	0	5	0	0	0	0	0	0	0	0	0	0	0	0	0	0	0	0	0	0	0	0	0	0	0	0	0

Species		1	2	3	4	5	6	7	8	9	10	11	12	13	14	15	16	17	18	19	20	21	22	23	24	25	26	27	28
Navicula elginensis	O-I	0	0	0	0	0	0	0	0	0	0	0	1	0	0	0	0	0	0	0	0	0	0	0	0	0	0	0	0
Navicula elginensis var neglecta	O-I	0	0	0	0	0	0	6	0	0	0	0	0	0	0	0	0	0	0	0	0	0	0	0	0	0	0	0	0
Navcula rhynchoceptoa	O-I	0	0	0	0	0	0	0	0	0	0	0	0	0	0	0	0	0	0	0	0	0	0	0	0	0	0	50	0
Navicula pupula	O-I	0	0	0	0	0	0	0	0	0	0	0	0	0	0	0	0	1	0	0	0	0	0	0	0	0	0	0	0
Navicula ramosissima	O-I	0	0	0	0	0	0	1	0	0	0	0	0	0	0	0	0	0	0	0	0	0	0	0	0	0	0	0	0
Navicula radiosa	O-I	0	0	0	1	0	0	0	0	0	0	0	0	0	0	0	1	0	14	17	4	3	6	1	4	2	6	0	0
Navicula rhynchocephala	O-I	0	0	0	0	0	0	0	0	0	0	0	0	0	0	0	0	0	1	0	0	0	0	0	0	0	0	0	0
Navicula viridula	O-I	0	0	0	0	0	0	0	0	0	0	0	0	0	0	0	0	0	5	0	0	0	0	0	0	0	0	0	0
Navicula vulpina	O-I	3	0	0	0	0	1	0	0	0	0	0	0	0	0	0	0	0	0	0	0	0	0	0	0	0	0	0	0
Nedium dubium	O-I	0	0	0	0	0	0	0	0	0	0	0	0	0	0	0	0	0	1	0	0	0	0	0	0	0	0	0	0
Nitzschia fonticola	O-I	0	0	0	0	0	0	0	0	0	0	0	0	0	0	0	0	0	0	3	0	21	16	2	7	1	0	0	0
Nitzschia palea	O-I	0	0	0	0	0	0	0	0	0	0	0	0	0	0	0	1	0	0	1	0	0	0	0	0	0	0	0	0
Pinnularia abaujensis	O-I	0	0	0	0	0	0	0	0	0	0	0	0	0	0	0	0	0	1	0	0	0	0	0	0	0	0	0	0
Pinnularia brebissonii	O-I	0	0	3	8	1	0	1	0	2	4	1	0	0	0	0	0	0	0	0	0	0	0	0	0	0	0	0	0
Pinnularia major	O-I	0	0	0	0	0	0	0	0	0	0	0	0	0	0	0	0	0	1	0	0	0	0	0	0	0	0	0	0
Pinnularia sudetica	O-I	0	0	2	3	0	0	0	0	1	1	0	0	1	0	0	0	0	0	0	0	0	0	0	0	0	0	0	0
Pseudostauros-ira brevistriata	O-I	0	11	7	1	1	0	0	0	0	0	1	1	0	1	4	0	0	0	0	0	0	2	33	17	2	1	0	0
Rhopalodia gibba var parallela	O-I	0	0	0	0	0	0	0	0	0	0	0	0	0	0	0	1	0	2	2	0	0	2	0	0	0	0	0	0

96

Species	Cat																												
Stauroneis phoenicenter-on	O-I	0	0	0	0	0	0	0	0	0	0	0	0	0	0	0	0	0	1	3	1	1	0	1	1	0	0	0	0
Stauroneis prominula	O-I	1	0	0	0	0	0	0	0	0	0	0	0	0	0	0	0	0	0	0	0	0	0	0	0	0	0	0	0
Staurosira elliptica	O-I	140	98	41	0	1	1	1	1	1	4	0	8	2	2	4	0	1	0	0	0	0	2	0	0	0	2	0	0
Staurosirella pinnata	O-I	0	1	5	73	125	72	93	125	67	80	104	99	93	47	75	68	56	2	7	6	2	2	5	21	9	1	4	0
Synedra rumpens	O-I	0	1	0	0	0	0	0	0	0	0	0	0	0	0	0	0	0	0	0	0	0	0	0	0	0	0	0	0
Amphora normanii	H	0	0	0	0	0	0	0	0	0	0	0	0	0	0	0	0	0	0	0	0	0	0	0	0	0	1	0	0
Denticula tenuis	H	0	0	0	0	0	0	0	0	0	0	0	0	0	0	0	0	1	0	0	0	2	6	23	6	10	0	0	0
Cymbella Hebridica	H	0	0	0	0	0	0	0	0	0	0	0	0	0	0	0	1	0	0	6	0	3	7	3	6	2	2	0	0
Eunotia arcus	H	0	0	1	0	0	0	0	0	0	0	0	0	0	0	0	1	1	14	10	3	5	7	1	2	1	0	0	2
Eunotia exigua	H	0	0	0	0	0	0	0	0	0	0	0	0	0	0	0	0	0	0	0	0	1	0	0	0	0	0	0	0
Eunotia fallax	H	0	0	0	0	0	0	0	0	1	0	0	0	0	0	0	0	0	0	0	0	0	0	0	0	0	0	0	0
Eunotia Praerupta	H	0	0	0	1	0	0	0	0	0	0	0	0	0	0	0	0	0	0	0	0	0	0	0	0	0	0	0	0
Navicula cocconeiformis	H	0	2	0	0	0	0	0	0	0	0	0	0	0	0	0	0	0	0	0	0	0	0	0	0	0	0	0	0
Navicula laevissima	H	0	0	0	0	0	0	0	0	0	0	0	0	0	0	0	0	0	1	0	0	0	0	0	0	0	0	0	0
Tabellaria fennostrata	H	0	0	0	0	0	0	0	0	0	0	0	6	0	0	0	0	0	0	11	2	7	1	1	2	0	0	0	0
Tabellaria flocculosa	H	0	2	0	0	0	0	1	0	5	0	0	0	0	0	1	2	0	0	27	7	31	13	5	5	2	0	0	0
Achnanthes gibberula	U	0	0	0	0	0	0	0	0	0	0	0	0	0	0	0	0	0	0	0	0	0	0	1	0	0	0	0	0
Achnanthes trinodis	U	0	0	0	0	0	0	0	0	0	0	0	0	0	0	0	0	0	0	0	0	0	0	1	0	0	0	0	0
Amphora copulata	U	0	0	0	0	0	0	1	0	0	0	0	0	1	0	1	0	0	0	0	0	0	0	0	0	0	0	0	0

Species																													
Caloneis molaris	U	0	0	0	0	0	1	0	0	0	0	0	0	0	0	0	0	0	0	0	0	0	0	0	0	0	0	0	0
Cocconeis confusa	U	0	0	0	0	0	0	0	0	0	0	0	1	0	0	3	0	0	0	0	0	0	0	0	0	0	0	0	0
Cocconeis dirupta	U	0	0	0	0	0	2	4	1	5	1	0	1	2	0	1	0	0	0	0	0	0	0	0	0	0	0	0	0
Cocconeis guttata	U	0	0	1	0	0	3	1	1	0	1	2	2	2	0	2	0	1	0	0	0	0	0	0	0	0	0	0	0
Cocconeis sp	U	0	0	0	0	0	0	0	0	0	0	0	0	0	0	2	3	0	0	0	0	0	0	0	0	0	0	0	0
Cyclotella distinguenda	U	0	0	0	0	0	0	0	0	0	0	0	0	0	0	0	0	0	0	0	0	13	9	4	1	0	0	0	0
Cyclotella glomerata	U	0	0	0	0	0	0	0	0	0	0	0	0	0	0	0	0	0	1	0	0	0	0	0	0	0	0	0	0
Cymbella alpina	U	0	0	0	0	0	0	0	0	0	0	0	0	0	0	0	0	0	0	0	0	0	0	0	0	0	0	2	0
Cymbella caespitosa	U	0	0	0	0	0	0	0	0	0	0	0	0	0	0	0	0	0	0	2	0	0	0	0	0	0	0	0	0
Cymbella delicatula	U	0	0	0	0	0	0	0	0	0	0	0	0	0	0	0	1	0	0	1	0	1	0	0	0	0	0	0	0
Cymbella laevis	U	0	0	0	0	0	0	0	0	0	0	0	0	0	0	0	0	0	2	0	0	0	0	0	0	0	0	0	0
Cymbella perpusilla	U	0	0	0	0	0	0	0	0	0	0	0	0	0	0	0	0	0	0	0	0	0	0	1	0	3	0	0	0
Cymbella pusilla	U	0	0	0	0	0	0	0	0	0	0	0	0	0	0	0	1	0	0	1	0	0	0	0	0	0	0	0	0
Cymbella silesiaca	U	0	0	0	0	0	0	0	0	0	0	0	0	0	0	0	0	0	1	0	0	0	0	0	0	0	0	0	0
Cymbella stauroneiformis	U	0	0	0	0	0	0	0	0	0	0	0	0	0	0	1	1	0	0	0	0	0	0	0	0	0	0	0	0
Diploneis crabro	U	0	0	0	0	0	0	0	0	0	0	1	0	0	0	0	0	0	0	0	0	0	0	0	0	0	0	0	0
Denticula kuetzingii	U	0	0	0	0	0	0	0	0	0	0	0	0	0	0	0	0	0	0	1	3	8	9	2	1	0	0	0	0
Eucocconeis	U	0	0	0	0	0	0	0	0	0	0	0	0	0	0	0	0	0	4	4	2	4	3	1	0	0	0	0	0
Eunotia septentrionalis	U	0	0	0	0	0	0	0	0	0	0	0	0	0	0	0	0	0	0	0	0	0	0	4	0	0	0	0	0
Eunotia tibia	U	0	0	0	0	0	0	0	0	0	0	0	0	0	0	0	0	0	0	0	0	0	0	16	0	0	0	0	0

Species		1	2	3	4	5	6	7	8	9	10	11	12	13	14	15	16	17	18	19	20	21	22	23	24	25	26	27	28
Fragilaria crotonensis	U	0	0	0	0	0	0	0	0	0	0	0	0	0	0	0	0	0	0	0	0	0	0	0	0	0	1	0	0
Gomphonema amoenum	U	0	0	0	0	0	0	0	0	0	0	0	0	0	4	0	0	0	0	0	0	0	0	0	0	0	0	0	0
Gomphonema unknown	U	0	0	0	0	0	0	0	0	0	0	0	0	0	0	1	0	0	0	0	0	0	0	0	0	0	0	0	0
Mastogloia unknown	U	0	0	0	0	0	0	0	0	0	0	0	0	0	0	0	2	0	0	0	0	0	0	0	0	0	0	0	0
Navicula angusta	U	0	0	0	0	0	0	0	0	0	0	0	1	0	0	0	0	0	0	0	0	0	0	0	0	0	0	0	0
Navicula delognei	U	0	0	0	0	0	0	0	0	0	0	0	0	0	1	0	0	1	0	0	0	0	0	0	0	0	0	0	0
Navicula theinmannii	U	0	0	2	0	0	0	0	0	0	0	0	0	0	0	0	0	0	0	0	0	0	0	0	0	0	0	0	0
Navicula striolata	U	0	0	0	0	0	0	0	0	0	0	0	0	0	0	0	0	0	1	0	0	0	0	0	0	0	0	1	0
Navicula subinflatoides	U	0	0	0	0	0	0	0	0	0	0	0	0	0	0	0	0	0	0	1	0	0	0	0	0	0	0	0	0
Nitzschia frequens	U	0	0	1	0	0	0	0	0	0	0	0	0	0	0	0	0	0	0	0	0	0	0	0	0	0	0	0	0
Nitzschia paleacea	U	0	0	1	0	0	0	0	0	1	0	0	0	0	0	0	0	0	0	0	0	1	8	0	0	0	0	0	0
Nitzschia pumila	U	0	0	0	0	0	0	0	0	0	0	0	1	0	0	0	0	0	0	0	0	0	0	0	0	0	0	0	0
Nitzschia sociablis	U	0	0	0	0	0	0	0	0	0	0	0	0	0	0	0	0	0	0	0	0	1	0	2	0	0	0	0	0
Nitzschia supralittorea	U	0	0	0	0	0	0	0	0	0	0	0	0	0	0	0	0	0	0	0	0	0	2	0	1	1	0	0	0
Pinnularia divergens	U	0	0	0	0	0	0	0	0	0	0	0	0	0	0	0	0	0	1	0	0	0	0	0	0	0	0	0	0
Pinnularia ergandensis	U	0	0	0	2	0	2	0	0	0	1	0	0	0	0	0	0	0	0	0	0	0	0	0	0	0	0	0	0
Rhopadia musculus	U	0	0	0	0	0	0	0	0	0	0	0	0	0	0	1	0	0	0	0	0	0	0	0	0	0	0	0	0
Rhopalodia musculus	U	0	0	0	0	0	0	0	0	0	0	0	0	0	0	0	1	0	0	0	0	0	0	0	0	0	0	0	0

Stauroneis alpina	U	0	0	0	0	0	0	0	0	0	0	0	0	0	3	0	0	0	0	0	0	0	0	0	0	0	0	0	0
Stauroneis lapponica	U	0	0	0	0	0	0	0	0	0	0	0	0	0	0	0	0	1	0	0	0	0	0	0	0	0	0	0	0
Stauroneis muriella	U	0	0	0	0	0	0	0	0	0	0	0	0	0	0	0	0	0	0	0	0	0	0	0	0	0	1	0	0
Stauroneis tackei	U	0	0	1	0	0	0	0	0	0	0	0	0	0	0	0	0	0	0	0	0	0	0	0	0	0	0	0	0
Stauroneis sp	U	0	0	0	0	0	0	0	0	0	0	0	0	0	0	0	1	0	0	0	0	0	0	0	0	0	0	0	0
Stauroneis sp 1	U	0	0	0	0	0	0	0	0	0	0	0	0	0	1	0	0	0	0	0	0	0	0	0	0	0	0	0	0
Tabularia fasciculata	U	0	0	0	0	0	4	0	0	0	0	0	0	0	0	1	0	0	0	0	0	0	0	0	0	0	0	0	0
Navicula comoides	U	0	0	0	0	0	0	0	0	0	0	0	0	0	0	1	1	0	0	0	0	0	0	0	0	0	0	0	0
Delphineis surirella	U	0	0	0	0	0	0	0	0	0	0	0	0	0	0	3	0	0	0	0	0	0	0	0	0	0	0	0	0
Total # of species:		263	245	251	260	263	250	265	266	253	262	267	257	256	274	270	269	273	263	272	269	267	276	262	277	259	250	104	98

Appendix 3

A3_1 Qualitative pollen analysis (J. Innes, personal communication 2014)

<u>Duart Bog</u>
Depth: 415 cm

Empetrum   18
Cyperaceae   7
Artemisia   1
Pinus   1
Betula nana   1
Saxifragaceae 1
Myriophyllum alterniflorum   3
Lycopodium selago   4
Type 128 algae   lots
Cyanobacteria   lots
ENVIRONMENT: Late Glacial or Loch Lomond Stadial sedge- heath with floating aquatic plants and algae (pond)

<u>Loch Duart Marsh</u>
Depth: 112 cm

Betula 27
Alnus   14
Quercus   3
Ulmus 1
Corylus   6
Pinus   1
Salix   1
Calluna   1
Cyperaceae   3
Poaceae   1
Cruciferae   1
Plantago maritime   7
Foram test linings   5
Spiniferites (dinoflagellate cyst)   1
ENVIRONMENT: Mid-Holocene wooded with saltmarsh indicators (coastal)

Depth: 195 cm
Poaceae   5
Cyperaceae   1
Rumex   5
Artemisia   2
Empetrum   1
Labiatae   1
Equisetum   1
Pediastrum   1
Myriophyllum alterniflorum   130
Botryococcus lots
Debarya   1
ENVIRONMENT: Lateglacial arctic tundra with open, cold water (deep pond)

Appendix 4

A4_1 RSL reconstruction of the regressive salt marsh sequence from Loch Duart Marsh based on the regional 'coastal transition' model of modern diatom in north west Scotland developed by Barlow et al. (2013).

Sample Depth (m)	m OD	SWLI	SWLI_SE	PMSE	RSL	SE (m)	MinDC
0.24	1.82	164.34	17.45	1.55	0.27	0.34	159.95
0.40	1.66	162.15	18.06	1.51	0.16	0.35	154.49
0.49	1.57	173.42	16.86	1.74	-0.17	0.33	136.72
0.65	1.41	177.61	17.50	1.83	-0.42	0.34	119.47

A4_2 Scatterplot of the observed standardised water level index (SWLI) against the WA-PLS transfer function model predicted SWLI for the regional Scotland 'coastal transition' diatom training set for the second component.
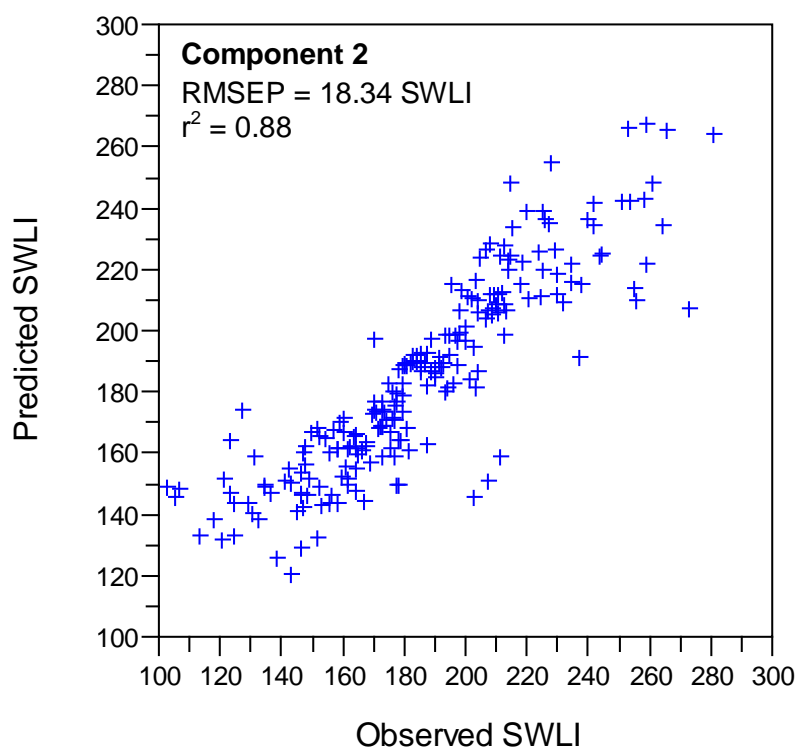
Appendix 5

A5_1 Radiocarbon Date Certificates

Christine Hamilton
Durham University
South Road
Durham DH1 3LE
United Kingdom

[14]CHRONO Centre
Queens University Belfast
42 Fitzwilliam Street
Belfast BT9 6AX
Northern Ireland

Radiocarbon Date Certificate

Laboratory Identification: UBA-26500
Date of Measurement: 2014-09-05
Site: Loch Duart Marsh (LDM 13/1)
Sample ID: LDM 13/1 40 CM
Material Dated: peat (bulk)
Pretreatment: AAA
Submitted by: Christine Hamilton

Conventional [14]C Age:	332±34 BP
Fraction corrected	using AMS $\delta^{13}C$

Queen's University Belfast

14 CHRONO

Centre for Climate, the Environment, and Chronology

Radiocarbon Date Certificate

Laboratory Identification: UBA-26501
Date of Measurement: 2014-09-12
Site: Loch Duart Marsh (LDM 13/1)
Sample ID: LDM 13/1 160 CM
Material Dated: peat (bulk)
Pretreatment: AAA
Submitted by: Christine Hamilton

Conventional [14]C Age:	8887 ± 36 BP
Fraction corrected	using AMS $\delta^{13}C$

Radiocarbon Date Certificate

Christine Hamilton
Durham University
South Road
Durham DH1 3LE
United Kingdom

Queen's University Belfast
14 CHRONO
Centre for Climate, the Environment, and Chronology

14CHRONO Centre
Queens University Belfast
42 Fitzwilliam Street
Belfast BT9 6AX
Northern Ireland

Laboratory Identification: UBA-26502
Date of Measurement: 2014-09-12
Site: Duart Bog (DB 13/3)
Sample ID: DB 13/3 423 CM
Material Dated: peat (bulk)
Pretreatment: AAA
Submitted by: Christine Hamilton

Conventional ^{14}C Age:	10810±41 BP
Fraction corrected	using AMS δ^{13}C

BETA ANALYTIC INC.

BETA

DR. M.A. TAMERS and MR. D.G. HOOD

4985 S.W. 74 COURT
MIAMI, FLORIDA, USA 33155
PH: 305-667-5167 FAX:305-663-0964
beta@radiocarbon.com

REPORT OF RADIOCARBON DATING ANALYSES

Dr. Jeremy Lloyd

Report Date: 10/1/2014

University of Durham

Material Received: 9/12/2014

Sample Data	Measured Radiocarbon Age	13C/12C Ratio	Conventional Radiocarbon Age(*)
Beta - 390107	12550 +/- 40 BP	-17.9 o/oo	12670 +/- 40 BP
SAMPLE : LDM13-1-199			
ANALYSIS : AMS-Standard delivery			
MATERIAL/PRETREATMENT : (organic sediment): acid washes			
2 SIGMA CALIBRATION : Cal BC 13240 to 13060 (Cal BP 15190 to 15010)			

References

Allen, J.R.L., 2000. Morphodynamics of Holocene salt marshes : a review sketch from the Atlantic and Southern North Sea coasts of Europe. *Quaternary Science Reviews*, 19, pp.1155–1231.

Ascough, P.L. et al., 2011. An Icelandic freshwater radiocarbon reservoir effect: Implications for lacustrine 14C chronologies. *The Holocene*, 21(7), pp.1073–1080.

Balesdent, J., 1987. The turnover of soil organic fractions estimated by radiocarbon dating. *The Science of the Total Environment*, 62, pp.405–408.

Ball, D., 1964. Loss-on-ignition as an estimate of organic matter and organic carbon in non-calcareous soils. *Journal of Soil Science*, 15(1), pp.84–92.

Balco, G. et al., 2008. A complete and easily accessible means of calculating surface exposure ages or erosion rates from 10 Be and 26Al measurements. *Quaternary Geochronology*, 3(3), pp.174–195.

Ballantyne, C., 1990. The Late Quaternary glacial history of the Trotternish Escarpment, Isle of Skye, Scotland, and its implications for ice sheet reconstruction. *Proceedings of the Geologists' Association*, 101(3), pp.171–186.

Ballantyne, C.K. et al., 1998. the Last Ice Sheet in North-West Scotland: Reconstruction and Implications. *Quaternary Science Reviews*, 17(12), pp.1149–1184.

Ballantyne, C. & Hall, A., 2008. The altitude of the last ice sheet in Caithness and east Sutherland , northern Scotland. *Scottish Journal of Geology*, 44(2), pp.169–181.

Ballantyne, C.K., 2010. Extent and deglacial chronology of the last British-Irish Ice Sheet: implications of exposure dating using cosmogenic isotopes. *Journal of Quaternary Science*, 25(4), pp.515–534.

Ballantyne, C.K., 2012. Chronology of glaciation and deglaciation during the Loch Lomond (Younger Dryas) Stade in the Scottish Highlands: implications of recalibrated 10 Be exposure ages. *Boreas*, 41(4), pp.513–526.

Ballantyne, C.K., Rinterknecht, V. & Gheorghiu, D.M., 2013. Deglaciation chronology of the Galloway Hills Ice Centre, southwest Scotland. *Journal of Quaternary Science*, 28(4), pp.412–420.

Barland, K., 1991. Trapped seawater in two Norwegian lakes: Kilevannet, a "new" lake with old trapped seawater, and Rorholtfjorden. *Aquatic Sciences*, 53(1), pp.90–98.

Barlow, N.L.M. et al., 2013. Salt marshes as late Holocene tide gauges. *Global and Planetary Change*, 106, pp.90–110.

Barlow, N.L.M. et al., 2014. Salt-marsh reconstructions of relative sea-level change in the North Atlantic during the last 2000 years. *Quaternary Science Reviews*, 99, pp.1–16.

Bassett, S. et al., 2005. Ice Sheet and Solid Earth Influences on Far-Field Sea-level Histories. *Science*, 309, pp.925–928.

Battarbee, R., 1986. Diatom Analysis. In B. Berglund, ed. *Handbook of Holocene Palaeoecology and Palaeohydrology*. Chichester: Wiley, pp. 527–570.

Benn, D., Lowe, J. & Walker, M., 1992. Response to climatic change during the Loch Lomond Stadial and early Flandrian: geomorphological and palynological evidence from the Isle of Skye, Scotland. *Journal of Quaternary Science*, 7, pp.125–144.

Benn, D.I. & Ballantyne, C.K., 2005. Palaeoclimatic reconstruction from Loch Lomond Readvance glaciers in the West Drumochter Hills, Scotland. *Journal of Quaternary Science*, 20(6), pp.577–592.

Beta Analytic, 2014. Accelerator Mass Spectrometry Radiocarbon Dating. Available at: http://www.radiocarbon.com/accelerator-mass-spectrometry.htm.

Bjorck, S. & Wohlfarth, B., 2002. 14C Chronostratigraphic Techniques in Paleolimnology. In W. Last & J. Smol, eds. *Tracking Environmental Change Using Lake Sediments Volume 1: Basin Analysis, Coring and Chronological Techniques*. Kluwer Academic Publishers, pp. 205–245.

Boomer, I., von Grafenstein, U. & Moss, A., 2012. Lateglacial to early Holocene multiproxy record from Loch Assynt, NW Scotland. *Proceedings of the Geologists' Association*, 123(1), pp.109–116.

Boulton, G. & Clark, C.D., 1990. A highly mobile Laurentide ice sheet revealed by satellite images of glacial lineations. *Nature*, 346, pp.813–817.

Boulton, G. & Hagdorn, M., 2006. Glaciology of the British Isles Ice Sheet during the last glacial cycle: form, flow, streams and lobes. *Quaternary Science Reviews*, 25, pp.3359–3390.

Bowen, D.Q. et al., 1986. Correlation of Quaternary glaciations in England, Ireland, Scotland and Wales. *Quaternary Science Reviews*, 5, pp.299–340.

Bowen, D.. et al., 2002. New data for the Last Glacial Maximum in Great Britain and Ireland. *Quaternary Science Reviews*, 21(1-3), pp.89–101.

Boyle, J., 2004. A comparison of two methods for estimating the organic matter content of sediments. *Journal of Paleolimnology*, 31, pp.125–127.

Bradley, S. et al., 2008. Modelling sea-level data from China and Malay–Thai Peninsula to infer Holocene eustatic sea- level change. In *American Geophysical Union, Fall Meeting 2008, abstract #GC33A-0763*.

Bradley, S.L. et al., 2011. An improved glacial isostatic adjustment model for the British Isles. *Journal of Quaternary Science*, 26(5), pp.541–552.

Bradwell, T., 2006. The Loch Lomond Stadial glaciation in Assynt: A reappraisal. *Scottish Geographical Journal*, 122(4), pp.274–292.

Bradwell, T., Stoker, M. & Larter, R., 2007. Geomorphological signature and flow dynamics of The Minch palaeo-ice stream, northwest Scotland. *Journal of Quaternary Science*, 22(January), pp.609–617.

Bradwell, T. et al., 2008. The northern sector of the last British Ice Sheet: Maximum extent and demise. *Earth-Science Reviews*, 88(3-4), pp.207–226.

Bradwell, T., Stoker, M. & Krabbendam, M., 2008. Megagrooves and streamlined bedrock in NW Scotland: The role of ice streams in landscape evolution. *Geomorphology*, 97(1-2), pp.135–156.

Brain, M.J. et al., 2012. Modelling the effects of sediment compaction on salt marsh reconstructions of recent sea-level rise. *Earth and Planetary Science Letters*, 345-348, pp.180–193.

Briggs, D. & Smithson, P., 1987. *Fundamentals of Physical Geography* 3rd ed., Hutchinson.

Brooks, A. et al., 2008. Postglacial relative sea-level observations from Ireland and their role in glacial rebound modelling. *Journal of Quaternary Science*, 23(October 2007), pp.175–192.

Charlesworth, J., 1956. The late-glacial history of the highlands and the islands of Scotland. *Transactions of the Royal Society of Edinburgh*, 62, pp.769–928.

Clark, C.D. et al., 2012. Pattern and timing of retreat of the last British-Irish Ice Sheet. *Quaternary Science Reviews*, 44, pp.112–146.

Clark, J.A., Farrell, W.E. & Peltier, W.R., 1978. Global Changes in Postglacial Sea Level : A Numerical Calculation. *Quaternary Research*, 9, pp.265–281.

Cleve-Euler, A., 1923. Forsok til analys av Nordens senkvartara nivaforandringar jamte nagra konsekvenser. *Geol.Foren.Stockholm Forh.*, 45, pp.19–107.

Cleve-Euler, A., 1944. Die Diatomeen als quartargeologische Indikatoren. *Geol.Foren.Stockholm Forh.*, 66, pp.383–410.

Colman, S.M. et al., 1996. AMS Radiocarbon analyses from Lake Baikal, Siberia: Challenges of dating sediments from a large, oligotrophic lake. *Quaternary Science Reviews (Quaternary Geochronology)*, 15, pp.669–684.

Davies, H.C., Dobson, M.R. & Whittington, R.J., 1984. A revised seismic stratigraphy for Quaternary deposits on the inner continental shelf west of Scotland between 55°30' and 57°30' N. *Boreas*, 13, pp.49–66.

Dawson, A.G., 1984. Quaternary sea-level changes in Western Scotland. *Quaternary Science Reviews*, 3(4), pp.345–368.

Dawson, S., Dawson, A.G. & Edwards, K.J., 1998. Rapid Holocene relative sea-level changes in Gruinart, Isle of Islay, Scottish Inner Hebrides. *The Holocene*, 8(2), pp.183–195.

Dean, W., 1974. Determination of carbonate and organic matter in calcareous sediments and sedimentary rocks by loss on ignition: comparison with other methods. *Journal of Sedimentary Petrology*, 44(1), pp.242–248.

Denys, L. & De Wolf, H., 1999. Diatoms as indicators of coastal paleo-environments and relative sea-level change. In E. Stoermer & J. Smol, eds. *The Diatoms: Applications for the Environmental and Earth Sciences*. Cambridge University Press.

Devoy, R.J., 1979. Flandrian Sea Level Changes and Vegetational History of the Lower Thames Estuary. *Philosophical transactions of the Royal Society of London, Series B, Biological*, 285(1010), pp.355–407.

Devoy, R.J., 1982. Analysis of the geological evidence for Holocene sea-level movements in southeast England. *Proceedings of the Geologists' Association*, 93(1), pp.65–90.

Dias, C., 2014. *Late Holocene sea-level reconstruction in Northwest Scotland in relation to situation of Iron Age archaeology*. University of Bristol.

Edwards, R.J., 2006. Mid- to late-Holocene relative sea-level change in southwest Britain and the influence of sediment compaction. *The Holocene*, 16(4), pp.575–587.

Environment Agency, 2009. *Investing for the future: Flood and coastal risk management in England*, Bristol.

Evans, D.J., Clark, C.D. & Mitchell, W. a., 2005. The last British Ice Sheet: A review of the evidence utilised in the compilation of the Glacial Map of Britain. *Earth-Science Reviews*, 70(3-4), pp.253–312.

Everest, J.D. et al., 2013. New age constraints for the maximum extent of the last British-Irish Ice Sheet (NW sector). *Journal of Quaternary Science*, 28(1), pp.2–7.

Fabel, D., Ballantyne, C.K. & Xu, S., 2012. Trimlines, blockfields, mountain-top erratics and the vertical dimensions of the last British–Irish Ice Sheet in NW Scotland. *Quaternary Science Reviews*, 55, pp.91–102.

Faegri, K. & Iversen, J., 1989. *Textbook of Pollen Analysis* 4th ed., The Blackburn Press.

Farrell, W.E. & Clark, J. a., 1976. On Postglacial Sea Level. *Geophysical Journal of the Royal Astronomical Society*, 46(3), pp.647–667.

Finlayson, A. et al., 2011. Evolution of a Lateglacial mountain icecap in northern Scotland. *Boreas*, 40(3), pp.1–33.

Firth, C. & Haggart, B., 1989. Loch Lomond Stadial and Flandrian shorelines in the inner Moray Firth area , Scotland. *Journal of Quaternary Science*, 4(1), pp.37–50.

Flemming, N.C., 1982. Multiple regression analysis of earth movements and eustatic sea-level change in the United Kingdom in the past 9000 years. *Proceedings of the Geologists' Association*, 93(1), pp.113–125.

Florin, M.-B., 1946. Clypeusfloran i postglaciala fornsjolagerfoljder i ostra Mellansverige. *Geol.Foren.Stockholm Forh.*, 68, pp.429–458.

Fromm, E., 1938. Geokronologisch datierte Pollendiagramme und Diatomeenanalysen aus Angermanland. *Geol.Foren.Stockholm Forh.*, 60, pp.365–381.

Gehrels, W.R. et al., 1995. Modeling the contribution of M2 tidal amplification to the Holocene rise of mean high water in the Gulf of Maine and the Bay of Fundy. *Marine Geology*, 124, pp.71–85.

Geikie, J., 1878. On the glacial phenomena of the long isle or outer Hebrides. *Journal of the Geological Society of London*, 34, pp.819–866.

Gillen, C., 2003. *Geology and landscapes of Scotland*, Terra Publishing.

Glew, J., Smol, J. & Last, W., 2001. Sediment Core Collection & Extrusion. In W. Last & J. Smol, eds. *Tracking Environmental Change Using Lake Sediments Volume 1: Basin Analysis, Coring and Chronological Techniques*. Kluwer Academic Publishers.

Godwin, H., 1940. Pollen analysis and forest history of England and Wales. *New Phytologist*, 39(4), pp.370–400.

Golledge, N.R., 2010. Glaciation of Scotland during the Younger Dryas stadial: a review. *Journal of Quaternary Science*, 25(4), pp.550–566.

Graham, D. et al., 1990. The biostratigraphy and chronostratigraphy of BGS borehole 78/4, North Minch. *Scottish Journal of Geology1*, 26, pp.65–75.

Gray, J., 1974. Lateglacial and postglacial shorelines in western Scotland. *Boreas*, 3(4), pp.129–138.

Greensmith, J.T. & Tucker, E. V., 1986. Compaction and consolidation. In O. van de Plassche, ed. *Sea-level Research: a manual for the collection and evaluation of data*. Geobooks, pp. 591–603.

Gregory, J., 1926. The Scottish kames and their evidence in the glaciation of Scotland. *Transactions of the Royal Society of Edinburgh1*, 54(395-432).

Grimm, E., 1987. CONISS: a FORTRAN 77 program for stratigraphically constrained cluster analysis by the method of incremental sum of squares. *Computers and Geosciences*, 13, pp.13–35.

Halden, B., 1929. Kvartargeologiska diatomaceestudier belysande den postglaciala trangressionen a Svenska Vastkusten. *Geol.Foren.Stockholm Forh*, 51, pp.311–366.

Hamilton, C., 2013. *A Reconstruction of the Lateglacial highstand in the Assynt region of North-west Scotland*. University of Bristol.

Hartley, B., Barber, H. & Carter, J., 1996. *An Atlas of British Diatoms* P. Sims, ed., Biopress Limited.

Haworth, E., 1976. Two Late-Glacial (Late Devensian) Diatom Assemblage Profiles from Northern Scotland. *New Phytologist*, 77(1), pp.227–256.

Heinrich, H., 1988. Origin and Consequences of Cyclic Ice Rafting in the Northeast Atlantic Ocean during the Past 130 , 000 Years. *Quaternary Research*, 29, pp.142–152.

Heiri, O., Lotter, A. & Lemcke, G., 2001. Loss on ignition as a method for estimating organic and carbon content in sediments: reproducibility and comparability of results. *Journal of Paleolimnology2*, 25, pp.101–110.

Hemphill-Haley, E., 1993. *Taxonomy of recent and fossil (Holocene) diatoms (Bacillariophyta) from northern Willapa Bay, Washington*.

Heyworth, A. & Kidson, C., 1982. Sea-level changes in southwest England and Wales. *Proceedings of the Geologists' Association*, 93(1), pp.91–111.

Hjulstrom, F., 1939. Transportation of detritus by moving water. In R. Trask, ed. *Recent Marine Sediments*. American Association for Petroleum Geologists, pp. 5–31.

Horton, B.P., Edwards, R.J. & Lloyd, J.M., 2000. Implications of a microfossil transfer function in Holocene sea-level studies. In I. Shennan & J. E. Andrews, eds. *Holocene Land-Ocean Interaction and Environmental Change around the North Sea*. Geological Society Special Publication 166: Geological Society Publishing House, pp. 41–54.

Horton, B.P. et al., 2005. Holocene sea levels and palaeoenvironments, Malay-Thai Peninsula, southeast Asia. *The Holocene*, 15(8), pp.1199–1213.

Horton, B.P. & Shennan, I., 2009. Compaction of Holocene strata and the implications for relative sealevel change on the east coast of England. *Geology*, 37(12), pp.1083–1086.

Horton, B.P. et al., 2013. Influence of tidal-range change and sediment compaction on Holocene relative sea-level change in New Jersey, USA. *Journal of Quaternary Science*, 28(4), pp.403–411.

Hubbard, A. et al., 2009. Dynamic cycles, ice streams and their impact on the extent, chronology and deglaciation of the British–Irish ice sheet. *Quaternary Science Reviews*, 28(7-8), pp.758–776.

Hustedt, F., 1937. Systematische und okologische Untersuchungen uber den Diatomeen-Flora von Java, Bali, Sumatra. *Archiv fuer Hydrobiologie*, 15 & 16.

Hustedt, F., 1953. Die Systematik der Diatomeen in ihren Beziehungen zur Geologie und Okologie nebst einer Revision des Halobien-systems. *Svensk Botanisk Tidskrift*, 47, pp.509–519.

Jevrejeva, S., Moore, J.C. & Grinsted, A., 2012. Sea level projections to AD2500 with a new generation of climate change scenarios. *Global and Planetary Change*, 80-81, pp.14–20.

Johnstone, G. & Mykura, W., 1989. *British Regional Geology: The Northern Highlands of Scotland* 4th ed., British Geological Survey.

Juggins, S., 2003. *C2 User guide. Software for ecological and palaeoecological data analysis and visualisation*, University of Newcastle, Newcastle Upon Tyne.

Kaland, P.E., Krzywinski, K. & Stabell, B., 1984. Radiocarbon-dating of transitions between marine and lacustrine sediments and their relation to the development of lakes. *Boreas*, 13(2), pp.243–258.

Keeling, P., 1962. Some experiments on the low-temperature removal of carbonaceous material from clays. *Clay Minerals Bulletin*, 28, pp.155–158.

Kjemperud, A., 1981. Diatom changes in sediments of basins possessing marine / lacustrine transitions in Frosta , Nord-Trondelag, Norway. *Boreas*, 10, pp.27–38.

Kjemperud, A., 1986. Late Weichselian and Holocene shoreline displacement in the Trondheimsfjord area, central Norway. *Boreas*, 15(1), pp.61–82.

Kolbe, R., 1927. Zur Okologie, Morphologie und Systematik der Brackwasser-Diatomeen. *Pflanzenforschung*, 7, pp.1–146.

Kuchar, J. et al., 2012. Evaluation of a numerical model of the British-Irish ice sheet using relative sea-level data: implications for the interpretation of trimline observations. *Journal of Quaternary Science*, 27(6), pp.597–605.

Kunze, G. & Dixon, J., 1987. Pretreatment for mineralogical analysis. In A. Klute, ed. *Methods of Soil Analysis Part 1: Physical and Mineralogical Methods1*. American Society of Agronomy, pp. 91–100.

Laidler, P.D., 2002. *Foraminiferal ecology of contemporary isolation basins in Northwest Scotland*. Durham University.

Lambeck, K., 1993a. Glacial rebound of the British Isles-1. Preliminary model results. *Geophysical Journal International*, 115, pp.941–959.

Lambeck, K., 1993b. Glacial rebound of the British Isles-II. A high-resolution, high-precision model. *Geophysical Journal International*, 115, pp.960–990.

Lawson, T.J., 1983. *Quaternary geomorphology of the Assynt area, N.W. Scotland*. University of Edinburgh unpublished PhD thesis.

Lambeck, K., 1995. Late Devensian and Holocene shorelines of the British Isles and North Sea from models of glacio-hydro-isostatic rebound. *Journal of the Geological Society*, 152(3), pp.437–448.

Lawson, T.J., 1995. *The Quaternary of Assynt and Coigach: Field Guide* T. J. Lawson, ed., Quaternary Research Association, Cambridge.

Lloyd, J.L., 2000. Combined foraminiferal and thecamoebian environmental reconstruction from an isolation basin in NW Scotland: Implications for sea-level studies. *Journal of Foraminiferal Research*, 30(4), pp.294–305.

Lloyd, J.M. & Evans, J.R., 2002. Contemporary and fossil foraminifera from isolation basins in northwest Scotland. *Journal of Quaternary Science*, 17, pp.431–443.

Lloyd, J.M. et al., 2009. Lateglacial to Holocene relative sea-level changes in the Bjarkarlundur area near Reykholar , North West Iceland. *Journal of Quaternary Science*, 24(7), pp.816–831.

Lloyd, J.M. et al., 2013. Holocene and Lateglacial relative sea-level change in north-west England: implications for glacial isostatic adjustment models. *Journal of Quaternary Science*, 28(1), pp.59–70.

Long, A.J., Waller, M.P. & Stupples, P., 2006. Driving mechanisms of coastal change: Peat compaction and the destruction of late Holocene coastal wetlands. *Marine Geology*, 225(1-4), pp.63–84.

Long, A.J. et al., 2011. Isolation basins, sea-level changes and the Holocene history of the Greenland Ice Sheet. *Quaternary Science Reviews*, 30(27-28), pp.3748–3768.

Lowe, J. & Walker, M., 1997. *Reconstructing Quaternary Environments*, Longman.

Lukas, S. & Bradwell, T., 2010. Reconstruction of a Lateglacial (Younger Dryas) mountain ice field in Sutherland, northwestern Scotland, and its palaeoclimatic implications. *Journal of Quaternary Science*, 25(4), pp.567–580.

MacLeod, A. et al., 2011. Timing of glacier response to Younger Dryas climatic cooling in Scotland. *Global and Planetary Change*, 79(3-4), pp.264–274.

McCarroll, D. et al., 1995. Nunataks of the last ice sheet in North-west Scotland. *Boreas*, 24(4), pp.305–323.

McIntyre, K., Howe, J. & Bradwell, T., 2011. Lateglacial ice extent and deglaciation of Loch Hourn, western Scotland. *Scottish Journal of Geology*, 47(2), pp.169–178.

Meyers, P. & Teranes, J., 2001. Sediment Organic Matter. In W. Last & J. Smol, eds. *Tracking Environmental Change Using Lake Sediments Volume 2: Physical and Geochemical Methods*. Kluwer Academic Publishers, pp. 239–269.

Milne, G. a., Mitrovica, J.X. & Schrag, D.P., 2002. Estimating past continental ice volume from sea-level data. *Quaternary Science Reviews*, 21(1-3), pp.361–376.

Mitrovica, J.X., 1996. Haskell [1935] revisited. *Journal of Geophysical Research*, 101(B1), pp.555–569.

Moore, P. & Webb, J., 1978. *An Illustrated Guide to Pollen Analysis*, Hodder and Stoughton.

Moore, P., Webb, J. & Collinson, M., 1991. *Pollen Analysis* 2nd ed., Blackwell Scientific Publications.

Murray-Wallace, C. & Woodroffe, C.D., 2014. *Quaternary Sea-Level Changes: A Global Perspective*, Cambridge University Press.

Neill, S.P., Scourse, J.D. & Uehara, K., 2010. Evolution of bed shear stress distribution over the northwest European shelf seas during the last 12,000 years. *Ocean Dynamics*, 60(5), pp.1139–1156.

Nelson, A.R. & Kashima, K., 1993. Diatom Zonation in Southern Oregon Tida Marshes relative to Vascular Plants , Foraminifera , and Sea Level. *Journal of Coastal Research*, 9(3), pp.673–697.

O'Cofaigh, C. et al., 2003. Palaeo-ice streams , trough mouth fans and high-latitude continental slope sedimentation. *Boreas*, 32, pp.37–55.

Olsson, I.U., 1991. Accuracy and precision in sediment chronology. *Hydrobiologia*, 214, pp.25–34.

Ordnance Survey, 2014. Benchmark Locator. *Ordnance Survey Benchmarks*. Available at: http://www.ordnancesurvey.co.uk/benchmarks/ [Accessed October 7, 2014].

Palmer, A. & Abbott, W., 1986. Diatoms as indicators of sea-level change. In O. van de Plassche, ed. *Sea-level Research: a manual for the collection and evaluation of data*. Geo books.

Peach, B. & Horne, J., 1892. The ice-shed in the North-West Highlands during the maximum glaciation. *Reports of the British Association*, 720.

Peach, B. et al., 1913. The geology of the Fannich Mountains and the country around upper Loch Maree adn Strath Broom. In *Memoir of the Geological Survey of Scotland*.

Peck, V.L. et al., 2007. The relationship of Heinrich events and their European precursors over the past 60ka BP: a multi-proxy ice-rafted debris provenance study in the North East Atlantic. *Quaternary Science Reviews*, 26(7-8), pp.862–875.

Peltier, W.R., Farrell, W.E. & Clark, J.A., 1978. Glacial isostasy and Relative sea-level: A global finite element model. *Tectonophysics*, 50, pp.81–110.

Peltier, W.R., 1986. Deglaciation-induced vertical motion of the North American continent and transient lower mantle rheology. *Journal of Geophysical Research*, 91(B9), p.9099.

Peltier, W.R., 1988. Lithospheric thickness, Antarctic deglaciation history, and ocean basin discretization effects in a global model of postglacial sea level change: A summary of some sources of nonuniqueness. *Quaternary Research*, 29(2), pp.93–112.

Peltier, W.R., 1998. Postglacial variations in the level of the sea: Implications for climate dynamics and solid-earth geophysics. *Reviews of Geophysics*, 36(4), pp.603–689.

Peltier, W., 2002. On eustatic sea level history: Last Glacial Maximum to Holocene. *Quaternary Science Reviews*, 21, pp.377–396.

Peltier, W.R. et al., 2002. On the postglacial isostatic adjustment of the British Isles and the shallow viscoelastic structure of the Earth. *Geophysical Journal International*, 148(3), pp.443–475.

Pennington, W. et al., 1972. Lake Sediments in northern Scotland. *Philosophical transactions of the Royal Society of London, Series B, Biological*, 264(86), p.191.

Pennington, W. & Sackin, M., 1975. An application of principal components analysis to the zonation of two Late-Devensian profiles. *New Phytologist*, p.419.

Preuss, H., 1979. Progress in computer evaluation of sea-level data within the IGCP project no. 61. In I. Flexor, ed. *International Symposium on Coastal Evolution in the Quaternary*. Sao-Paulo, Brazil, pp. 104–134.

Pye, K., 1994. *Sediment Transport and Depositional Processes*, Blackwell Scientific Publications.

Reimer, P.J. et al., 2013. IntCal13 and MARINE13 radiocarbon age calibration curves 0-50000 years cal BP. *Radiocarbon*, 55(4).

Robinson, M., 1982. Diatom Analysis of Early Flandrian Lagoon Sediments from East Lothian , Scotland. *Journal of Biogeography*, 9(3), pp.207–221.

Scherer, R.P., 1994. A new method for the determination of absolute abundance of diatoms and other silt-sized sedimentary particles. *Journal of Paleolimnology*, 12(2), pp.171–179.

Sejrup, H.P. et al., 2005. Pleistocene glacial history of the NW European continental margin. *Marine and Petroleum Geology*, 22(9-10), pp.1111–1129.

Selby, K. a. et al., 2000. Late Devensian and Holocene relative sea level and environmental changes from an isolation basin in southern Skye. *Scottish Journal of Geology*, 36(1), pp.73–86.

Shennan, I., 1982. Interpretation of Flandrian sea-level data from the Fenland, England. *Proceedings of the Geologists' Association*, 93(1), pp.53–63.

Shennan, I., 1989. Holocene crustal movements and sea-level changes in Great Britain. *Journal of Quaternary Science*, 4, pp.77–89.

Shennan, I.. et al., 1994. Late Devensian and Holocene relative sea-level changes at Loch nan Eala, near Arisaig, northwest Scotland. *Journal of Quaternary Science*, 9, pp.261–283.

Shennan, I., Innes, J.B., Long, A.J., et al., 1995. Holocene relative sea-level changes and coastal vegetation history at Kentra Moss , Argyll , northwest Scotland. *Marine Geology*, 124, pp.43–59.

Shennan, I. et al., 1995. Late Devensian and Holocene relative sea-level changes in Northwestern Scotland: New data to test existing models. *Quaternary International*, 26(94), pp.97–123.

Shennan, I. et al., 1996. Late glacial sea level and ocean margin environmental changes interpreted from biostratigraphic and lithostratigraphic studies of isolation basins in northwest Scotland. *Geological Society, London, Special Publications*, 111(1), pp.229–244.

Shennan, I. et al., 1996. Evaluation of Rapid Relative Sea-Level Changes in North-West Scotland During the Last Glacial- Interglacial Transition : Evidence from Ardtoe and Other Isolation Basins. *Journal of Coastal Research*, 12(4), pp.862–874.

Shennan, I., 1999. Global meltwater discharge and the deglacial sea-level record from northwest Scotland. *Journal of Quaternary Science*, 14(7), pp.715–719.

Shennan, I. et al., 2000. Late Devensian and Holocene records of relative sea-level changes in northwest Scotland and their implications for glacio-hydro-isostatic modelling. *Quaternary Science Reviews*, 19(11), pp.1103–1135.

Shennan, I. et al., 2002. Global to local scale parameters determining relative sea-level changes and the post-glacial isostatic adjustment of Great Britain. *Quaternary Science Reviews*, 21(1-3), pp.397–408.

Shennan, I. & Horton, B., 2002. Holocene land- and sea-level changes in Great Britain. *Journal of Quaternary Science*, 17(5-6), pp.511–526.

Shennan, I. et al., 2005. A 16000-year record of near-field relative sea-level changes, North-west Scotland, United Kingdom. *Quaternary International*, 133-134, pp.95–106.

Shennan, I., et al., 2006a. Relative sea-level changes, glacial isostatic modelling and ice-sheet reconstructions from the British Isles since the Last Glacial Maximum. *Journal of Quaternary Science*, 21, pp.585–599.

Shennan, I., et al., 2006b. Relative sea-level observations in western Scotland since the Last Glacial Maximum for testing models of glacial isostatic land movements and ice sheet reconstructions. *Journal of Quaternary Science*, 21, pp.601–613.

Shennan, I., 2007. Sea-level studies; Overview. In S. Elias, ed. *Encyclopedia of Quaternary Science*. Elsevier, pp. 2967–2974.

Shennan, I., Barlow, N. & Combellick, R., 2008. Palaeoseismological records of multiple great earthquakes in south-central Alaska – a 4000 year record at Girdwood. In J. Freymueller et al., eds. *Active tectonics and seismic potential of Alaska. In: Geophysical Monograph Series, vol. 179*. American Geophysical Union Washington, pp. 185–199.

Shennan, I., Milne, G. & Bradley, S., 2012. Late Holocene vertical land motion and relative sea-level changes: lessons from the British Isles. *Journal of Quaternary Science*, 27(1), pp.64–70.

Sissons, J.B., 1963. Scottish Raised Shoreline Heights with Particular Reference to the Forth Valley. *Geografiska Annaler*, 45(2/3), pp.180–185.

Sissons, J.B. & Smith, D.E., 1966. Late-glacial and post-glacial shorelines in south-east Scotland. *Transactions of the Institute of British Geographers*, 39, pp.9–18.

Sissons, J.B., 1967. *The Evolution of Scotland's Scenery*, Edinburgh: Oliver and Boyd.

Sissons, J., 1977. The Loch Lomond Readvance in the Northern Mainland of Scotland. In J. Gray & J. Lowe, eds. *Studies in the Scottish Lateglacial Environment*. Pergamon Press, pp. 45–60.

Sissons, J.B., 1983. Shorelines and isostasy in Scotland. In D. E. Smith & A. G. Dawson, eds. *Shorelines and Isostasy*. Academic Press, London, pp. 209–226.

Smith, D.E., Cullingford, R.A. & Firth, C.R., 2000. Patterns of isostatic uplift during the Holocene: evidence from mainland Scotland. *The Holocene*, 10, pp.489–501.

Smith, D.E., 2005. Evidence for secular sea surface level changes in the Holocene raised shorelines of Scotland, UK. *Journal of Coastal Research*, (42), pp.26–42.

Smith, D.E. et al., 2006. Towards improved empirical isobase models of Holocene land uplift for mainland Scotland, UK. *Philosophical transactions. Series A, Mathematical, physical, and engineering sciences*, 364(1841), pp.949–72.

Smith, D.E. et al., 2012. Patterns of Holocene relative sea level change in the North of Britain and Ireland. *Quaternary Science Reviews*, 54, pp.58–76.

Snyder, J. a. et al., 1997. Postglacial relative sea-level history: sediment and diatom records of emerged coastal lakes, north-central Kola Peninsula, Russia. *Boreas*, 26, pp.329–346.

Stoker, M. & Bradwell, T., 2005. The Minch palaeo-ice stream, NW sector of the British-Irish Ice Sheet. *Journal of the Geological Society*, 162(3), pp.425–428.

Stoker, M.S. et al., 2009. Lateglacial ice-cap dynamics in NW Scotland: evidence from the fjords of the Summer Isles region. *Quaternary Science Reviews*, 28(27-28), pp.3161–3184.

Stokes, C.R. & Clark, C.D., 2001. Palaeo-ice streams. *Quaternary Science Reviews*, 20, pp.1437–1457.

Sugden, D.E., Bentley, M.J. & O Cofaigh, C., 2006. Geological and geomorphological insights into Antarctic ice sheet evolution. *Philosophical transactions. Series A, Mathematical, physical, and engineering sciences*, 364(1844), pp.1607–25.

Sullivan, M. & Currin, C., 2000. Community Structure and Functional Dynamics of Benthic Microalgae in Salt Marshes. In M. Weinstein & D. Kreeger, eds. *Concepts and controversies in Tidal Marsh Ecology*. Springer, pp. 81–106.

Sutherland, D.G., 1984. The Quaternary Deposits and Landforms of Scotland and the Neighbouring Shelves: A Review. *Quaternary Science ReviewsQuaternary Science Reviews*, 3, pp.157–254.

Thomas, C., 2014. *Investigating postglacial relative sea-level change, Duart, NW Scotland*. University of Bristol.

Tooley, M.J., 1982. Sea-level changes in northern England. *Proceedings of the Geologists' Association*, 93(1), pp.43–51.

Troels-Smith, J., 1955. Karakterisaring af l+se jordarter (Characterisa- tion of Unconsolidated Sediments). *Geological Survey of Denmark IV*, 3, pp.1–73.

Uehara, K. et al., 2006. Tidal evolution of the northwest European shelf seas from the Last Glacial Maximum to the present. *Journal of Geophysical Research*, 111(C9), p.C09025.

United Nations Environment Programme, 2010. Human Settlements on the Coast. *UN Atlas of the Oceans*.

Van de Plassche, O., 1986. Introduction. In O. van de Plassche, ed. *Sea-level Research: a manual for the collection and evaluation of data*. Geobooks.

Veres, D., 2002. A comparative study between loss on ignition and total carbon analysis on minerogenic sediments. *Studia Universitatis Babes-Bolyai, Geologia*, XLVII(1), pp.171–182.

Vos, P.C. & De Wolf, H., 1988. Methodological aspects of paleo-ecological diatom research in coastal areas of the Netherlands. *Geologie en Mijnbouw*, 67, pp.31–40.

Vos, P.C. & De Wolf, H., 1993. Diatoms as a tool for reconstructing sedimentary environments in coastal wetlands ; methodological aspects. *Hydrobiologia*, 269/270, pp.285–296.

Watcham, E.P., Shennan, I. & Barlow, N.L.M., 2013. Scale considerations in using diatoms as indicators of sea-level change: lessons from Alaska. *Journal of Quaternary Science*, 28(2), pp.165–179.

Wentworth, C., 1922. A scale of grade and class terms for clastic sediments. *The Journal of Geology*, 5, pp.377–392.

Whitehouse, P.L. et al., 2012. A new glacial isostatic adjustment model for Antarctica: calibrated and tested using observations of relative sea-level change and present-day uplift rates. *Geophysical Journal International*, 190(3), pp.1464–1482.

Whittington, G. & Hall, A.M., 2002. The Tolsta Interstadial, Scotland: correlation with D–O cycles GI-8 to GI-5? *Quaternary Science Reviews*, 21(8-9), pp.901–915.

Zong, Y., 1997. Implications of Paralia Sulcata Abundance in Scottish Isolation Basins. *Diatom Research*, 12(1), pp.125–150.

Zong, Y. & Horton, B.P., 1998. Diatom zones across intertidal flats and coastal saltmarshes in Britain. *Diatom Research*, 13.

Zong, Y. & Horton, B.P., 1999. Diatom-based tidal-level transfer functions as an aid in reconstructing Quaternary history of sea-level movements in the UK. *Journal of Quaternary Science*, 14(2), pp.153–167.

Zong, Y. & Tooley, M.J., 1999. Evidence of mid-Holocene storm-surge deposits from Morecambe Bay, northwest England: A biostratigraphical approach. *Quaternary International*, 55(1), pp.43–50.

Zong, Y., 2004. Mid-Holocene sea-level highstand along the Southeast Coast of China. *Quaternary International*, 117(1), pp.55–67.

Zwartz, D. et al., 1998. Holocene sea-level change and ice-sheet history in the Vestfold Hills, East Antarctica. *Earth and Planetary Science Letters*, 155, pp.131–145.